Distribution Agreement

In presenting this thesis or dissertation as a partial fulfillment of the requirements for an advanced degree from Emory University, I hereby grant to Emory University and its agents the non-exclusive license to archive, make accessible, and display my thesis or dissertation in whole or in part in all forms of media, now or hereafter known, including display on the world wide web. I understand that I may select some access restrictions as part of the online submission of this thesis or dissertation. I retain all ownership rights to the copyright of the thesis or dissertation. I also retain the right to use in future works (such as articles or books) all or part of this thesis or dissertation.

Signature:

_____ _____

Douglas E. Terry Date

Local ecdysone synthesis in a wounded epithelium sustains developmental delay and promotes regeneration in *Drosophila*

By

Douglas Emmons Terry

Doctor of Philosophy

Genetics and Molecular Biology
Graduate Division of Biological and Biomedical Sciences
Laney Graduate School
Emory University

_____
Kenneth Moberg, Ph.D.
Advisor

_____
Dorothy Lerit, Ph.D.
Committee Member

_____
Eric Ortlund, Ph.D.
Committee Member

_____
Melissa Gilbert-Ross, Ph.D.
Committee Member

_____
William G. Kelly, Ph.D.
Committee Member

Accepted:

_____
Kimberly Jacob Arriola, Ph.D., MPH
Dean of the James T. Laney School of Graduate Studies

_____
Date

Local ecdysone synthesis in a wounded epithelium sustains developmental delay and promotes regeneration in *Drosophila*

By

Douglas Emmons Terry
B.S., Georgia Institute of Technology 2012

Kenneth H. Moberg, Ph.D.
Advisor

An abstract of
A dissertation submitted to the Faculty of the James T. Laney School of Graduate Studies of Emory University in partial fulfillment of the requirements for the degree of Doctor of Philosophy in the Division of Biology and Biomedical Sciences,
Genetics and Molecular Biology Program
2023

Abstract

Local ecdysone synthesis in a wounded epithelium

sustains developmental delay and promotes regeneration in *Drosophila*

By Douglas Emmons Terry

The capacity for regeneration is often lost as animals mature past embryonic or juvenile stages, suggesting a dependence on redirecting developmental signals away from patterned growth and toward localized regenerative growth. This generally corresponds with a pause in growth of uninjured tissues that avoids developmental asynchrony by allowing the injured tissue to repair before rejoining a normal developmental trajectory. Yet, how local and systemic endocrine signaling are coordinated to promote tissue regeneration while stalling systemic developmental growth remains poorly understood.

Loss of regeneration competence in a commonly used *Drosophila* wing injury system parallels the rapid rise in levels of the steroid hormone ecdysone (Ec) that peaks at the larval-to-pupal transition. This apparently inverse relationship has led to the hypothesis that high level Ec inhibits wing regeneration. However, low level Ec is present throughout regeneration-competent larval stages, and Ec has been shown to promote cell proliferation and tissue growth. Moreover, low level Ec and its receptor EcR are required for activity of the pro-growth Dpp and Wg pathways, which promote normal and regenerative wing disc growth.

The apparent paradox that injury results in systemic depletion of the Ec larval growth hormone at a time when the wing blastema is undergoing regenerative growth led us to assess Ec roles and activity within injured wing discs. We find that as EcR activity drops elsewhere in the disc, it rises in the blastema region. In parallel, local depletion of Ec biosynthesis enzymes

consistently impairs regrowth of injured wings, while local depletion of the Ec catabolic enzyme Cyp18a1 enhances regeneration. We trace these effects to a requirement for Ec in both injury-induced developmental delay and coordinated growth reduction and find that expression of mRNAs encoding the key regeneration regulators Ets21C and Upd3 expression are responsive to Ec produced locally at the site of injury. These findings suggest that 20E promotes elements of the regenerative transcriptional program in the wing disc, and that the blastema is a unique signaling environment that generates its own Ec to sustain a tissue repair program. Thus, the studies described in this dissertation provide a novel addition to our understanding of how local and systemic Ec production are coordinated to create a privileged transcriptional environment to support tissue repair that may provide insight into regulation of endocrine signaling molecules during tissue regeneration in diverse species.

Local ecdysone synthesis in a wounded epithelium sustains developmental delay and promotes regeneration in *Drosophila*

By

Douglas Emmons Terry
B.S., Georgia Institute of Technology 2012

Kenneth H. Moberg, Ph.D.
Advisor

A dissertation submitted to the Faculty of the James T. Laney School of Graduate Studies of Emory University in partial fulfillment of the requirements for the degree of Doctor of Philosophy in the Division of Biology and Biomedical Sciences,
Genetics and Molecular Biology Program
2023

Acknowledgements

I would like to thank my advisor, Dr. Ken Moberg, for his mentorship throughout my time at Emory. Your enthusiasm for research and the process of scientific discovery has always shown through and provided inspiration and encouragement, whether the results of a given experiment made any sense to us at the time or not. I would also like to thank you for your constructive criticism of my figures and scientific writing. Knowing that I could rely on you to help polish my work has been a great comfort and, I believe, has greatly benefited the clarity of my own figure building and writing.

Thank you to the members of my committee: Drs. Dorothy Lerit, Melissa Gilbert-Ross, Eric Ortlund, and Bill Kelly. Your comments and suggestions have helped me stay on track and move my research forward. Perhaps even more importantly, your encouragement has helped motivate me throughout my graduate career. Thank you.

To all the current and previous members of the Moberg Lab, thank you for providing a positive and friendly laboratory environment. I would also like to thank the 'Hippo' side of the lab for help with experimental design and techniques: especially Drs. Joanna Wardwell-Ozgo, Can Zhang, and Shilpi Verghese. Carly Lancaster thank you for providing me access to the Corbett Lab when I needed it and always being a good lab mate. Colby Schweibenz thank you for being gracious loser in both the lab dart game and ping pong. Seriously though, thank you for being a great friend, lab would not have been nearly as enjoyable without you. I sincerely hope you all have a nice life.

To my graduate school friends, thank you for your support and friendship. The road through graduate school was a long one, but you have made the years immensely enjoyable. It is

bittersweet as we move on, and often away, but I know that the experiences we have shared throughout our time in graduate school will make reconnecting easy when we get the chance.

To my family, it has been wonderful to have you so close here in Georgia. Knowing that you will always be there for me has been, and continues to be, a great support.

Table of Contents

List of figures

List of tables

Chapter 1. Introduction

1.1 Regeneration as a scientific field of study

Regeneration refers to the replacement of lost tissue by an organism. In the early 1900s Thomas Hunt Morgan refined the definition to denote the difference between physiological and restorative regeneration: physiological regeneration refers to regeneration that is part of the regular life cycle of the organism (e.g., replacement of feathers, teeth, antlers, lining of the gut) and restorative regeneration refers to regeneration of "all other kinds"[1]. These definitions nicely differentiate between two distinct yet related types of growth following tissue loss. While these two types of regeneration share certain aspects, this dissertation will largely focus on restorative regeneration following acute injury. Here I present a brief overview of how the scientific study of regeneration began and outline the rest of the chapter.

The first recorded documentation of regeneration as a natural phenomenon goes back to a brief note in Aristotle's *History of Animals* in the fourth century BC: "The tails of lizards and of serpents, if they be cut off, will grow again" (taken from [2]). However, the rise of the scientific study of regeneration did not come for another two thousand years with the depiction and characterization of crayfish limb and claw regeneration in 1712 [1, 3]. Reaumur's detailed characterization of the regeneration of a complex organ caught the imagination of other scientists of his time and helped to kickstart and interest in the study of regeneration. Now, over 300 years later, we know from more recent work on fiddler crabs that this regeneration very likely required ecdysteroid hormone signaling [4], whose role in regeneration is the primary focus of this thesis.

Interest in regeneration intensified in the latter half of the 18th century as proponents of the two main theories of generation (the study of what has come to be known as embryogenesis

and development) believed they could test their theories by studying the mechanisms of regenerative growth. Regeneration appeared to offer an experimentally feasible context in which to study generation. Preformationists believed they would find evidence for a preformed limb within salamander regenerate. Likewise, epigenists believed they would discover roles for Newtonian forces to account for generation [5, 6]. The intense competition between these theories of generation would lead to the study and description of regeneration across numerous model systems including snails, hydra, and salamanders [1, 6, 7].While these theories of generation would eventually be overthrown with the development of cell theory and developmental biology as we now know it, the theoretical underpinning of regeneration as a process that reuses key programs of developmental growth has remained [1, 6, 7].

The idea that regeneration could help us understand development was picked up by Thomas Hunt Morgan in the late 19th and early 20th century. In 1901, he synthesized much of the previous work of the past two centuries as well as his own studies on regeneration in his book *Regeneration* [1]. This synthesis helped set the groundwork for the scientific investigation of regeneration in the 20th century. However, Morgan himself eventually abandoned regenerative research, reportedly, in favor of the 'easier' problem of heredity [6]. Morgan is now most well-known for his pioneering genetic research using *Drosophila* that led to the discovery of the role chromosomes play in heredity and the Nobel Prize in Physiology and Medicine in 1933. As a *Drosophila* geneticist, I can be happy Morgan made this switch even as I use *Drosophila* to study regeneration today.

Since Morgan's abandonment of the regeneration field over 120 years ago, key advances in our techniques to probe and our understanding of the molecular underpinnings that control development and growth have been leveraged to study regeneration. Indeed, it has only been in

the previous two decades that we have made the advances in methodologies that allow us to investigate the specific effects of gene manipulation within regenerating organs. The regeneration field, since its inception in the 1700s, has taken advantage of comparative study of many model organisms and this trend continues to this day. In this introductory chapter, I will begin by discussing what has been and still can be learned about regeneration by studying multiple model organisms. I then describe the relevant aspects of *Drosophila* as a regenerative model organism and highlight the strengths of *Drosophila* as a model organism to study regeneration. From there we will turn to what is known about the mechanisms of *Drosophila* wing disc regeneration and the ecdysone steroid hormone signaling pathway. Finally, I will provide a framework for how the research presented in the following chapters of this dissertation fit into our current understanding of regeneration and steroid hormone signaling.

1.2 Comparative study of regeneration

Restorative regeneration can be found across the metazoan phyla [8, 9] (**Fig. 1.1**). This has led to the hypothesis that regeneration is an ancestral trait that has been suppressed in those lineages that do not display regeneration. However, both the extent of regenerative capacity and the cellular contributors to the regenerate vary across the model systems that have been studied. Planarians, for example, are capable of whole-body regeneration and make use of a specialized pool of stem cells to fuel their whole-body regeneration. Salamanders, on the other hand, are only capable of regenerating certain body structures (e.g., limbs) and appear to take advantage of both resident stem cell populations and transdetermination of mature cell types to fuel regenerative growth. Similarly, the key signaling pathways and gene regulatory networks (GRNs) required to drive regenerative growth show both variation and commonalities between

organisms [9-11]. While the extent to which shared aspects of regeneration between different lineages represent true homology or convergent evolution remains unclear, by comparing these similarities and differences in species with divergent regenerative capacities we can identify key factors that can be leveraged to promote regeneration. The remainder of this section will focus on the shared aspects of regeneration, especially between species that display restricted structural restorative regeneration (e.g., arthropods and vertebrates).

Regenerative capacity that is relegated to specific tissues of an organism is known as structural regeneration. Structural regeneration of specific tissues is often further restricted by the developmental stage of the animal. For example, salamanders can only regenerate their eye lens to a certain developmental stage and this stage varies between species of salamander [12]. Mammals often demonstrate a form of this restricted regeneration in which they can regenerate heart and fingertips as neonates but quickly lose this ability as they develop [13, 14]. Holometabolous arthropods, such as *Drosophila*, display regenerative capacity, which is similarly restricted to the larval imaginal discs, the precursors of their external adult tissues [15, 16]. Recently, in both vertebrates and arthropods, the presence of enhancer elements that are specific to or at least preferential toward regeneration over development have been discovered. These tissue regeneration enhancer elements (TREEs) offer the prospect for explaining part of the differences in regenerative capacity that occurs through the development of an animal, as they may become silenced as an animal ages [10, 11]. Overall, the existence of strong regenerative capacity at specific early developmental timepoints supports the idea that regenerative capacity of these organisms could be improved with a better understanding of the molecular underpinnings of regeneration.

Scientists studying regeneration as early as the 18th century noted the similarities between regenerative growth and developmental growth. More recent studies indicate that many of the same signaling pathways that are utilized for developmental growth are turned on during regenerative growth, these include the Wnt/Wingless, Jun N-terminal kinase (JNK), JAK/Stat, and Hippo pathways [15, 16]. However, key differences have been discovered as well. Foremost among these is that regenerative growth takes place adjacent to more mature tissue. One common mechanism to allow for regenerative growth in mature tissues appears to be the formation of what is known as a regeneration blastema. The blastema is a collection of cells, often derived both from local progenitor cell populations as well as dedifferentiated mature cell populations, that proliferates and respecifies to reform the injured tissue. Many of the key studies that provided evidence for the formation of the blastema following injury were performed in salamanders [17]. Since then, blastema formation has been recognized as a key aspect in many lineages that display restricted restorative regeneration, including the mouse digit tip, zebrafish fin, and *Drosophila* imaginal discs. However, key gaps in knowledge remain around the precise signaling pathways that control both formation and sustenance of the blastema throughout the duration of regeneration.

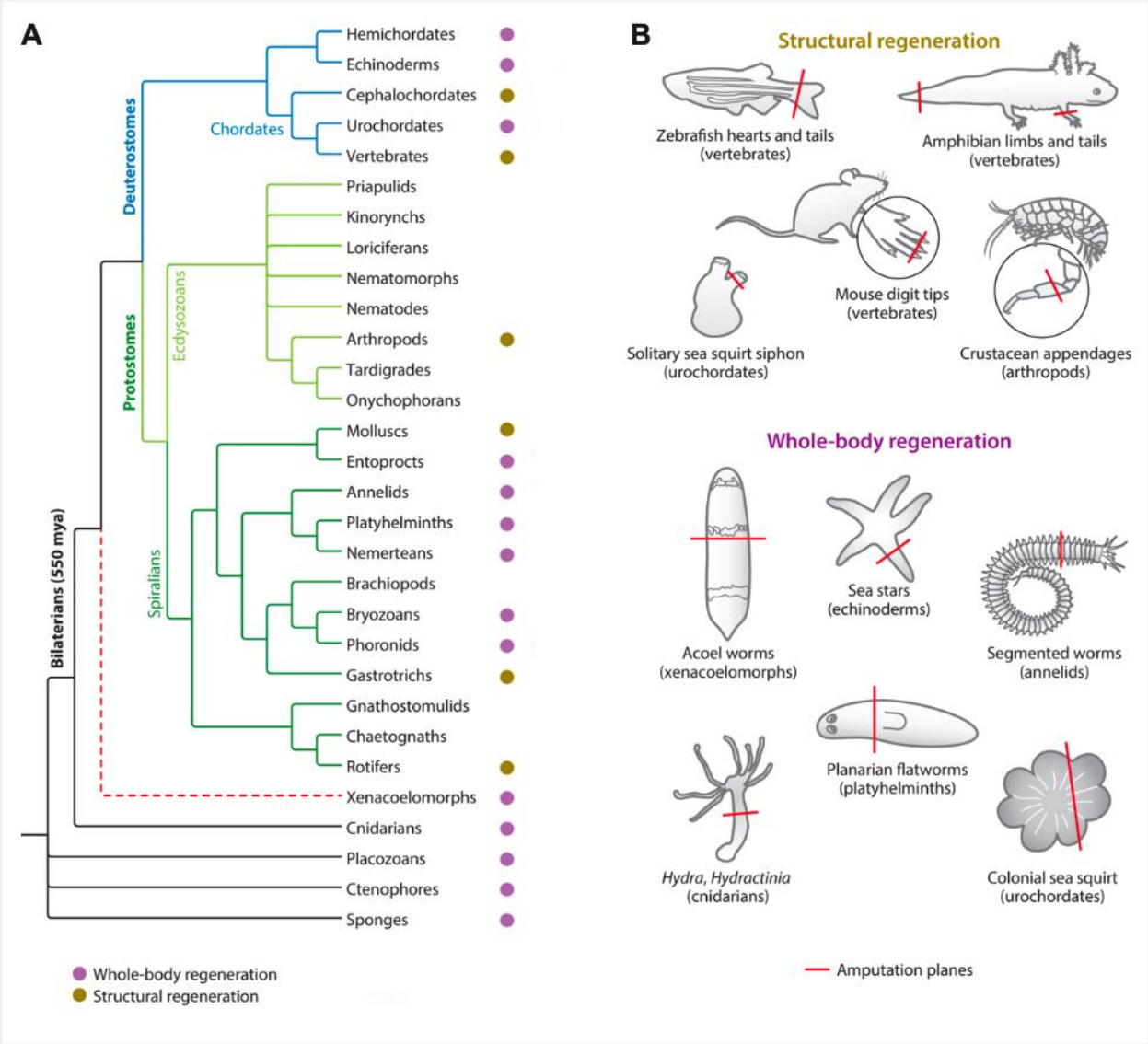

Figure 1.1. Distribution of regenerative capacity. (**A**) Phylogenetic tree indicating the broad conservation of restorative regenerative capacity across lineages. Whole-body regeneration is indicated by purple dots and structural regeneration is indicated by gold dots. (**B**) Examples of animals that display regeneration from the lineages listed in the phylogenetic tree.

Adapted from [9].

1.3 Features of *Drosophila* as a model organism to understand regeneration

1.3.1 The strengths of *Drosophila* as a model organism

The fruit fly *Drosophila melanogaster* became a preeminent model organism in the 20th century. To date, 5 Nobel prizes have been given to research primarily originating in the fruit fly [18]. These Nobel prize winning research programs demonstrate the qualities that make *Drosophila* a powerful model organism. The first of these Nobel prizes was won by Thomas Hunt Morgan in 1933 "for his discoveries concerning the role played by the chromosome in heredity." Morgan's research took advantage of the fruit fly's short life cycle and fecundity coupled with the tractable, visually apparent phenotypes of genetic mutations and the relatively small fly genome (consisting of only 4 chromosomes and with ~13,000 protein coding genes) to track the linkage of genes along chromosomes. The next fly Nobel prize was given in 1946 for Hermann Joseph Muller's "discovery of the production of mutations by means of X-ray irradiation." With the advent of technologies such as RNA interference (RNAi) and clustered regularly interspaced short palindromic repeats (CRISPR), X-ray irradiation is no longer the favored method of genetic manipulation in fruit flies; however, fruit flies continue to be one of the fastest and best model organisms for adapting new genetic manipulation technologies. The final three Nobel prizes given to fruit fly research 1995, 2011, and 2017 all make use of the qualities described earlier: fast generation, small genome, and ease of genetic manipulation. In addition, they took advantage of the remarkably highly conserved nature of core genetic pathways to uncover the key components that control early embryonic development, innate immunity, and circadian rhythms respectively. These same features lend themselves to the study of regeneration: the speed of growth (regeneration of appendage precursor tissue takes place in a matter of days rather than the months it takes vertebrate models to regenerate appendages) and fecundity of flies

make them useful for genetic screens; the ease of genetic manipulation allows us to test the requirements for specific genes in specific tissues at specific times; and the conservation of signaling pathways involved allows us to extrapolate to regeneration in higher eukaryotes.

1.3.2 Regenerative capacity of *Drosophila*

Drosophila display restorative regeneration that is restricted both to specific tissues and time points in development. To understand the interplay between regenerative capacity and development, we first need to familiarize ourselves with the *Drosophila* life cycle. *Drosophila* are holometabolous insects: they progress from embryo, through three larval stages (i.e., 1st through 3rd instars), into pupa, and finally into their imago (i.e., mature adult) form (**Fig. 1.2**). Like other holometabolous insects, *Drosophila* only display restorative regeneration of larval imaginal discs. The imaginal discs are larval organs comprised of two layers of epithelial cells separated by a lumen that metamorphose into the external structures of the mature adult (**Fig. 1.2**). The regenerative capacity of the imaginal discs remains high throughout most the larval stages before declining at the end of the 3rd and final larval instar. Regeneration has been observed for the eye, wing, genital, leg, and haltere imaginal discs [15]. However, the majority of recent regeneration studies, including the research presented here, have been performed in the wing disc due to the wealth of patterning information available and the ease of using the adult wing as a phenotypic readout for the extent of regeneration. The key features of imaginal disc regeneration will be covered more fully in the next section.

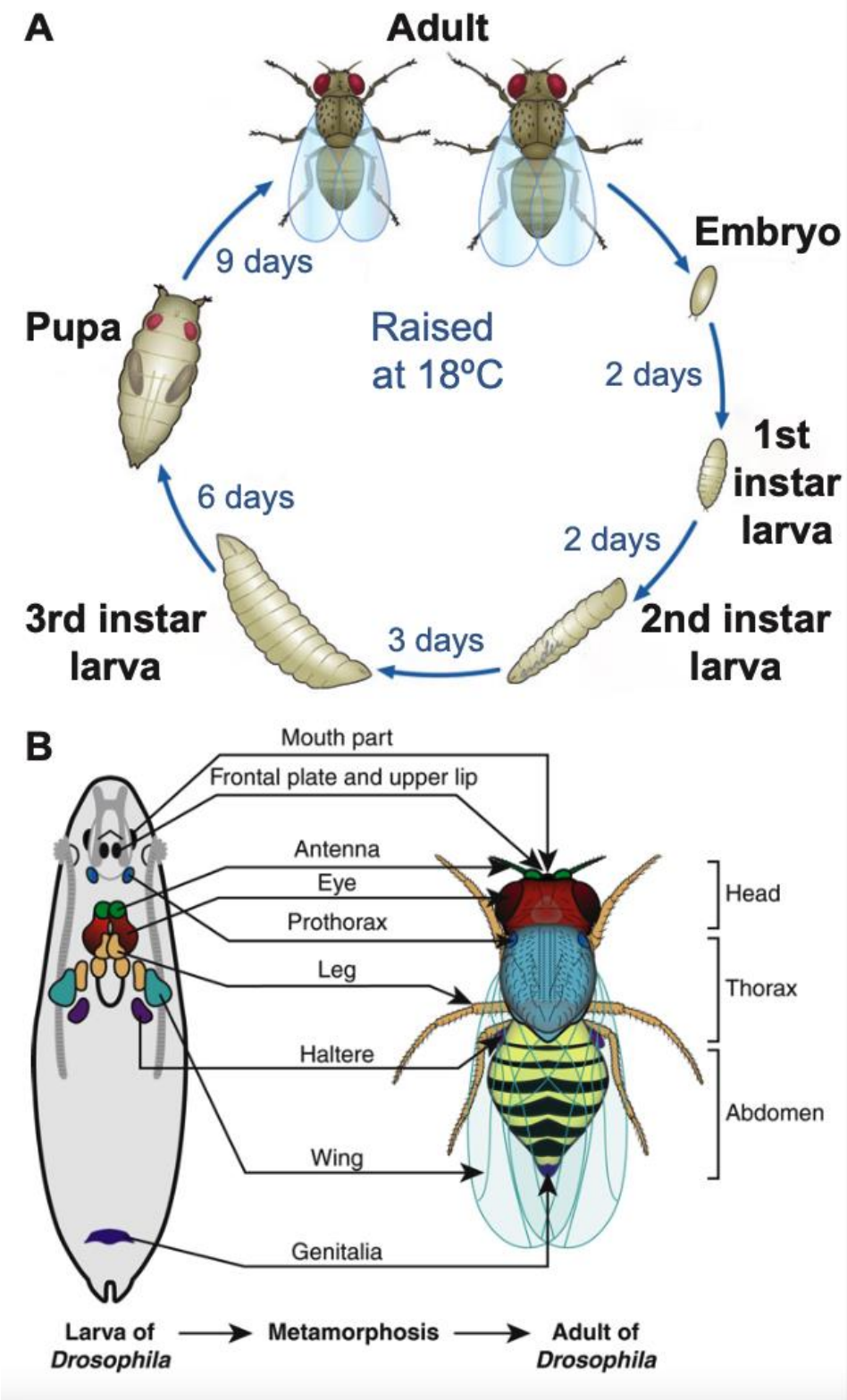

Figure 1.2. *Drosophila* lifecycle and imaginal discs. (**A**) A representation of the *Drosophila* lifecycle. Approximate durations for each stage are listed for *Drosophila* reared at 18°C, which is

the temperature used for the regeneration experiments presented in chapter 2. (**B**) A depiction of the location of the imaginal discs in the *Drosophila* larvae and the external structures of the adult they become through metamorphosis.

Adapted from [19, 20]

1.3.3 Imaginal wing disc development and patterning

The primordia of the imaginal discs can first be observed in the early embryo by their distinct cellular morphology. By embryonic stage 14, the discs have separated from each other and the wing discs can be specifically identified by expression of distinct transcription factors [21]. This initial wing disc primordium is estimated to contain only 25-30 cells and little to no cell division occurs until the end of the 1st larval instar. At embryonic stage 14, the wing disc primordia also invaginates to form the distinctive epithelial sac structure of the imaginal discs. As the wing disc develops, the cells on one side of the sack flatten to form a squamous epithelium. This is referred to the peripodial epithelium (PE). These cells will only make up a small fraction of the wing disc, ~5%, but they are necessary for the morphogenetic transformation of the wing disc during metamorphosis and may have further signaling roles during development [21]. The cells on the other side of the disc elongate to form a columnar epithelium. This columnar epithelial side of the disc, which will comprise the majority of the wing disc by the end of the larval stages, is known as the disc proper. The disc proper cells undergo ~10 cell divisions during the 2nd and 3rd larval instars, resulting in a final disc size of ~30,000-40,000 cells densely packed into together to form a wing disc ~40 μm long and 2 μm wide. While local variations in proliferation rates can be detected across the disc proper at specific temporal stages, the development growth rates are largely uniform across the disc.

The wing disc proper is divided into three regions: the notum, hinge, and pouch. Each region of the disc proper will metamorphose into a different external structure of the adult fly. The notum region becomes part of the thorax, the hinge region becomes the hinge between the thorax and the wing, and the pouch region becomes the wing of the adult fly (**Fig. 1.3**). The

specification of these cell fates occurs during the third larval instar, however full differentiation of these cells does not occur until metamorphosis.

Studies of the signaling pathways and morphogen gradients required for the wing disc regions to achieve their proper specification have greatly enhanced our understanding of tissue compartmentalization and patterning [21]. A full examination of these pathways is beyond the scope of this dissertation; however, the Wingless (Wg) and Decapentaplegic (DPP) morphogen gradients offer an illustrative demonstration of how wing disc patterning is accomplished. Wg and DPP are respectively produced along the dorsal-ventral and anterior-posterior compartment boundaries between the regions of the disc and then spread from these compartment boundaries to form perpendicular gradients across the wing disc proper (**Fig 1.3**). These concentration gradients, combined with the patterns of other morphogen gradients and transcription factors, assign cells their proper specification by driving expression of transcription factors (e.g., Vestigial (Vg), Rotund (Rn), Nubbin (Nub)) [21].

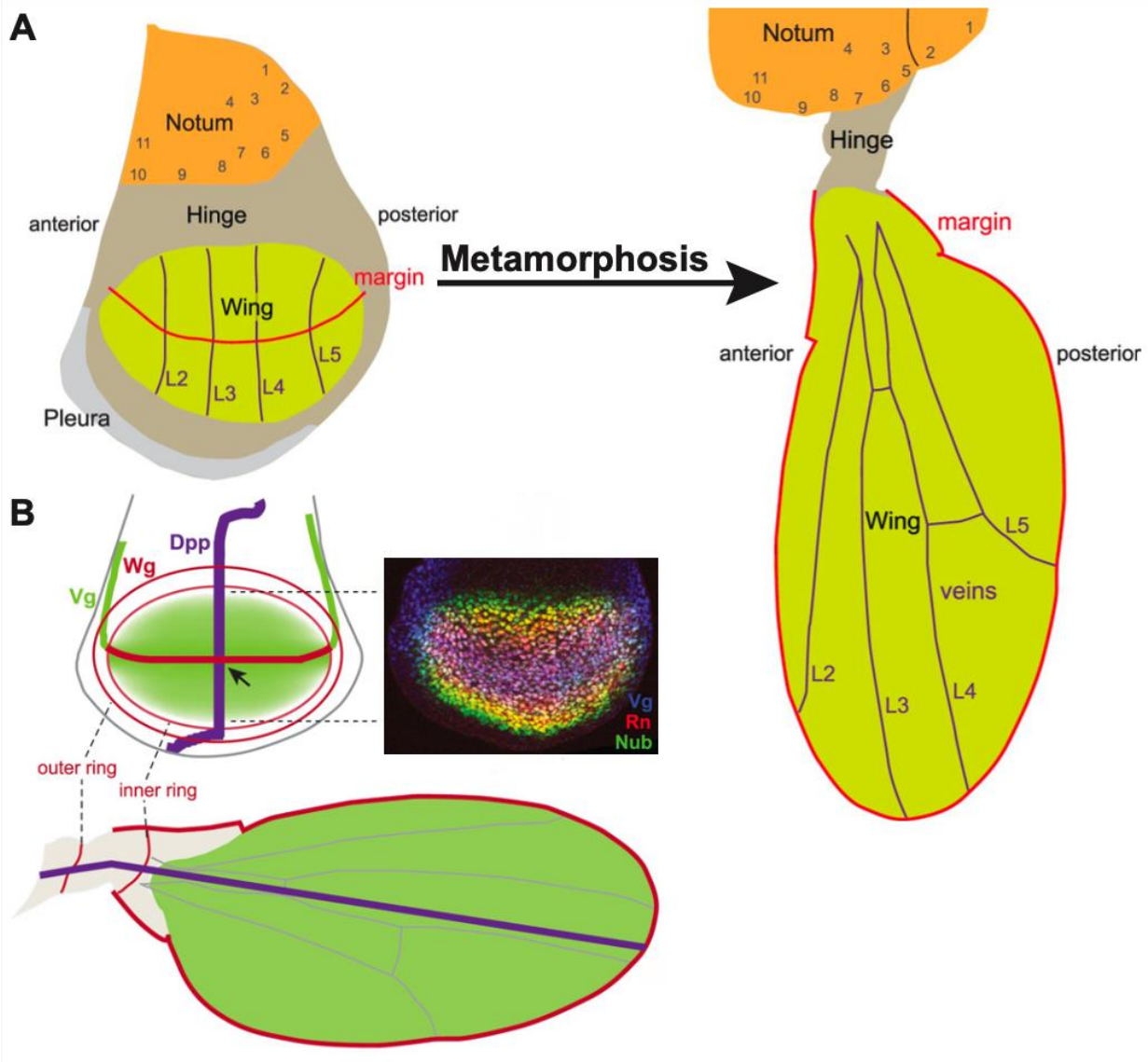

Figure 1.3. The regions and patterning of the imaginal wing disc. (**A**) An illustration of the regions of the imaginal wing disc. The regions specified in the wing disc as the notum, hinge, and wing pouch become the adult fly upper thorax, wing hinge, and wing. (**B**) A depiction of the compartment boundaries at which the morphogens Wg and Dpp are produced as well as the expression pattern of the transcription factor Vg. Inset is a confocal microscopy image of Vg, Rn, and Nub protein staining in the imaginal disc. Of note, it is the rn promoter which is used to direct tissue injury in the genetic ablation system used in chapter 2 of this dissertation.

Adapted from [21]

1.4 *Drosophila* imaginal wing disc regeneration

1.4.1 Injury models

Initial studies of wing disc regeneration were performed by dissecting out discs and physically fracturing them before implanting the injured discs back into either the larval or adult female abdomen [15]. These original studies were born of the desire to fate map the imaginal discs. By fracturing the discs and implanting them back into late 3rd instar larvae, researchers could allow the larvae to undergo metamorphosis and then look in the adult abdomen to see which portions of the adult structure emerged. Interestingly, these experiments also demonstrated the regenerative capacity of imaginal discs. Researchers discovered that fractured discs implanted into late 3rd instar larvae do not regenerate, but discs implanted into early 3rd instar larvae or adult abdomens are capable of regeneration without differentiation. Later experiments using these methods discovered several key aspects of wing disc regeneration which will be further explored in this section. These include localized cell proliferation (resembling the blastema formed during salamander limb regeneration), loss of cell fate specification, and organismal level responses [15, 16].

More recently, a targeted genetic ablation system has been developed to allow for specific injury of the wing disc pouch for a specified duration. This system takes advantage of the Gal4/UAS-system derived from yeast to drive expression of pro-apoptotic genes specifically in the wing disc pouch [22, 23]. In this system, the wing disc pouch specific promoter *rn* is used to drive expression of a pro-apoptotic gene, either *reaper* (*rpr*) or *eiger* (*egr*). Further control over the timing and duration of injury is gained by employing the temperature-sensitive (ts) repressor Gal80^{ts} [22, 24] (**Fig. 1.4**). These genetic ablation systems, abbreviated as *rn^{ts}>rpr* and *rn^{ts}>egr* respectively, allow for reproducible injury of large numbers of animals at the same time.

Combining the rn^{ts}>*rpr* and rn^{ts}>*egr* systems with *UAS* driven RNAi lines has proven to be an effective approach to identify factors required for larval disc regeneration by measuring their effects on adult wing size [25-29]. This allows researchers to take advantage of the full power of the *Drosophila* toolkit to identify regulators of regeneration and study the molecular mechanism they employ to promote regeneration.

The research presented in the following chapters used both *rpr* and *egr* driven cell death. Overexpression of either gene leads to apoptosis; however, the pathways through which they act are different and may lead to differences in the regenerative response [22, 30]. The rn^{ts}>*rpr* system drives apoptosis by directly binding to and inhibiting Death-associated inhibitor of apoptosis 1 (dIAP1) [31]. In contrast, the rn^{ts}>*egr* induces injury through activation of the JNK pathway, which eventually activates the apoptosis pathway [32]. This leads to a swifter injury time course in the rn^{ts}>*rpr* system, requiring only a 20 hour temperature shift to kill ~95% of wing pouch cells, whereas the rn^{ts}>*egr* system requires a 40 hour temperature shift to kill approximately the same percentage of pouch cells [22]. Since JNK pathway activation has been shown to be required for proper wing disc regeneration, it has also been hypothesized that the rn^{ts}>*egr* system primes regeneration regulators that are activated by the JNK signaling pathway [22]. Thus, comparison of regenerating discs injured with these two systems may allow for identification of pathways that are influenced by JNK signal priming.

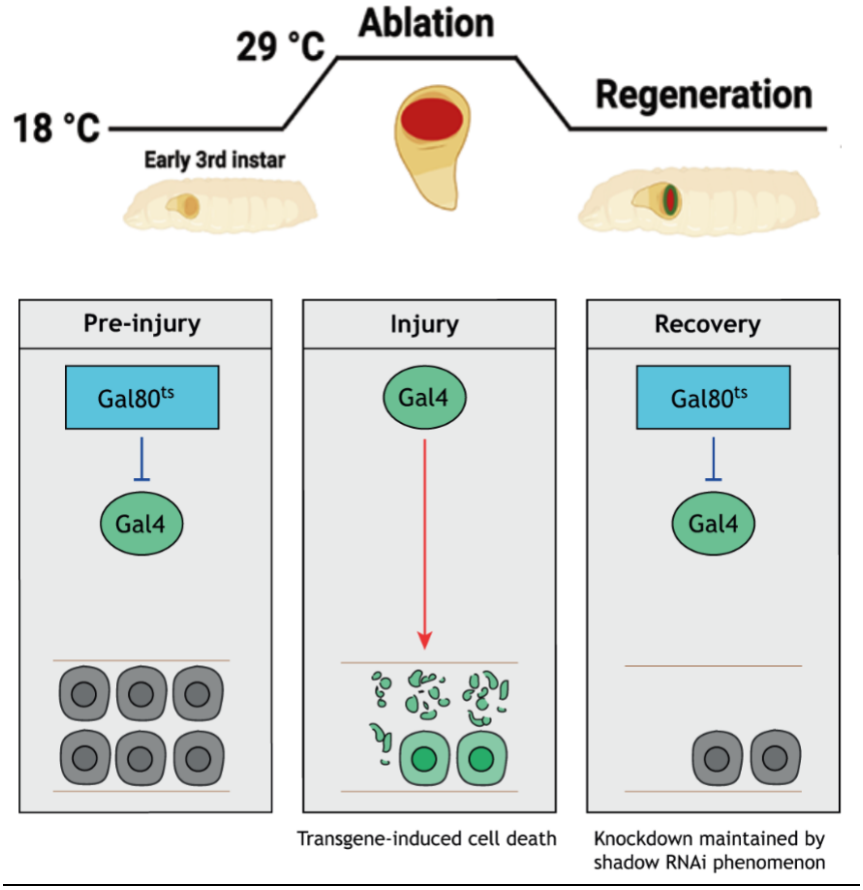

Figure 1.4. Genetic ablation of the system in the imaginal wing disc. Schematic of the genetic ablation system used to injure imaginal wing discs in *Drosophila* larvae. The Gal4/*UAS* system is used to drive expression of a pro-apoptotic signal under the control of a temperature-sensitive version of the Gal80 repressor. This allows for reproducible *in vivo* injury of large numbers of imaginal wing discs simultaneously as well as the co-expression of RNAi depletion of putative regeneration regulators.

Adapted from [16] and (Terry et al., 2023 submitted).

1.4.2 Wing disc regeneration blastema

Injury to the wing disc, whether by physical fragmentation or genetically induced ablation, results in localized cell proliferation that restores the injured tissue. A localized zone of de-differentiated, proliferating cells is a well-conserved aspect of restorative regeneration in animal systems ranging from simple invertebrates to mammals and is referred to as the regeneration blastema. This section will describe what is known about the cellular composition and key signaling pathways of the blastema.

Lineage-tracing experiments indicate that the wing disc blastema forms from a combination of surviving wing pouch cells and fate-switched inner hinge cells [22, 33-37]. The fate-switching of inner hinge cells is possible due to localized, injury-induced loss of cell fate gene expression. For example, the normal stripe of Vg at the dorsal-ventral boundary of the wing disc pouch is lost immediately following injury; before eventually being re-established ~48 hours into regeneration [22]. Recent single-cell RNA-sequencing (scRNA-seq) experiments comparing uninjured discs to genetically ablated discs 24 hours following injury further indicate that the blastema is composed of at least two distinct cellular states, distinguished as inner Blastema1 cells and outer Blastema2 cells (**Fig. 1.5**) [38]. Cells can transition through these states and into more mature cell fates allowing for restoration of the damaged tissue. Loss of cell fate gene expression and transformation into a less specified state that can then proliferate to restore the injured tissue is also a hallmark of the salamander limb blastema and likely a well-conserved feature of regeneration of complex tissues [22, 39-41]. In *Drosophila*, regeneration of the wing pouch continues for ~72 hrs following injury and proliferation requires a localized increased level of signaling of several pathways involved in developmental proliferation, including the highly conserved JNK, JAK-STAT, ROS, Wnt/Wg, and Hippo pathways (**Fig. 1.5**) [15, 16, 37].

However, these are likely not the only pathways involved in initiating and sustaining the blastemal environment throughout regeneration; indeed, research has implicated other mechanisms and pathways, such as the transcription factor Ets21C, in maintenance of expression of key blastemal genes [38]. Gaining a better understanding of the interplay between the signaling pathways that promote blastema proliferation and sustain the blastema state remains a crucial research objective of the regeneration field.

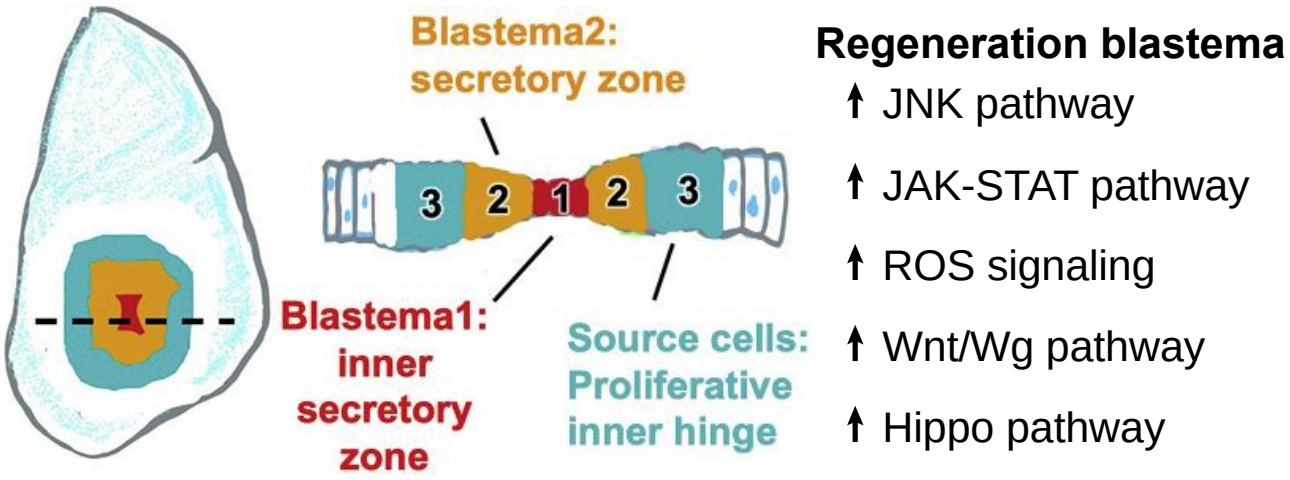

Figure 1.5. The imaginal wing disc regeneration blastema. Schematic of the larval imaginal wing disc with the inner (Blastema1) and outer (Blastema2) zone cells identified by scRNA-seq indicated. Major conserved pathways between imaginal wing disc regeneration and vertebrate regeneration are listed.

Adapted from [38].

1.4.3 Organismal aspects of regeneration

Injury to larval imaginal discs produces systemic developmental delay in addition to the local changes described in the previous section. This delay extends the 3rd instar larval phase and is thought to allow time to regenerate before the loss of regenerative capacity that occurs in late 3rd instar animals [16, 37, 42]. Developmental delay is achieved through the inhibition of the large systemic pulse of steroid hormone Ec synthesis in the prothoracic gland that drives maturation. This Ec synthesis inhibition involves signaling from the injured disc that involves the secreted peptide Ilp8, retinoids, and the Jak/STAT ligand Upd3 [43-49]. Since Ec signaling is required for developmental growth as well as maturation, the inhibition of Ec synthesis in the prothoracic gland also induces coordinated growth reduction throughout the rest of the animal. The details of Ec signaling are further explored in the next section.

1.5 Ecdysteroid synthesis and signaling

1.5.1 Ecdysone signaling overview

Ecdysone steroid hormone signaling is the central regulator for driving the developmental transitions in the superphylum Ecdysozoa. The Ec molecule gets its name from the Ancient Greek *ecdysis*, meaning 'shedding' or 'sloughing off,' as occurs during molting. In *Drosophila,* the prohormone Ec is synthesized in the prothoracic gland (PG), which is located adjacent to the larval brain, and released into the hemolymph before being converted into active 20-hydroxyecdysone (20E) in peripheral tissues. Active 20E can then bind the EcR to regulate transcription. Large pulses of Ec synthesis in the PG drive the major developmental transitions in *Drosophila* by activating transcriptional cascades of 'early' and 'late' response genes (**Fig 1.6**) [50-52]. These transcriptional cascades are further modified in a tissue- and stage-dependent

manner by the presence or absence of competence factors to orchestrate systemic responses to Ec pulses [52]. Subsequent research has revealed additional roles for Ec outside of these major systemic pulses in both promoting larval imaginal disc proliferation and supporting adult fertility. This section will describe the ecdysone hormone synthesis pathway, the mechanism of EcR signaling, and the role of ecdysone signaling in promoting local growth of larval tissues.

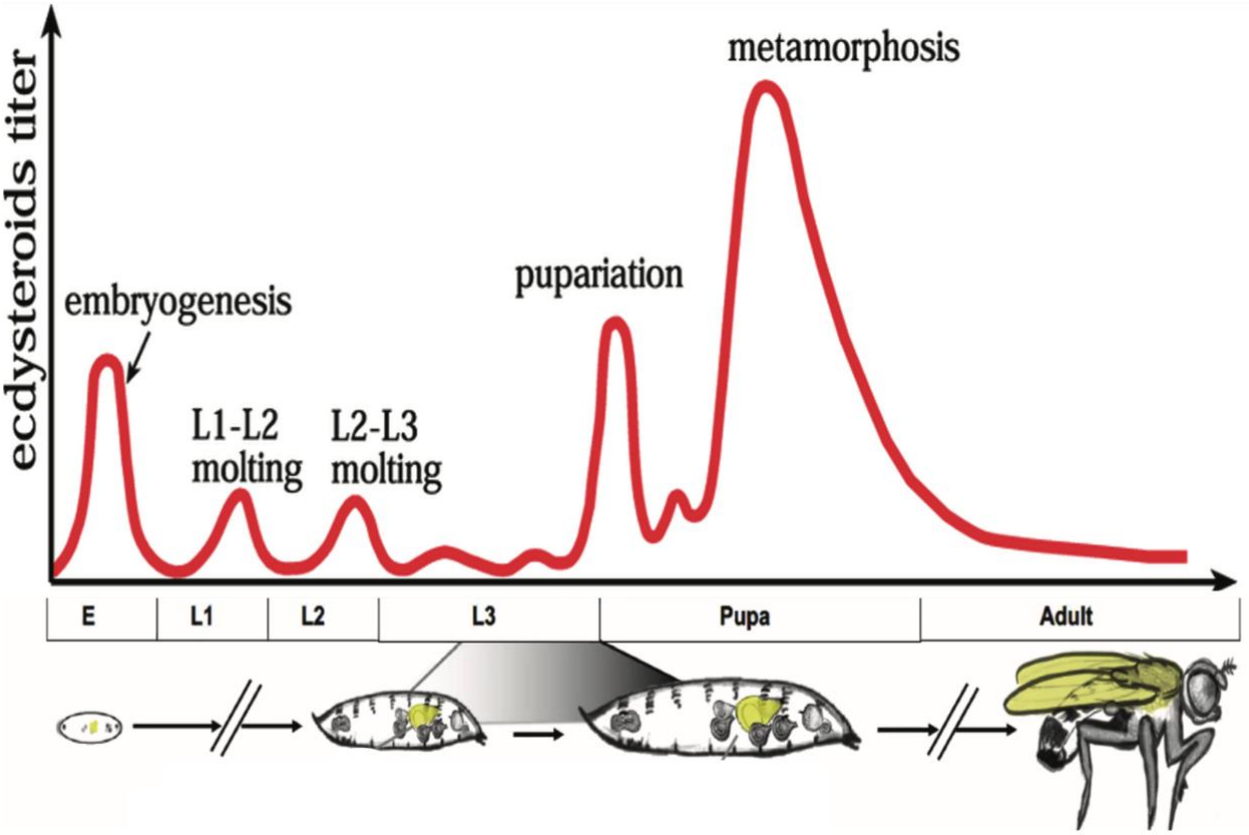

Figure 1.6. Systemic pulses of Ec drive the major developmental transitions in *Drosophila*.

Schematic indicating the level of ecdysteroid titers during *Drosophila* development. Large pulses of Ec are synthesized by the larval PG to drive the major developmental transitions.

Adapted from [51, 53].

1.5.2 Ecdysone synthesis: The Halloween gene family

Ecdysone is synthesized from dietary sterols by a series of biosynthetic enzymes. These steps first involve the conversion of dietary sterols into 5β-ketodiol in a series of steps that are still referred to as the Black Box reactions due to their nature not being fully elucidated (**Fig. 1.7**) [54, 55]. Subsequently 5β-ketodiol is converted to 20E by the sequential addition of OH groups catalyzed by the cytochrome P450 enzymes phantom (phm), disembodied (dib), shadow (sad), and shade (shd). These ecdysone biosynthesis enzymes are classically referred to as the Halloween genes due to the "empty, and ghost-like" embryonic cuticles formed by loss-of-function mutants [55, 56]. Active 20E can then be inactivated through 26-hydroxylation catalyzed by the cytochrome P450 enzyme Cyp18a1 and subsequent conversion into 20-hydroxecdysonoic acid [57].

Halloween gene expression and ecdysone synthesis primarily occurs in the prothoracic gland (PG) located adjacent to the larval brain. The PG has been shown to respond to inputs from neurons that innervate the PG, as well as inputs from circulating hormones, to regulate ecdysone synthesis. These inputs allow the PG to integrate external cues, such as nutritional status or tissue damage, to correctly time the pulses of ecdysone synthesis that drive developmental transitions [55]. For example, following wing disc injury, secreted signals from the injured wing disc circulate through the hemolymph and bind cognate receptors in the larval brain and PG to coordinate the inhibition of ecdysone synthesis, allowing time for regeneration to occur (**Fig. 1.7**) [43-49].

Similar to mammalian steroids, ecdysone steroid hormone signaling is also required for fertility in *Drosophila*. However, unlike the systemic production of ecdysone in the PG required for developmental transitions, the ecdysone required for fertility is produced locally in the

follicular epithelium of the female egg chamber. This local ecdysone synthesis requires the Halloween genes *phm, sad,* and *shd*. Mutations that effect these ecdysone biosynthesis genes impair border cell migration and ovulation [58].

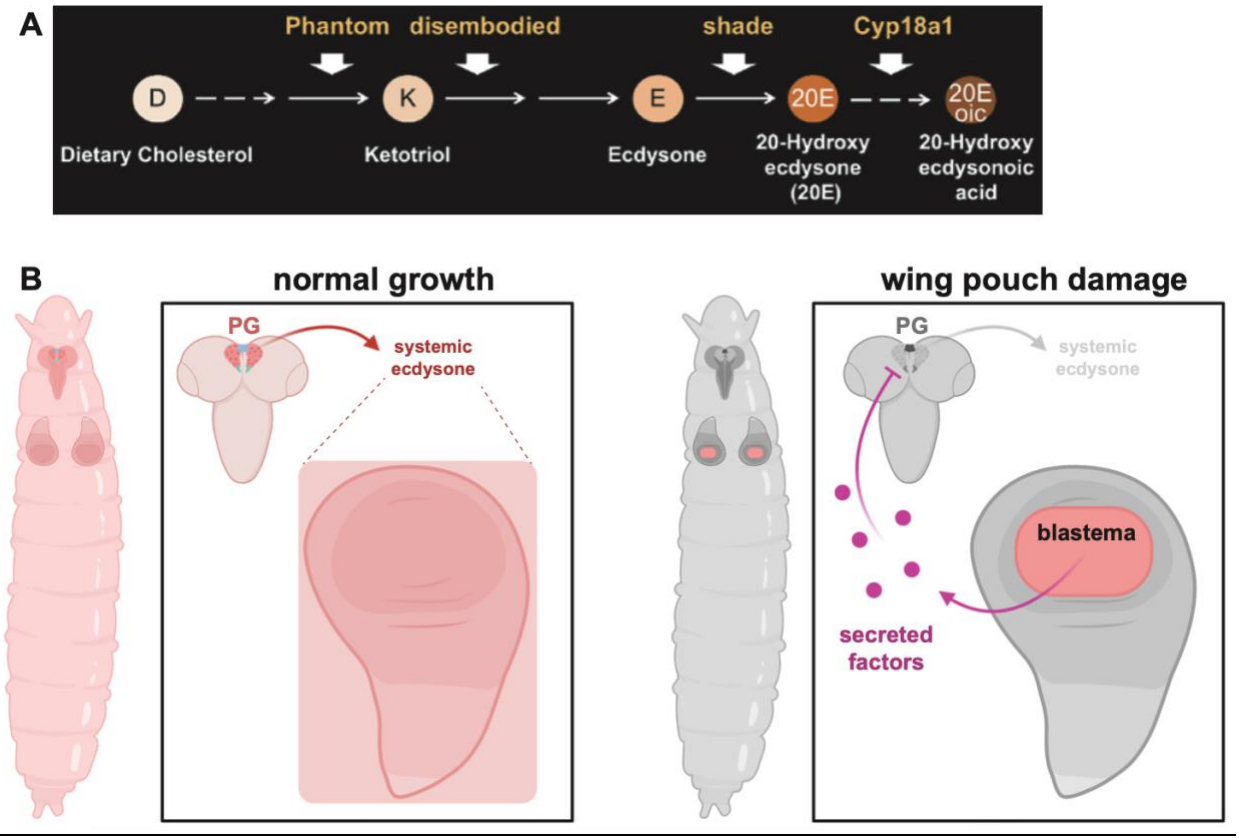

Figure 1.7. Ecdysone synthesis and injury-induced synthesis inhibition. (**A**) Simplified schematic of the ecdysone biosynthesis and catabolic pathways. The key cytochrome P450 enzymes (known as the Halloween genes) and ecdysteroid intermediates are indicated. (**B**) During normal larval growth ecdysone (Ec) is synthesized in the prothoracic gland (PG) and secreted into the hemolymph to bath the animal and promote imaginal disc growth. Following wing disc injury, secreted factors from the injury tissue (e.g., Ilp8, upd3, retinoids) signal to the PG gland and inhibit systemic Ec. This acts to stall development and allow time for the injury tissue to recover.

Adapted from (Terry et al., 2023 submitted)

1.5.3 Ecdysone receptor structure and mechanism

The Ecdysone receptor (EcR) is a member of the nuclear receptor superfamily. Nuclear receptors share a common domain structure composed of a highly conserved DNA-binding domain (DBD) connected via a flexible hinge region to a less conserved ligand binding domain (LBD) (**Fig. 1.8**). The LBD also contains the principal dimerization interface for nuclear receptor proteins as well as binding sites for co-activators and co-repressors [59]. The nuclear receptor superfamily is further divided into four subtypes based on their localization prior to ligand binding (cytosolic vs nuclear), dimerization partners (homodimeric vs heterodimeric), and the orientation of the paired hormone response element (HRE) DNA sequences which they bind (direct vs inverted vs half-site) [60]. The EcR is a member of the Type 2 nuclear hormone receptors, it resides in the nucleus as a heterodimer prior to ligand binding and binds to direct HRE repeats [59].

The EcR forms a heterodimer with its binding partner, Ultraspiracle (USP). The EcR/USP heterodimer localizes to the nucleus and binds DNA sequences referred to as ecdysone response elements (EcREs) in the presence or absence of its active ligand, 20E [59, 61, 62]. In the absence of 20E, the EcR can bind co-repressors (e.g., SMRT-related ecdysone receptor-interacting protein (Smr)) and has been shown to repress genes that are required for developmental transitions [62, 63]. Presence of 20E functions to activate transcription via a combination of de-repression and direct activation through the recruitment of transcriptional co-activators [62] (**Fig. 1.8**). These transcriptional co-activators of the EcR notably include Taiman (Tai), the homolog of the vertebrate family of p160 Steroid Receptor Coactivators (SRC-1,2,3) [64, 65]. Overall, EcR/USP is structurally homologous to human LXR/RXR and FXR/RXR nuclear receptors but has the most functional similarity to the mammalian sex steroid hormone receptors (e.g., estrogen and androgen receptors) that drive developmental transitions, tissue growth, and fertility [59, 62].

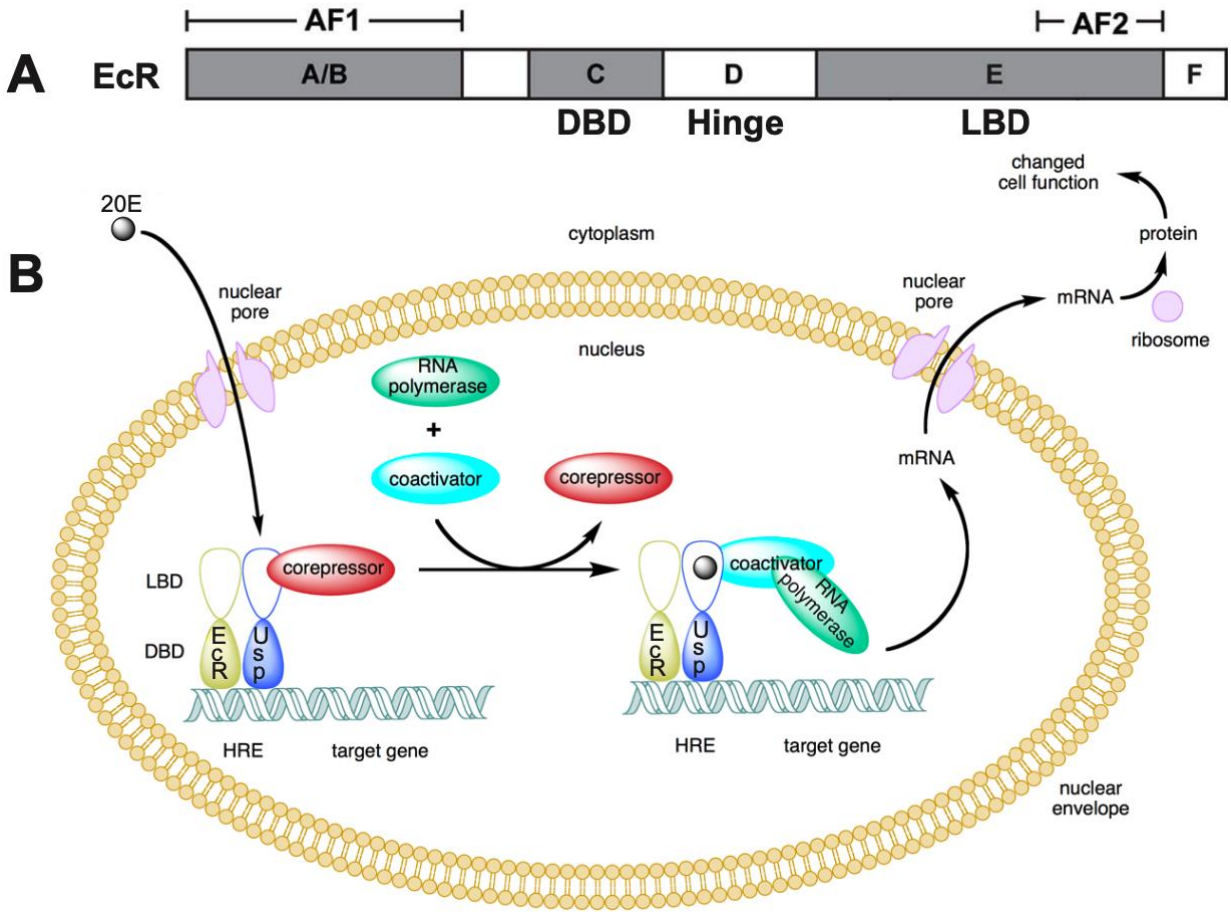

Figure 1.8. EcR Structure and signaling pathway. (**A**) The EcR is a nuclear receptor composed of the standard A/B, C (DNA binding domain), D (hinge region), E (Ligand binding domain), and F (C-terminal) domains. The A/B domain and E domain contain activation function 1 (AF1) and activation function 2 (AF2). (**B**) As a type 2 nuclear receptor, the EcR forms a heterodimeric complex with its binding partner USP and can bind DNA at its hormone response element sequences in the absence of ligand. When not bound by ligand, the EcR/USP heterodimer is bound by corepressors. Upon binding to its cognate ligand, 20E, EcR/USP release corepressors and can recruit coactivators to promote transcription of target genes.

Adapted from (Wardwell-Ozgo et al., 2022 submitted) and [66].

1.5.4 Ecdysone as a promoter of growth

Ecdysone has been most well studied for its roles in driving developmental transitions. However, research in recent years has discovered key requirements for low level 20E concentrations in promoting growth of imaginal discs [67, 68]. Multiple independent studies showed that ablation of the prothoracic gland (i.e., the systemic source of Ec) not only prevents developmental transitions but also greatly reduces growth rates of imaginal discs [68, 69]. This requirement for Ec signaling was further explored in cultured wing discs, where researchers demonstrated the physiologically low levels of active 20E present during the majority 3rd larval instar (i.e., ~4% of peak levels) are required to sustain proliferation and proper expression of wing patterning genes in cultured discs [67]. Subsequent *in vivo* research indicates that 20E may be responsible for 'gating' the wing disc growth in response to the major wing disc morphogens Wg and Dpp [70]. The requirement for 20E to promote imaginal disc proliferation also provides a mechanism for coordinated growth reduction of all other tissues following an injury or growth perturbation of a single imaginal disc: the systemic reduction in 20E levels stalls growth of other discs across the entire animal and opens a temporal window during which proliferation within regeneration blastema allows the injured disc to 'catch up' [43, 48, 71-73]. However, a key unknown in this model is how the regeneration blastema can drive regrowth in the absence of 20E, which is otherwise required for imaginal disc growth.

1.6 Scope of dissertation

The following chapter of this dissertation examines the local role of Ec signaling in imaginal wing disc regeneration. As discussed earlier in this introductory section, injury to the imaginal wing disc causes a systemic suppression of ecdysone synthesis from the PG that leads to a delay in developmental maturation, as well as coordinated growth reduction of other imaginal discs. Yet this appears to present a paradox that led to the experiments presented in Chapter 2: if systemic 20E levels are reduced following injury and 20E is normally required for imaginal disc growth, how does the injured imaginal wing disc grow in the absence of systemic 20E? One possibility is that, in the context of injury, regenerating imaginal discs can synthesize their own 20E in a fashion similar to the local 20E synthesis that has been shown to be required for *Drosophila* border cell migration and ovulation. I performed a screen using RNAi lines locally targeting 20E biosynthesis and turnover during injury in the imaginal wing disc. These experiments indicate that locally inhibiting 20E biosynthesis inhibits regeneration, while locally inhibiting 20E turnover promotes regeneration. We trace these effects to a requirement for local 20E in promoting injury induced EcR activity, developmental delay, and coordinated growth reduction. We go on to find that the requirement for local 20E may be due to a requirement for 20E signaling to sustain expression of expression of mRNAs encoding the regeneration regulators Ets21C and Upd3, suggesting a key, local transcriptional role for EcR/USP within the blastema.

Chapter 3 of this dissertation details experiments I performed using two new tools recently created by postdoctoral fellows in the Moberg lab. The first is a *UAS*-transgene created to encode the fragment of the *EcR* coding sequence containing the LBD, which I will refer to as the *UAS-EcR*^{LBD} transgene. This new tool can be expressed in a tissue- and developmental time-

specific manner to disrupt LBD-dependent interactions between endogenous EcR and its coregulators. I tested the functionality of the *UAS-EcR^{LBD}* transgene as a tool for investigating EcR signaling by examining the effect of *UAS-EcR^{LBD}* expression EcR signaling regulated process of salivary glue protein production, secretion, and expectoration. These experiments demonstrate the differences between using the *UAS-EcR^{LBD}* transgene, which specifically disrupts LBD-dependent interactions between endogenous EcR and its coregulators, and previous methods EcR disruption. The second tool is an endogenous CRISPR allele of the EcR co-activator Tai. This CRISPR allele contains mutations that convert the two PPxY motifs in Tai to PPxA's. The Tai PPxY motifs have previously be shown by our lab to be required for physical interaction with Yorkie (Yki), the transcriptional coactivator of the Hippo pathway, and are required for Yki-driven overgrowth of imaginal wing discs [74]. Here, I test the effect on imaginal wing disc regeneration and injury-induced developmental delay of heterozygosity for the CRISPR *tai^{PPxA}* mutant.

Finally, in Chapter 4, I discuss how the research presented in this dissertation fits into the fields of regeneration and ecdysone steroid hormone signaling as well as the limitations of these experiments and the implications for future research. Overall, these studies highlight the requirement for a local increase of active 20E over the regenerating blastema. This mechanism is a novel addition to our understanding of how local signals create a privileged transcriptional environment to support tissue repair.

Chapter 2. Local ecdysone synthesis in a wounded epithelium sustains developmental delay and promotes regeneration in *Drosophila*

This chapter was adapted from the following paper in review:

Douglas Terry, Colby Schweibenz, and Kenneth Moberg. *Local ecdysone synthesis in a wounded epithelium sustains developmental delay and promotes regeneration in Drosophila*. Development. (*in review*).

2.1 Abstract

Regenerative ability often declines as animals mature past embryonic and juvenile stages, suggesting a dependence on redirecting pathways that promote developmental growth toward localized, regenerative growth. Signals that distinguish local regenerative growth from developmental growth remain poorly defined. Intriguingly, systemic decline in growth hormone ecdysone (Ec) is required for regeneration in a *Drosophila* model of epithelial injury while rising Ec coincides with loss of regenerative potential in late-stage larvae. Examining local Ec dynamics more closely, we find that while transcriptional activity of the Ec-receptor (EcR) drops in uninjured regions, it surprisingly rises in the blastema. In parallel, blastema depletion of *Halloween* genes encoding Ec biosynthesis enzymes blocks EcR activity and impairs regeneration but has no effect on uninjured wings. We trace these local Ec/EcR roles to injury-induced pupation delay and find that expression of key regeneration regulators *Ets21C* and *upd3* are responsive to excess Ec produced at the site of injury. Collectively, these data indicate that injury induces a local source of Ec within the wing blastema that sustains a unique transcriptional signature necessary for tissue repair.

2.2 Introduction

Regeneration of damaged or lost tissue often involves cells around the injury site reentering the cell cycle to generate new cells that repopulate the missing region. In some cases, this injury-induced proliferation is driven by local stem cells, while in others it involves partial dedifferentiation and proliferation of uninjured cells. The capacity for regeneration varies widely between different species and is often lost as animals mature past embryonic or juvenile stages, suggesting a dependence on redirecting developmental signals away from patterned growth and toward localized, regenerative growth. The resultant pause in growth of uninjured tissues avoids developmental asynchrony by allowing the injured tissue to repair before rejoining a normal developmental trajectory.

In *Drosophila melanogaster* larvae, genetically induced death of epithelial cells in the wing pouch results in proliferation of surviving cells (the regeneration 'blastema') that replaces lost cells and restores final adult wing size. This regenerative proliferation is accompanied by concentration of the pro-proliferative morphogen Wingless (Wg) within the blastema and its depletion elsewhere in the tissue, and by blastema-specific expression of genes such as *Ets21C*, which sustains a regenerative program that includes secreted factors *upd3* and *Ilp8* (*Drosophila* insulin-like peptide-8) that signal through their receptors to enhance blastema proliferation and suppress production of the steroid hormone ecdysone (Ec) in the prothoracic gland [22, 38, 44-48]. The systemic drop in levels of circulating Ec, which promotes major developmental transitions through its receptor EcR [50, 75-78], halts organism growth and delays the larval-to-pupal transition to allow blastema proliferation to fully replace missing cells. As a result of these mechanisms, mutations that impair key elements of the regenerative program reduce wing regeneration efficiency, due to either insufficient proliferation in the blastema or failure to induce developmental delay.

Loss of regeneration competence in a commonly used *Drosophila* wing injury system occurring at late 3rd instar and parallels the rapid rise in Ec levels that peaks at the larval-to-pupal transition [22, 30]. This apparently inverse relationship has led to the hypothesis that high level Ec inhibits wing regeneration [29]. However, low level Ec is present throughout regeneration-competent larval stages, and Ec promotes cell proliferation, tissue growth, and even a regeneration response in certain species [4, 67, 68, 79]. Moreover, low level Ec and its receptor, EcR, are required for activity of the pro-growth growth Dpp and Wg pathways, which promote normal and regenerative wing disc growth [22, 70, 79].

The apparent paradox that injury results in systemic depletion of the Ec larval growth hormone at a time when the wing blastema is undergoing regenerative growth led us to assess Ec roles and activity within injured wing discs. We find that as EcR activity drops elsewhere in the disc, it rises in the blastema region. In parallel, local depletion of Ec biosynthesis enzymes has little effect on normal wing growth but consistently impairs regrowth of injured wings, while local depletion of the Ec catabolic enzyme Cyp18a1 enhances regeneration. We trace these effects to a requirement for Ec in the injury-induced developmental delay and find that expression of mRNAs encoding the key regeneration regulators Ets21C and Upd3 expression are responsive to Ec produced locally at the site of injury. These findings suggest that 20E promotes elements of the regenerative transcriptional program in the wing disc, and that the blastema is a unique signaling environment that generates its own Ec to sustain a tissue repair program.

2.3 Results

Local knockdown of 20E synthesis/degradation genes modulates wing disc regeneration

An established genetic ablation system was used to assay the local effect of Ec during regeneration of *Drosophila* imaginal wing discs [22]. This system uses a combination of *rotund (rn)-GAL4* and *tubulin-GAL80^{ts}* to express a pro-apoptotic gene (*UAS-reaper*) in a spatially and temporally restricted manner (hereafter *rn^{ts}>rpr*) (**Fig. 2.1A**). Briefly, flies were raised at 18°C for 7 days. They were then transferred, as early 3rd instar larvae, to a 30°C water bath for 20 hours to induce ablation of ~95% of wing pouch cells before being shifted back down to 18°C to allow for recovery and regeneration [22]. Flies with same genetic background and subject to the same temperature shifts, but lacking *UAS-rpr*, are used as uninjured ('mock injured' or *rn^{ts}>+*) controls. Combining the *rn^{ts}>rpr* system with *UAS* driven RNAi lines has proven to be an effective approach to identify factors required for larval disc regeneration by their effects on adult wing size [25-29].

We adapted this local knockdown (KD) approach to assess roles of enzymes that synthesize Ec or its bioactive derivative 20-hydroxyecdysone (20E) using a series of RNAi lines targeting *Halloween* genes (i.e., the cytochrome P450 enzymes that catalyze steps in Ec/20E biosynthesis) as well as the 20E degradation enzyme Cyp18a1 [56, 57, 80-82] (**Fig. 2.1B**). Binning adult wings into approximate "percent regenerated" groups reveals that local KD of the 20E biosynthesis genes *phantom* (*phm*), *disembodied* (*dib*), or *shade* (*shd*) in *rn^{ts}>rpr* animals each significantly impair wing regeneration relative to *rn^{ts}>rpr* alone, while KD of the *Cyp18a1* enzyme that inactivates 20E [57] has the inverse effect of enhancing regeneration (**Fig. 2.1C**). As reported previously [26, 44-47, 72, 83, 84], these data confirm that local KD of the injury-induced peptide hormone *Ilp8* impairs regeneration and show that local wing disc pouch KD of *torso* (*tor*), a receptor that promotes *Halloween* gene expression in the prothoracic gland (PG) [52, 85], has no effect on wing regeneration.

We chose to verify these semi-quantitative findings for phm^{KD} and $Cyp18a1^{KD}$. Wing area was quantified for phm^{KD} and $Cyp18a1^{KD}$ in rn^{ts}>+ mock uninjured controls and rn^{ts}>*rpr* driven injury (**Fig. 2.1D** and **Fig. 2.2A-B**). Surprisingly, KD of either *phm* or *Cyp18a1* in rn^{ts}>+ controls is sufficient to induce a slight but significant reduction in adult wing size (**Fig. 2.2A-B**). This slight reduction in wing size of uninjured discs may indicate a growth interference caused by activating RNAi machinery in the developing wing disc pouch or a requirement for local regulation of 20E levels even in uninjured wing discs. The data for each genotype shown in **Fig.2.1D** is normalized back to its respective rn^{ts}>+ control to account for these growth differences in uninjured discs. This analysis confirms that local phm^{KD} in the blastema impairs regeneration, while $Cypa18a1^{KD}$ enhances it.

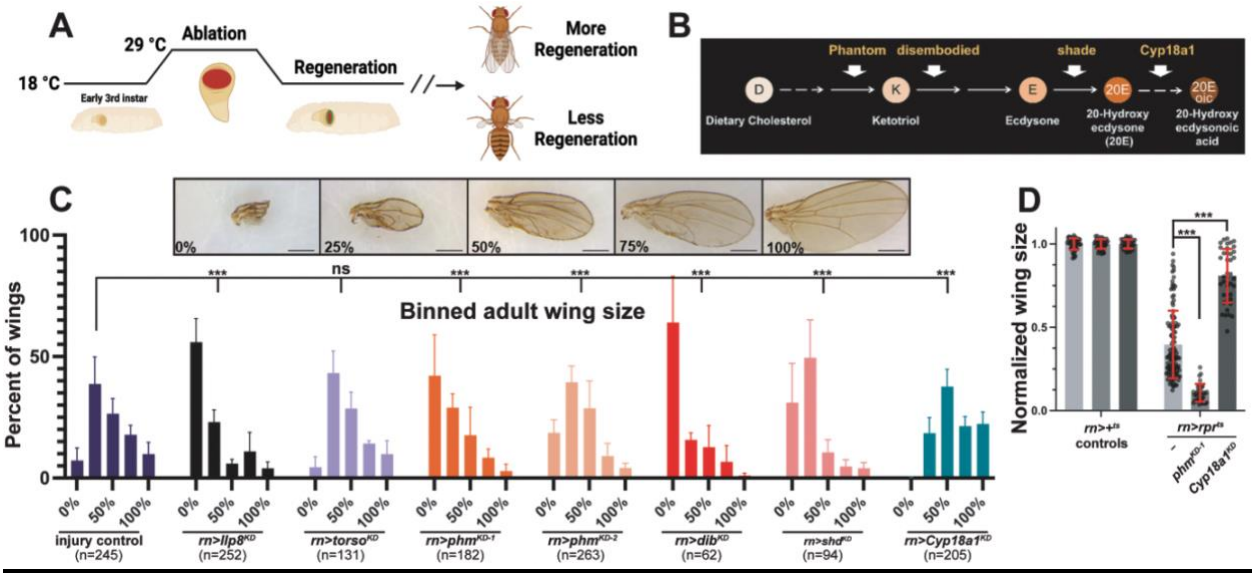

Figure 2.1. Local 20E synthesis gene knockdown impairs regeneration **(A)** Schematic of genetic ablation system. **(B)** Simplified schematic of ecdysteroidogenesis. **(C)** Examples of adult wing bin sizes after regeneration from 0-100%, and distribution of female adult wing sizes binned into five categories from 0-100% regenerated following injury and regeneration (n=number of wings and is cumulative for three experiments). Scale bars: 0.5 mm. Statistical significance determined by the χ^2 test. ***p<0.0001, ****p<0.00001, n.s.=not significant. Error bars are s.e.m. **(D)** Normalized wing area of mock ablated controls (rn>rpr^{ts}) used for normalization of their respective injured (rn>rpr^{ts}) counterparts. Wing area for injured (rn>rpr^{ts}) control w^{1118} (n=174), injured phm^{KD-1} (n=100), injured *Cyp18a1*^{KD} (n=78) fly wings normalized back to mock ablated of the same genotype. Samples are female wings only. n is cumulative of at least two experiments. Student's t-test. ***p<0.0001, n.s.=not significant. Error bars are s.d.

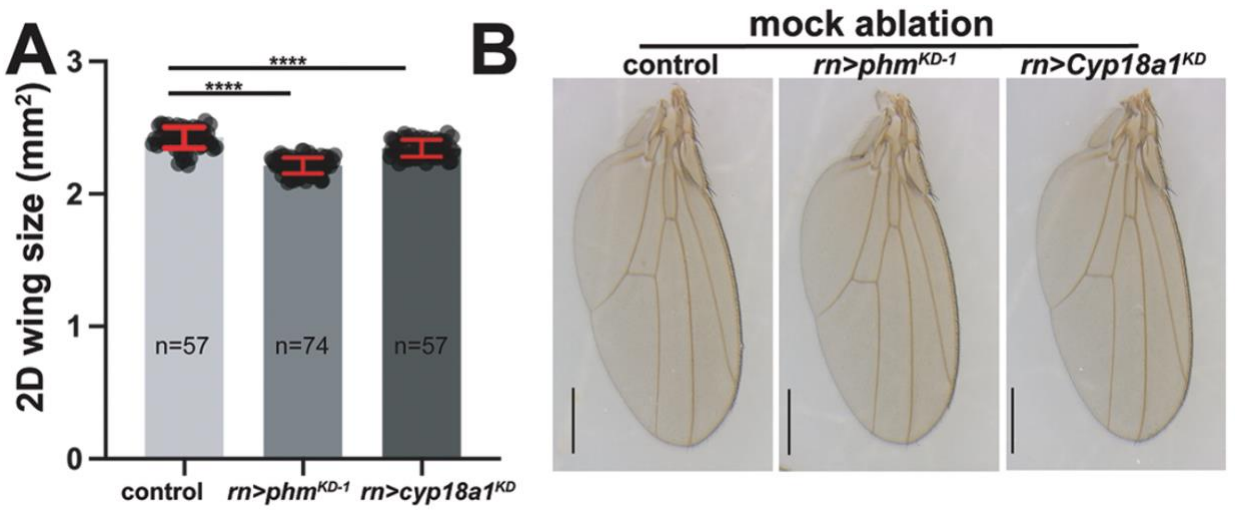

Figure 2.2. Local 20E knockdown in mock ablation. **(A)** Wing area for mock ablated control w^{1118}, *rn>phm*$^{KD-1}$, and *rn>Cyp18a1*^{KD}. Samples are female wings only. n is cumulative of three experiments. Student's t-test. **(B)** Representative mock ablated wings. Scale bars are 0.5 mm.

EcR is transcriptionally active in regenerating wing discs

In *Drosophila melanogaster* larvae, genetically induced death of epithelial cells in the wing pouch results in localized proliferation of surviving pouch cells and cells derived from the inner hinge region (which together form the regeneration 'blastema') to replace lost cells and restores final adult wing size [22, 35, 38, 41, 86, 87]. This regenerative proliferation is accompanied by concentration of pro-proliferative signals (e.g., the morphogen Wg) within the blastema and depletion of these signals elsewhere in the wing disc, and by blastema-specific expression of genes such as the stress-inducible transcription factor *Ets21C*, which sustains a regenerative program that includes expression of secreted factors *upd3* and *Ilp8* (*Drosophila* insulin-like peptide-8) [22, 38, 44-48].

Given the evidence of a requirement for 20E biosynthesis enzymes in the regenerating wing disc, we checked for evidence of 20E-regulated EcR activity in the regenerating blastema using a reporter comprised of seven ecdysone-response elements (EcREs) upstream of *GFP* (*7xEcRE-GFP*) [88]. In the absence of rn^{ts}>*rpr* injury, *7xEcRE-GFP* expression increases between early third instar (L3) and mid-L3, with regions of elevated EcR activity detected in the hinge, pouch, and sensory organ precursors (SOPs) along the dorsoventral boundary (**Fig. 2.3A-B**). Consistent with the PG as the major source of Ec in uninjured larvae, these *7xEcRE-GFP* patterns are unaffected by local phm^{KD} in the pouch (**Fig. 2.3C-D**).

We next examined effects of rn^{ts}>*rpr* injury on *7xEcRE-GFP* expression. During the first 24hrs of regeneration (R0-R24), EcR activity drops to almost undetectable levels in wild-type and phm^{KD} injured discs (**Fig. 2.3E-H**). By R32, approximately midway through the regeneration process, *7xEcRE-GFP* expression begins to differ between wild-type and phm^{KD} injured discs. In wild-type injured discs at R32, *7xEcRE-GFP* expression rises in scattered, individual cells located

along the inner dorsal and ventral hinges and within the pouch proper (**Fig. 2.3I**) and by R48 becomes stronger along the ventral hinge and an area extending from the inner dorsal hinge toward the notum (**Fig. 2.3J**). Cells derived from the inner hinge region have been shown by several labs to be recruited into the regeneration blastema and contribute to the wing regenerate [22, 35, 38]. As discs near the end of regeneration at R72, which corresponds to the systemic rise in Ec signaling that promotes the developmental transition to the pupal stage, *7xEcRE-GFP* rises throughout the wing disc (**Fig. 2.3M**). This begins to resemble the developmental pattern of EcR activity in uninjured mid- and late-L3 wing discs (e.g., **Fig. 2.3B**). Importantly, local phm^{KD} in the blastema decreases EcR activity in mid-regeneration R32 and R48 discs (**Fig. 2.3K-L,O**), indicating a local requirement for 20E biosynthesis to induce EcR activity in the regenerating blastema. However, local phm^{KD} has little effect on EcR activity in R72 discs (**Fig. 2.3M-N**). This suggests a shift away from reliance on local *phm* as the systemic late-L3 rise in Ec levels takes precedence over local regeneration-specific Ec synthesis.

Use of the pro-apoptotic TNF receptor ligand *eiger* as an alternative to *rpr* (*rn>egr*^{ts}) also strongly induces *7xEcRE-GFP* expression, as well as expression of the similar *7xEcRE-lacZ* reporter, in the pouch while decreasing expression of these reporters in the hinge and notum, indicating that regional shifts in EcR activity are a feature of the *egr* injury system as well (**Fig. 2.4A-D**). The difference in timing of these shifts in the *rpr* and *egr* backgrounds may reflect the longer injury duration of the *rn>egr*^{ts} system or Egr-induction of JNK activity in regenerative program [22, 30, 32, 89]. Notably, *7xEcRE-GFP* expressing cells in *rn>egr*^{ts} injured discs overlap the Wg-positive blastema, contain nuclear EcR protein, and lie adjacent to cells positive for the apoptotic marker cleaved Dcp-1 (**Fig. 2.4E-G**). *rn>egr* regeneration is also impaired by local shd^{KD} or a shd^{2} null allele (**Fig. 2.4H**) For subsequent experiments, we continued to use the

rn>rpr^{ts} system due to its direct apoptotic mechanism and less crumpled morphology of *rn>rpr*^{ts} injured discs [22, 30, 32, 89, 90].

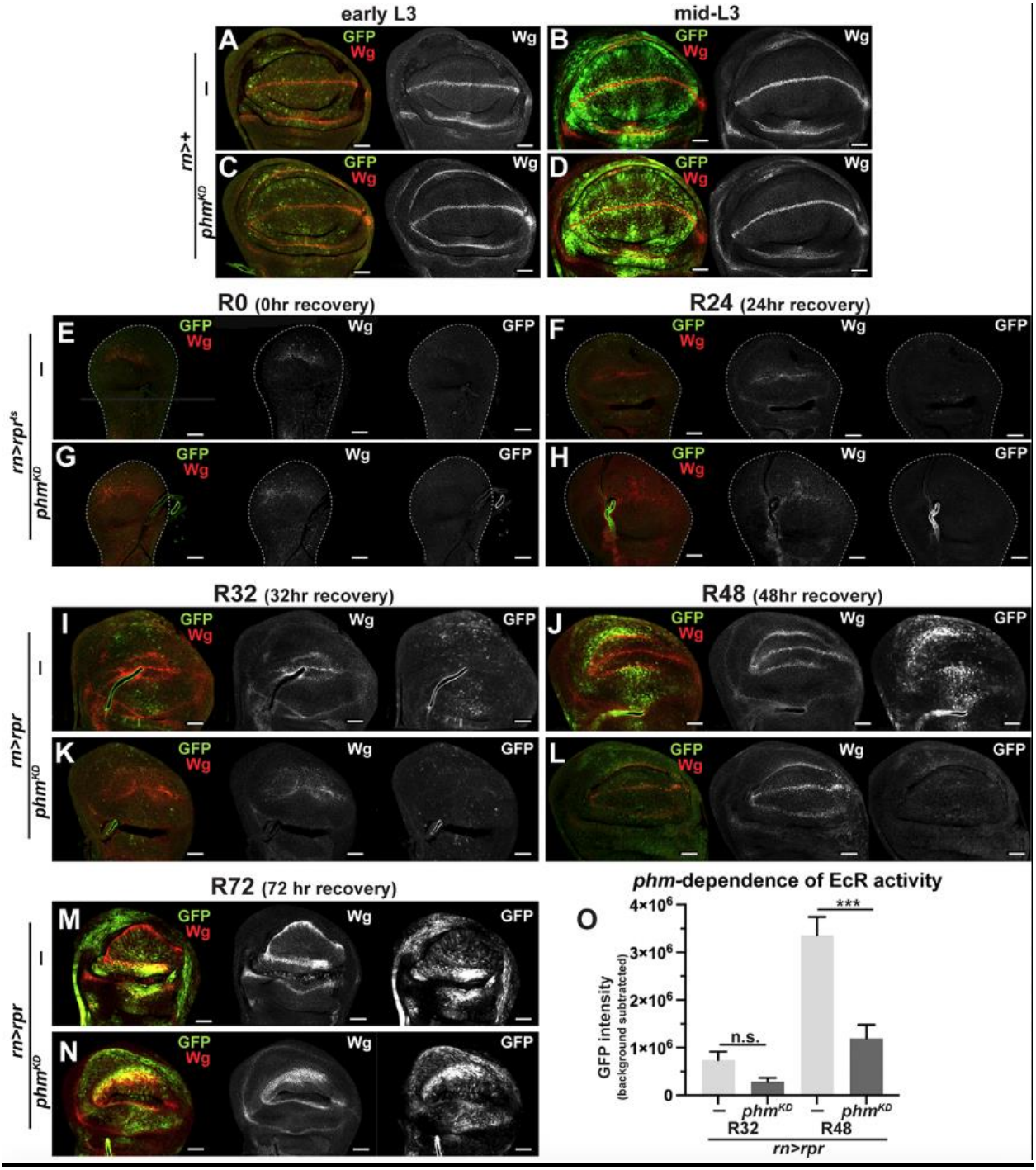

Figure 2.3. EcR is active in the blastema mid-regeneration. (A-D) Representative images of EcRE-GFP expression patterns in mock ablated control w^{1118} and phm^{KD-2} discs at early and late 3rd instar larval timepoints. **(E-N)** Representative images from a time-course of EcRE-GFP expression in regenerating wing discs at different time points into recovery following $rn>rpr^{ts}$

injury. **(O)** Quantification of EcRE-GFP expression in regenerating discs. R32: *7xEcRE-GFP* n=21 and phm^{KD-2}; *7xEcRE-GFP* n=16. R48: *7xEcRE-GFP* n=18 and phm^{KD-2}; *7xEcRE-GFP* n=20. n is cumulative of three experiments. Student t-test. ***p=0.0007, n.s.=not significant. GFP=EcRE-GFP is green and Wg=wingless is red antibody. All scale bars are 50 μm.

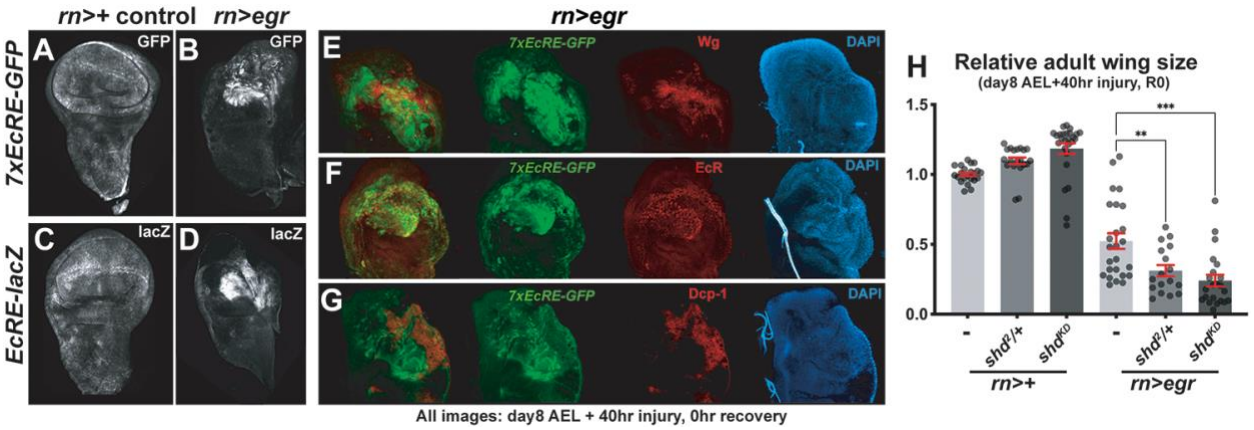

Figure 2.4. Ecdysone receptor activity reporter expression in *rn>eiger* ablation. (A-B) Representative images of 7xEcRE-GFP reporter expression in *rn>egr* discs. **(C-D)** Representative images of 7xEcRE-lacZ expression in *rn>egr*. **(E)** Representative images of 7xEcRE-GFP reporter expression in *rn>egr* discs co-stained with Wg=wingless antibody. **(F)** Representative images of 7xEcRE-GFP reporter expression in *rn>egr* discs co-stained with EcR=Ecdysone receptor antibody. **(G)** Representative images of 7xEcRE-GFP reporter expression in *rn>egr* discs co-stained with Dcp1 antibody. All animals were temperature shifted at Day 8 for 40 hours and dissected at 0 hours recovery. **(H)** Wing area of mock ablated controls (*rn>egr^{ts}*) normalized to OreR mock ablated controls. Wing area for injured (*rn>egrr^{ts}*) OreR (n=25), injured *shd^{2}*/+ (n=17), injured *shd^{KD-2}* (n=22) fly wings normalized back to mock ablated of the same genotype. Samples are female wings only. Student's t-test. **p<0.001, ***p<0.0001. Error bars are s.e.m.. All scale bars are 50 μm.

Injury-induced pupariation delay is regulated by *phm* and *Cyp18a1* in the wing pouch

Previous studies have found that an important aspect of the imaginal wing disc regenerative program is damaged-induced developmental delay. Wing discs lose their capacity to regenerate in late L3 larvae [30], however when early L3 wing discs are growth perturbed (e.g., genetic ablation, tumor growth, growth inhibition by ribosomal gene KD, etc.), larvae experience developmental delay that allows time for regeneration to occur. This developmental delay is caused by suppression of systemic production of the steroid hormone Ec in the PG that is required to drive developmental progression through activation of its cognate receptor EcR [50, 75-78].

Key advances have been made in determining the pathways that allow growth perturbed discs to signal to the PG to reduce systemic ecdysone production and cause developmental delay. The Unpaired family cytokine *upd3* and the insulin-like peptide *Ilp8* are secreted from the growth perturbed disc into the hemolymph. These signaling molecules then travel through the hemolymph to the larval brain and PG to signal through their respective receptors to suppress systemic production of Ec by reducing expression of 20E biosynthesis genes in the PG [22, 38, 43-48, 91]. The systemic drop in levels of circulating Ec slows developmental progression of the larvae to allow injured wing discs to regrow and equalize their developmental stage with uninjured larval tissues prior to pupation [26, 42, 43, 45, 46, 91].

phm^{KD} or $Cyp18a1^{KD}$ dependent changes in the duration of injury induced developmental delay could theoretically alter regeneration efficiency in $rn>rpr^{ts}$ injured wings. To test this hypothesis, we determined the extent of developmental delay following $rn>rpr^{ts}$ driven injury by measuring the time to pupation for $rn>rpr^{ts}$ injured wing discs in wild-type, $Ilp8^{KD}$, $torso^{KD}$, phm^{KD}, and $Cypa18a1^{KD}$ genetic backgrounds (**Fig. 2.5A-B**). Data were collected as survival curves (**Fig. 2.5A**) but are also presented as median time to pupation graphs for ease of

visualization (**Fig. 2.5B**). As expected, *Ilp8*^{KD} (i.e., KD of one of the key secreted signaling factors known to induce developmental delay) reduces the time to pupation compared to control. Further, as with regeneration efficiency, local imaginal wing disc KD of *torso* (the gene for a receptor that promotes expression of 20E biosynthesis genes in the PG) had no effect on pupation timing compared with injured controls (**Fig. 2.5A-B**). Interestingly, local *phm*^{KD} suppresses injury-induced pupariation delay to a similar extent as *Ilp8*^{KD} positive control, whereas local *Cypa18a1*^{KD} has the opposite effect of enhancing the delay (**Fig. 2.5A-B**). The ability of local 20E synthesis gene KD (*phm*^{KD}) to suppress injury-induced developmental delay and local 20E degradation gene KD (*Cypa18a1*^{KD}) to enhance injury-induced developmental delay strongly suggests that local 20E is critical for proper control of injury-induced developmental delay. We do note that all RNAi lines tested, regardless of target, slightly accelerated pupariation in mock ablated (i.e., no *rpr*) controls (**Fig. 2.6A-B**). This is similar to the slight reduction seen in our mock ablation wing size data (**Fig.2.2A-B)** and could suggest that activating RNAi processing machinery affects entry into pupation.

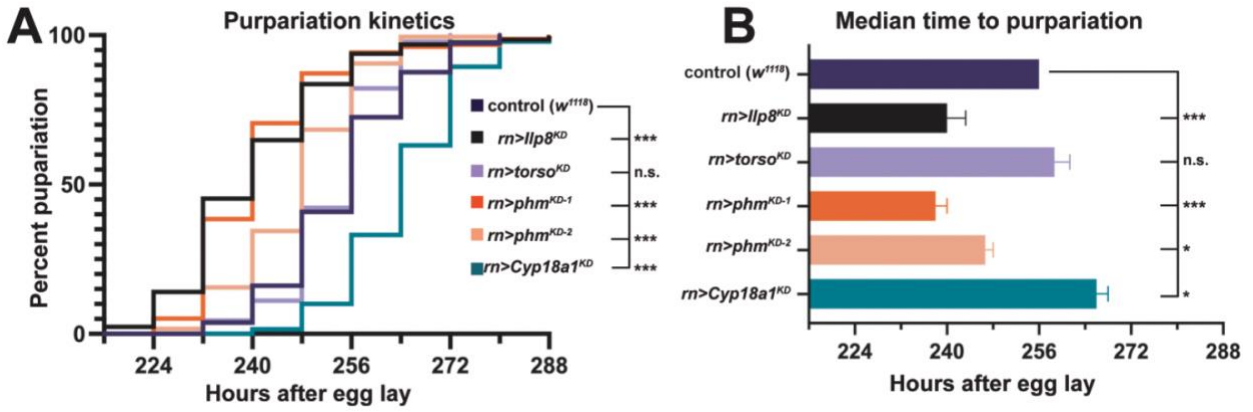

Figure 2.5. Injury induced pupariation delay is dependent on local 20E. (A) Kaplan-Meyer survival curve for pupariation time-points following injury with significance determined by the Log-rank (Mantel-Cox) test. n values are combined for 3 experiments: control w^{1118} n=186, phm^{KD-1} n=156; phm^{KD-2} n=180; $Cyp18a1^{KD}$ n=190; $torso^{KD}$ n=130; $ilp8^{KD}$ n=128. **(B)** Median time to pupariation following injury in the survival curve assays for pupariation time points. One-way Anova with Dunnett's test used to determine statistical significance.

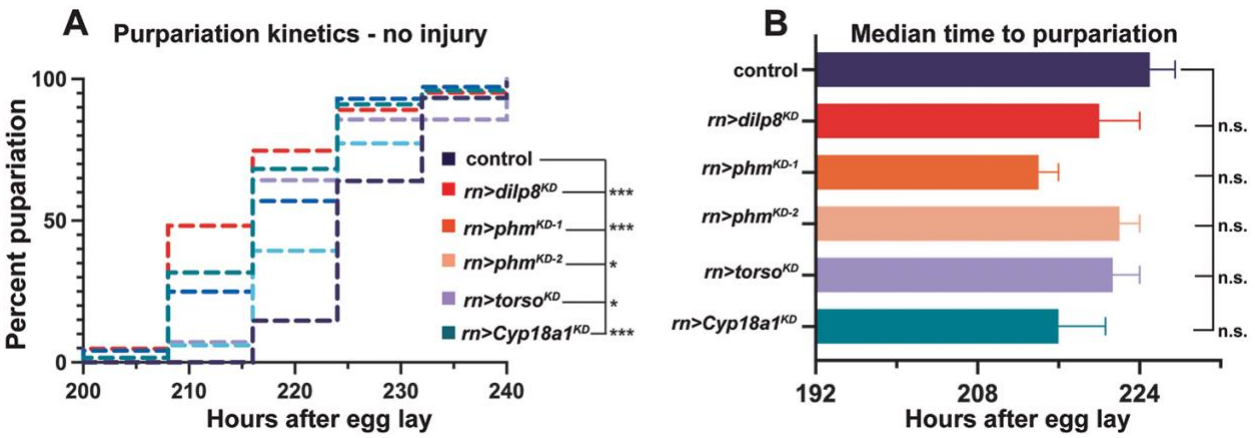

Figure 2.6. Pupariation kinetics of mock ablated animals. (A) Kaplan-Meyer survival curve for pupariation time-points following mock ablation with significance determined by the Log-rank (Mantel-Cox) test. n values are combined for 3 experiments: control w^{1118} n=136, phm^{KD-1} n=158; phm^{KD-2} n=237; $Cyp18a1^{KD}$ n=163; $torso^{KD}$ n=98; $ilp8^{KD}$ n=184. **(B)** Median time to pupariation following mock ablation in the survival curve assays for pupariation time points. One-way Anova with Dunnett's test used to determine statistical significance. ***p<0.0001, *p<0.05, n.s.=not significant.

Coordinated intra-organ growth reduction is local 20E dependent

Given the effect of 20E on disc growth [67, 68, 73, 79, 92], we also sought to test whether local depletion of *phm* or *Cyp18a1* alters cell division rates within the regenerating blastema, focusing on the R48 timepoint when EcR transcriptional activity is most sensitive to local phm^{KD} (see **Fig. 2.3I-J**). In mock ablated discs, intensity of the DNA replication marker EdU is unchanged by local phm^{KD} or $Cyp18a1^{KD}$ (**Fig. 2.7A-C**), which is consistent with data that phm^{KD} or $Cyp18a1^{KD}$ have little effect on wing size in the absence of injury (see **Fig. 2.2A-B**). Notably, we do not detect reduced EdU staining in injured phm^{KD} blastemas relative to injured control blastemas (**Fig. 2.7D-F**), suggesting that the detrimental effect of phm^{KD} on wing regeneration is not due to insufficient cell division within the regenerate. However, in these same phm^{KD} discs we noted a failure of $rn>rpr^{ts}$ injury to reduce EdU incorporation in areas outside the pouch relative to control injured discs, and an upward trend in total EdU signal within the blastema region of $rn>rpr^{ts}$ injured $Cyp18a1^{KD}$ discs (**Fig. 2.7D-G**). The drop in EdU in regions outside the blastema (referred to as coordinated growth reduction) is a well-documented feature of injury-induced growth perturbation and results from inhibition of Ec production in the PG, which systemically slows growth of uninjured imaginal discs [22, 26, 38, 42, 43, 72, 91, 93]. Consistent with a local role for 20E and EcR in this intra-organ feedback mechanism, phm^{KD} and $Cyp18a1^{KD}$ have regional effects on growth -- the blastema of phm^{KD} discs comprises a smaller percentage of the total disc area relative to injured controls, whereas the blastema of $Cyp18a1^{KD}$ discs is enlarged relative to total disc area (**Fig. 2.7H**). Further, phm^{KD} discs are larger than injured controls, and $Cyp18a1^{KD}$ discs are smaller than injured controls at the same time point in recovery (**Fig. 3I**). Overall, these data are consistent with local phm^{KD} impairing both $rn>rpr^{ts}$ developmental delay and intra-organ growth inhibition, and local $Cypa18a1^{KD}$ enhancing both effects.

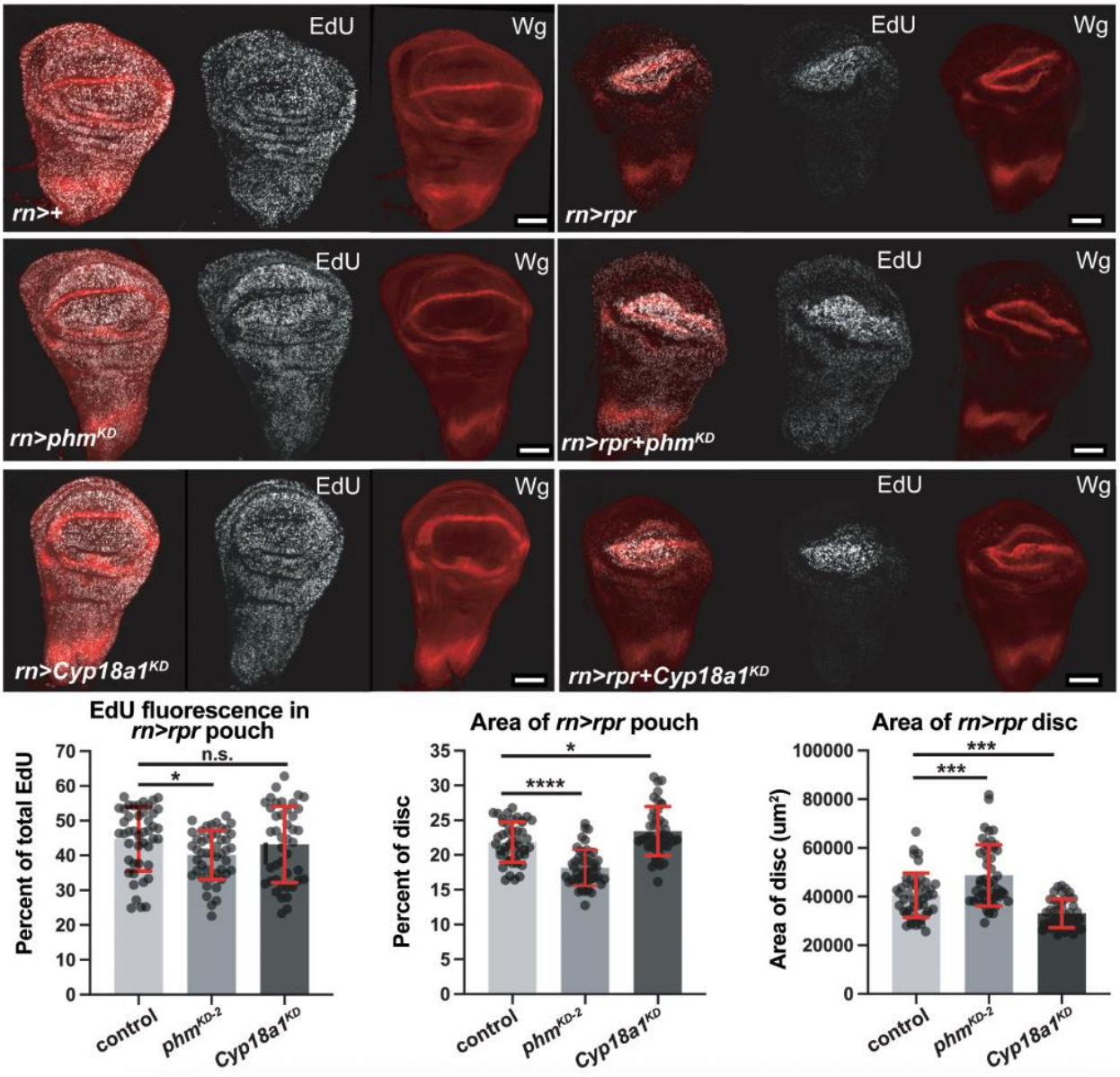

Figure 2.7. Injury induced coordinated intra-organ growth reduction is dependent on local 20E. (A-C) Representative images of EdU incorporation in mock ablated uninjured discs. **(D-F)** Representative images of EdU incorporation in ablated discs at R48. **(G)** Graph depicts the percent of total EdU fluorescence intensity coming from the blastema (blastema intensity/total intensity * 100%) at R48. **(H)** Area of blastema as percent of total disc (area of blastema/area of disc * 100%) at R48. **(I)** Total area of disc. **(G-I)** n values are combined for 3 experiments:

control w^{1118} n=45, phm^{KD-2} n=47; $Cyp18a1^{KD}$ n=43. Significance analyzed using One-way Anova with Dunnett's test. ***$p<0.0003$, *$p<0.05$. All scale bars are 50 μm.

The regeneration genes *Ets21c* and *upd3* are *Cyp18a1*-dependent

To test effects of phm^{KD} and $Cyp18a1^{KD}$ on regeneration regulators, we analyzed expression of candidate genes. Given the effects on injury-induced developmental delay and coordinated growth reduction we see with phm^{KD} and $Cyp18a1^{KD}$, the known injury-induced developmental delay regulator *Ilp8* was a strong candidate. The enhancer trap reporter of *Ilp8* expression, *Ilp8-GFP*, is not induced in either mock ablated control or phm^{KD} wing discs (**Fig. 2.8A-B**). Following injury, *Ilp8-GFP* is strongly induced in both control and phm^{KD} wing discs (**Fig. 2.8C-E)**. Further, *Ilp8* mRNA is induced to equivalent degrees in control injured wing discs and phm^{KD} or $cyp18a1^{KD}$ injured discs (**Fig. 2.8F**). These data suggest that phm^{KD} and $Cyp18a1^{KD}$ effects on developmental delay are not regulated through the expression of *Ilp8*. Based on recent work indicating that Ec signaling can affect the permeability of the epithelial membrane to secreted peptides such as *Ilp8* [94], we also measured the permeability of the epithelial barrier using fluorescein conjugated dextran (FITC-dextran) and found no evidence that local phm^{KD} alters this parameter (**Fig. 2.8G-J)**. We then analyzed two additional elements of the regeneration program: the *Ets21c* transcription factor, which sustains a regeneration specific transcriptional program [38], and the *upd3* cytokine, which is produced and secreted by wing blastema cells [38, 86, 95-97]. While phm^{KD} does not significantly impair induction of *Ets21c* or *upd3* mRNAs by $rn>rpr^{ts}$ injury, induction of both mRNAs is significantly enhanced by $Cyp18a1^{KD}$ (**Fig. 2.8K-L**). *Ets21C* is specifically expressed in the regeneration blastema and controls a regeneration-specific gene regulatory network (GRN) in injured wing discs that sustain the regeneration blastema transcriptional program [38]. The effect of $Cyp18a1^{KD}$ on levels of *Ets21c* and *upd3* mRNAs in injured wing discs suggests either that 20E/EcR promote blastemal fate, or that 20E/EcR directly or indirectly control transcription of these genes in the regenerate.

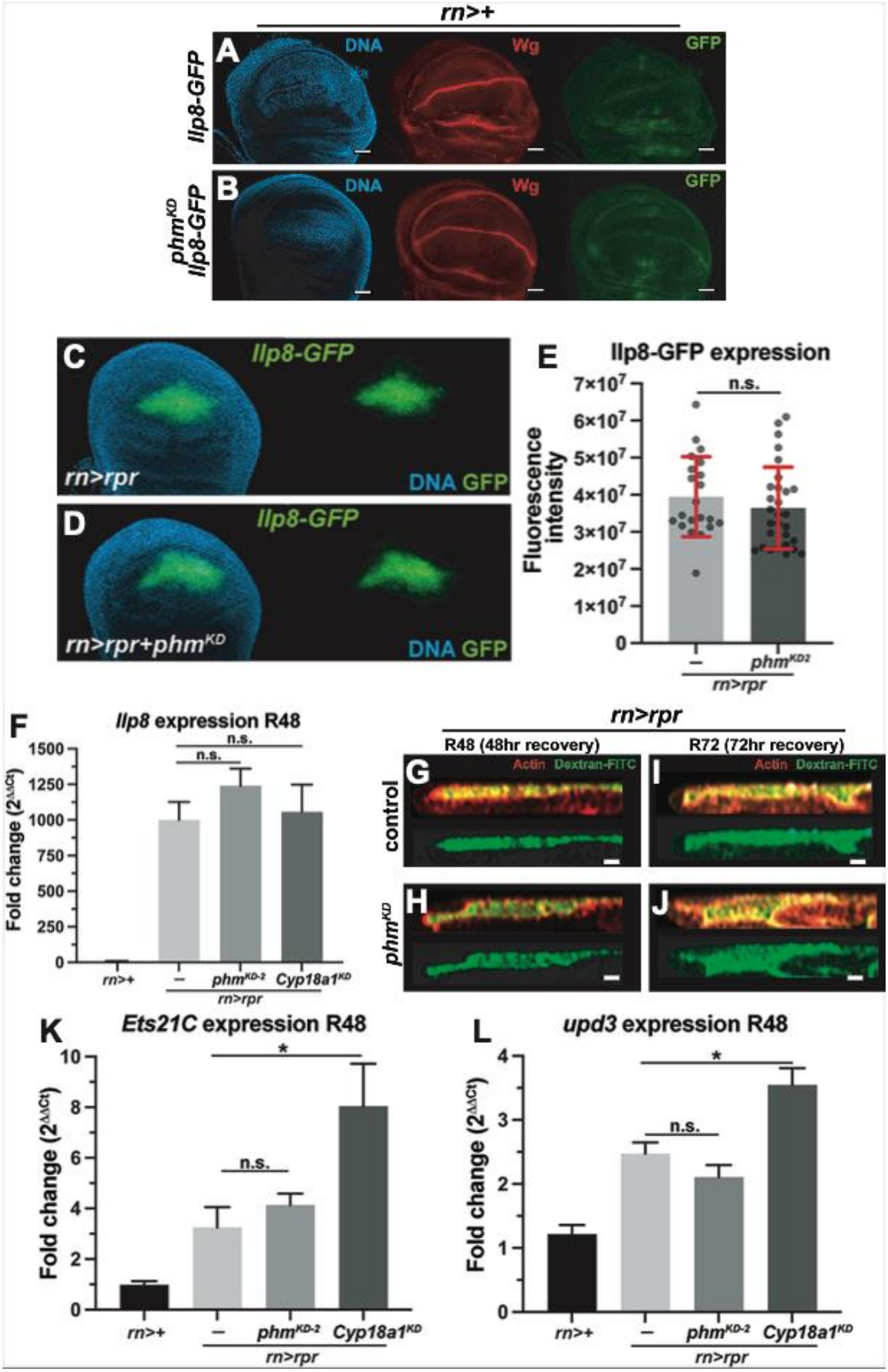
rn>+
A
DNA
Wg
GFP
Ilp8-GFP
B
DNA
Wg
GFP
phmKD
Ilp8-GFP
C
Ilp8-GFP
rn>rpr
DNA GFP
D
Ilp8-GFP
rn>rpr+phmKD
DNA GFP
E
Ilp8-GFP expression
n.s.
Fluorescence intensity
7×10^7
6×10^7
5×10^7
4×10^7
3×10^7
2×10^7
1×10^7
0
–
phmKD2
rn>rpr
F
Ilp8 expression R48
n.s.
n.s.
Fold change (2^ΔΔCt)
1500
1250
1000
750
500
250
0
rn>+
–
phmKD-2
Cyp18a1KD
rn>rpr
rn>rpr
R48 (48hr recovery)
R72 (72hr recovery)
G
Actin Dextran-FITC
I
Actin Dextran-FITC
control
H
J
phmKD
K
Ets21C expression R48
*
n.s.
Fold change (2^ΔΔCt)
10
8
6
4
2
0
rn>+
–
phmKD-2
Cyp18a1KD
rn>rpr
L
upd3 expression R48
*
n.s.
Fold change (2^ΔΔCt)
4
3
2
1
0
rn>+
–
phmKD-2
Cyp18a1KD
rn>rpr

Figure 2.8. Ets21C levels, but not Ilp8 levels, are dependent on local 20E. (A-B) Representative images of Ilp8-GFP expression in mock ablation discs with or without phm^{KD} respectively. Scale bars are 50 μm. **(C-D)** Representative images of *Ilp8-GFP* intensity during regeneration at R48. Quantification of *Ilp8-GFP* intensity using Student's t-test. n values are combined for 3 experiments: *Ilp8-GFP* n=21 and phm^{KD-2}; *Ilp8-GFP* n=29. **(E)** Quantification of *Ilp8-GFP* intensity using Student's t-test. n values are combined for 3 experiments: *Ilp8-GFP* n=21 and phm^{KD-2}; *Ilp8-GFP* n=29. **(F)** Change in *Ilp8* mRNA levels during regeneration in control, phm^{KD-2}, or $Cyp18a1^{KD}$ at R48 compared to mock ablated controls. **(G-J)** Representative images of wing disc epithelial barrier permeability to fluorescein conjugated dextran. Shown are orthogonal views of the wing disc pouch. Phalloidin staining marks actin of the peripodial and columnar cells. Fluorescein conjugated dextran marked in green can be seen in the lumen. **(K-L)** Change in *Ets21c* or *upd3* mRNA levels during regeneration in control, phm^{KD-2}, or $Cyp18a1^{KD}$ at R48 compared to mock ablated controls. Significance analyzed using Student's t-test. *$p<0.05$.

2.4 Discussion

Drosophila imaginal wing discs lose their regenerative capacity in the late-3rd instar larval stage, a developmental timepoint that is concomitant with the systemic increase of Ec steroid hormone levels that promote the transition from the larval stage to the pupal stage. Indeed, numerous studies have demonstrated that developmental progression is slowed following imaginal disc injury by suppression of systemic Ec synthesis in the PG [22, 38, 43-48, 91], and Ec signaling in late stage disc antagonizes expression of the pro-regeneration gene *Chinmo* (Narbonne-Reveau and Maurange, 2019). However, the relatively low levels of Ec present throughout most of the larval stages support imaginal disc growth. Further, a recent study using gamma irradiation to damage larvae proposed that Ec displays a biphasic role in wing disc regeneration such that low concentrations of Ec promote regeneration and high concentrations of Ec restrict regeneration as the tissue undergoes the changes necessary for pupariation [4, 67, 68, 79]. Yet, the source of local 20E during wing disc regeneration has not previously been explored. Here, we employ the rn^{ts}>*rpr* genetic ablation system combined with local *UAS* driven RNAi KD of 20E synthesis/degradation genes within the wing disc blastema to show that 20E synthesis enzymes are locally required within the blastema for proper wing disc regeneration.

When we look for EcR activity in the regenerating wing disc using a EcRE-based reporter, we do not detect evidence for EcR activity until near the mid-point of regeneration. This could indicate that the primary role of local EcR signaling is to sustain, rather than establish, the pro-regenerative environment. This would coincide with wing disc culture experiments that low level 20E extends proliferation of wing discs [67]. Alternatively, low levels of EcR activity below the limits of our EcRE-based reporters to detect may be required for early time points of wing disc regeneration.

The dependence on a local source of Ec in *rn>rpr^{ts}* wounded discs for EcR activation contrasts with cells in developing wing discs that normally activate EcR using Ec derived exclusively from the prothoracic gland [70]. As EcR activity and nuclear accumulation of EcR protein itself remains restricted to the pouch and hinge of *rn>rpr^{ts}* or *egr^{ts}* damaged discs (e.g., see **Figs. 2.4J-L and 2.3A-G**), the locally produced Ec appears to signal regionally within the disc over a relatively short range. This local Ec signaling role resembles the autocrine effect of Ec synthesis in a group of approximately 10 cells in the ovarian follicular epithelium [98], which respond to Ec by collective invasion through surrounding nurse cells [64]. How Ec is concentrated locally in these two scenarios is unclear, but could rely on secretion, uptake, or local sequestration.

Significantly, EcR activity has also been shown to be induced within larval wing discs damaged by exposure to gamma irradiation [79], which parallels the effect of *rn>rpr^{ts}* and *egr^{ts}* observed in this study. However, the source of Ec following irradiation was not examined and presumed to be derived from a systemic source. Intriguingly, feeding 20E to hyperactivate EcR in irradiated discs, or blocking EcR using a dominant-negative transgene (*EcR^{DN}*), affects expression of both the *Ilp8-GFP* reporter and Wg protein, which play key roles in regeneration [22]. Neither of these factors respond to knockdown of *Cyp18a1* or *Halloween* genes in our *rn>rpr^{ts}* damaged wing discs, implying potential differences in effects of Rpr-killing vs. ionizing radiation, or in methods used to identify EcR candidate targets.

Our data indicate that a primary role for local Ec signaling during regeneration is to support injury-induced developmental delay. KD of *phm* in the regenerating blastema is sufficient to reduce pupariation delay to nearly the same extent as KD of the key secreted signaling peptide *Ilp8*. Given that *phm^{KD}* and *Ilp8^{KD}* also display similar inhibition of wing disc

regeneration, the loss of injury-induced developmental delay can likely account for the *phm*^{KD} regeneration defect. Furthermore, proliferation (as measured by EdU incorporation) within the blastema of *phm*^{KD} discs is unchanged from controls, but proliferation of the other regions of the disc is increased in *phm*^{KD} discs. This indicates a loss of coordinated growth reduction. Like injury-induced developmental delay, coordinated growth reduction has been shown to be regulated by suppression of systemic Ec production in the PG [72, 73]. Importantly, local KD of the 20E degradation enzyme *Cyp18a1* has the opposite effect of *phm*^{KD} by enhancing both wing disc regeneration and injury-induced developmental delay. This provides strong support that the local effects of 20E biosynthesis gene KD on regeneration are indeed mediated through local 20E production.

Surprisingly, given the effects of *phm*^{KD} and *Cyp18a1*^{KD} on injured-induced developmental delay and coordinated growth reduction, we find that neither *phm*^{KD} nor *Cyp18a1*^{KD} significantly decreases Ilp8-GFP reporter or *Ilp8* mRNA expression in injured wing discs. Ec signaling is well-known to control a diverse set of biologic pathways in *Drosophila* and we cannot rule out that Ilp8 signaling influenced by local 20E levels downstream of *Ilp8* expression. Alternatively, this could provide evidence for additional signaling pathways having a more important role in suppression of systemic Ec during regeneration than previously realized. The Unpaired cytokine Upd3 is known to be expressed in the regenerating blastema and has recently been found to regulate developmental delay by activating the JAK/STAT pathway in the PG following tumor induced growth perturbation of the imaginal wing disc [15, 38, 48]. Here we find that *upd3* mRNA is significantly upregulated in *Cyp18a1*^{KD} regenerating discs. This suggests a direct or indirect role for Ec signaling in regulating *upd3* expression during regeneration. *Cyp18a1*^{KD} discs also display a significant increase in expression of the stress-

induced transcription factor *Ets21c*. A recent scRNA-seq study showed *Ets21c* controls a GRN, which includes *upd3*, that is required to sustain the pro-regenerative transcriptional program of the regenerating blastema [38]. Given the increased expression of *Ets21c* in $Cyp18a1^{KD}$ discs, the overlap between the Ets21c GRN and the influence of phm^{KD} and $Cyp18a1^{KD}$ on injury-induced developmental delay, and the likely role for EcR activity in sustaining wing disc regeneration; the requirement for local 20E for imaginal wing disc regeneration may be partly mediated through regulation of the *Ets21c* GRN. However, resolving how these complex signaling pathways interact during regeneration will require further experiments.

Our findings indicate that 20E synthesis enzymes are locally required within the blastema for proper wing disc regeneration and depleting these 20E synthesis enzymes modulates pupariation delay and concomitant intra-organ growth effects, while depleting the 20E degradation enzyme Cyp18a1 enhances wing disc regeneration and pupariation delay. Based on these findings we propose that local 20E levels influence wing disc regeneration in the $rn>rpr^{ts}$ injury model by enhancing local expression of *Ets21c*, *upd3*, and perhaps other genes that support regeneration (**Fig. 2.9**). Broadly, identification of gene targets that respond to local EcR activity detected in the pouch of $rn>rpr^{ts}$ and egr^{ts} models would reveal much about how a damaged wing disc evades the systemic loss of Ec from the PG by *Halloween* gene activity in the pouch, which in turn contributes to a unique signaling environment over the wound that requires Ec and sustains a transcriptional signature necessary for tissue repair. This mechanism is a significant and novel addition to our understanding of how a systemic endocrine signaling pathway is locally regulated to create a privileged transcriptional environment to support tissue repair.

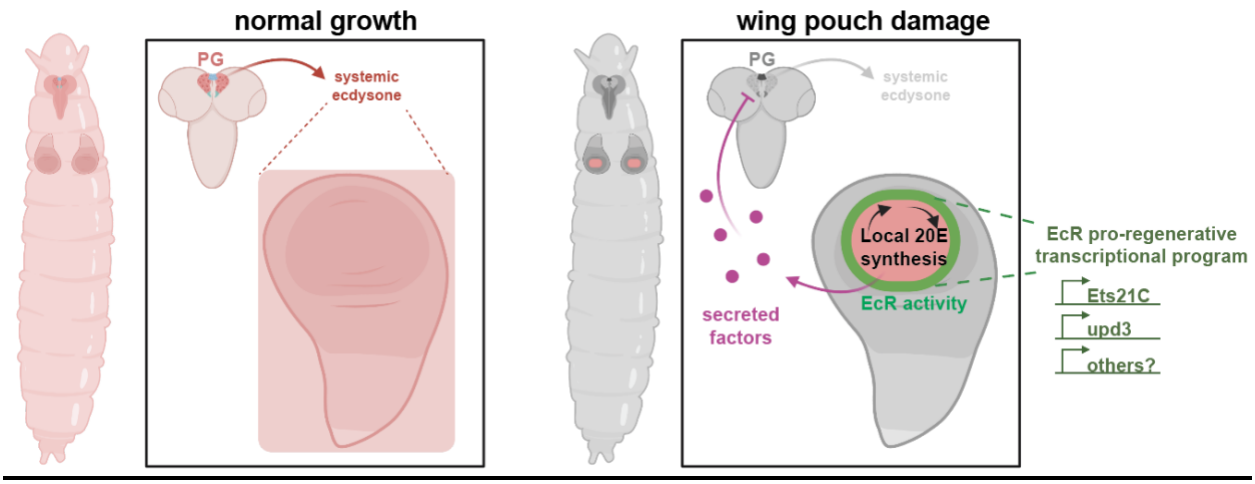

Figure 2.9. Model of local Ec synthesis supporting wing disc regeneration. Schematic depicting the role for system Ec in promoting wing disc growth during normal, uninjured development. Contrasted with our model for local Ec synthesis promoting regulators of regeneration to sustain developmental delay in the context of injury and wing disc regeneration.

2.5 Materials and methods

Experimental model and subject details

Drosophila husbandry

Drosophila lines used in this study are described in the Key resources table. Stocks were maintained under standard culture conditions in 12hr light:dark cycles in humidity controlled incubators at 25°C unless otherwise noted (see Regeneration experiments below). Animals of both sexes were used except where noted (see Adult wing size experiments below).

Method details

Regeneration experiments

We used the *w1118;; rn-GAL4, tub-GAL80ts, UAS-reaper* and *w1118;; rn-GAL4, tub-GAL80ts, UAS-eiger* genetic ablation systems to study regeneration, and *w1118;; rn-GAL4, tub-GAL80ts* as our mock ablation control [22]. These are abbreviated as rn^{ts}>*rpr*, rn^{ts}>*egr*, and rn^{ts}>+ respectively. Development was synchronized by collecting eggs on grape plates. Eggs were collected for 4 hours at 25°C then placed at 18°C. After 2 days at 18°C, 50 L1 larvae were picked and placed into churned fly food vials. For rn^{ts}>*rpr* experiments, on day 7 after egg lay (AEL) temperature shifts were performed to induce ablation. Vials were moved from 18°C to a 29°C circulating water bath for 20 hours. For rn^{ts}>*egr*, temperature shifts were performed at day 8 AEL for 40 hours. For wing disc experiments, dissections were performed at several time points during regeneration: immediately following ablation (R0), and after 24, 48, and 72 h of regeneration.

Adult wing imaging

Adult wings were plucked and mounted in Gary's Magic Mountant (Canada balsam dissolved in methyl salicylate). Images were taken on a Nikon SMZ800N microscope at 25X magnification (2.5x objective x 10x eyepiece) using a Leica MC170HD camera and a Nii-LED High intensity LED illuminator. Area of wing was measured using FIJI.

Immunohistochemistry

Larval discs were dissected in 1xPBS, fixed 20min in 4% paraformaldehyde at room temperature, rinsed 3x in 1xPBS, then permeabilized for 30min at room temperature (RT) in 1xPBS+0.3% Triton X-100 (1xPBST 0.3%). Samples were then blocked for 1 hour in 1xPBS+10% normal goat serum (NGS), and then incubated in primary antibody 1xPBST 0.1% + 10% NGS overnight at 4°C. The next day samples were washed for 5min 5x in 1xPBST 0.1%, incubated for 45min at RT in secondary antibody in 1xPBST 0.1% + 10% NGS, and washed for 5min 5x in 1xPBST 0.1%. Nuclei were then stained with DAPI/Hoescht for 10min and washed 2x in 1xPBS, before mounting discs in *n*-propyl gallate (4% w/v in glycerol). Wing discs were imaged on a Nikon A1R HD25 confocal system using 20x and 40x objectives. Refer to the Key Resources Table for a complete list of antibodies and reagents used.

EdU assay

For EdU staining, live discs were incubated in Schneider's medium with EdU at 100 μM concentration for 20min at RT in the dark. After incubation, discs were fixed in 4% PFA for 20min before proceeding with standard antibody staining as described above. Click-iT EdU

detection was then performed according to the Click-iT EdU proliferation Kit manufacturer's instructions.

Pupariation timing experiments

Pupariation rates were quantified by counting newly formed pupae every 8 h. Timing was reported as hours after egg lay (AEL), starting at the beginning of the 4-hour egg lay period. Pupariation was determined as when animals stopped moving and darken in color.

Quantitative reverse-transcription PCR (qPCR)

50 discs from equivalently staged larvae of each genotype were dissected and added to 100 μL of Trizol. RNA was extracted using the Qiagen RNeasy kit according to manufacturer's instructions. cDNA conversion was performed using SuperScript-III RT kit according to manufacturer's instructions using 1 μg of extracted RNA. qPCR analysis was performed in triplicate using SYBR green master mix on a QuantStudio6 Real-Time PCR System. The entire assay was repeated 3 times using discs from separate ablation experiments. Refer to the Key Resources Table for a full list of primers and reagents used.

Dextran assay

Larvae were dissected, inverted, and cleaned in Schneider's medium at the time points noted. Carcasses were then placed in 25mg/mL 10kD fluorescein-conjugated dextran diluted 1:8 in Schneider's medium and incubated for 30min at room temperature in the dark while rocking. Carcasses were then washed 1x with Schneider's medium and the fixed with 4%

paraformaldehyde for 20min, before proceeding with normal antibody staining as described above.

Quantification and statistical analysis

Adult wing size

Only female animals were used for these experiments, as previous research has indicated that female and male flies display statistically different regenerative capacity. Populations from separate ablation experiments cannot be meaningfully compared to one another as studies from other labs have indicated seasonal variation regeneration.

Semi-quantitative: for binning experiments, adult wing size was scored following injury and regeneration into 5 categories (0%, 25%, 50%, 75%, and 100%). Results were calculated per population, with n's representing data from at least 3 separate ablation experiments. Statistical analysis was performed in GraphPad Prism9 using the χ^2 test.

Quantitative: Results were calculated per population, with n's representing data from at least 2 separate ablation experiments. For injured wing size measurements, wings were normalized to the mean wing size of mock ablation wings from the same genotype. This was done to control for the small but statistically significant difference between mock ablation controls. Statistical analysis was performed in GraphPad Prsim9 using the Student's t-test.

Fluorescence intensity quantification

ImajeJ/FIJI software was used to quantify fluorescence intensity. All quantified images used the same imaging parameters within a given experiment.

EcRE-GFP intensity was quantified by measuring the fluorescence within the wing disc pouch as defined by the outer edge of hinge Wingless (Wg) expression. To control for background variations across discs, a 52x52 pixel non-regenerating region in the notum was used to determine background EcRE-GFP expression. Statistical analysis was performed in GraphPad Prism9 using the Student's t-test. N's represent 3 separate ablation experiments.

Ilp8-GFP intensity was quantified by measuring the total GFP fluorescence from the Ilp8-GFP positive region of the disc using summed z-stacks. Statistical analysis was performed in GraphPad Prism9 using the Student's t-test. N's represent 3 separate ablation experiments.

EdU assay quantification

ImajeJ/FIJI software was used to quantify fluorescence intensity. All quantified images used the same imaging parameters within a given experiment.

EdU intensity was measured from summed z-stacks of discs. For both intensity and area measurements, the pouch region of the disc was determined by the outer edge of hinge Wg expression. Percent of total EdU fluorescence in pouch was determined: pouch EdU intensity/total disc EdU intensity. This allowed for normalization of any variation in incorporation between discs. Area of pouch was determined: area of pouch/total disc area. Statistical analysis was performed in GraphPad Prism9 using One-way ANOVA with Dunnett's test for multiple comparisons.

Pupariation timing analysis

Survival curve analysis for pupariation timing experiments was performed in GraphPad Prism9 using the Log-rank (Mantel-Cox) test. Results are calculated per population, with n's representing data from at least 3 separate ablation experiments.

Quantitative reverse-transcription PCR (qPCR) analysis

Analysis was performed using the $\Delta\Delta C_T$ method and expression levels were normalized to *rp49*. Statistical analysis was performed in GraphPad Prsim9 using the Student's t-test.

REAGENT or RESOURCE	SOURCE	IDENTIFIER
Antibodies		
Mouse anti-Wg (4D4)	Developmental Studies Hybridoma Bank	RRID: AB_528512
Mouse anti-β-galactosidase (40-1a)	Developmental Studies Hybridoma Bank	RRID: AB_528100
Mouse anti-EcR common	Developmental Studies Hybridoma Bank	RRID: AB_10683834
Rabbit anti-DCP-1	Cell Signaling	RRID: AB_2721060
Goat anti-mouse-Cy3	Jackson ImmunoResearch	RRID: AB_2338683
Normal goat serum	Jackson ImmunoResearch	RRID: AB_2336990
Chemicals, peptides, and recombinant proteins		
Triton X-100	Sigma-Aldrich	9002-93-1
20% Paraformaldehyde	Electron Microscopy Sciences	15713
Trizol	Invitrogen	15596018
DAPI	Invitrogen	D1306
Hoescht 33342	Thermo Fisher Scientific	62249
n-Proply gallate	Sigma	P-3130
Glycerol	VWR International	56-81-5
Alexa Fluor 594 phalloidin	Invitrogen	A12381
Dextran, Fluorescein, 10,000 MW	Thermo Fisher Scientific	D1820
Schneider's *Drosophila* Media	Thermo Fisher Scientific	21720024
Canada balsam	Sigma	C1795
Methyl salicylate	Sigma	M6752
Critical commercial assays		
RNeasy mini kit	Qiagen	74106
SuperScript III RT	Thermo Fisher Scientific	18080093
EdU Assay: Click-iT EdU Cell Proliferation Kit	Thermo Fisher Scientific	C10340
Experimental models: Organisms/strains		
rn-GAL4, tub-GAL80^{ts}, UAS-egr	Smith-Bolton et al.	RRID: BDSC_51280
rn-GAL4, tub-GAL80^{ts}, UAS-rpr	Smith-Bolton et al.	N/A
rn-GAL4, tub-GAL80^{ts}	Smith-Bolton et al.	N/A
Ilp8-GFP (*Mi[99]Ilp8*^{MI00727})	Bloomington *Drosophila* Stock Center	RRID: BDSC_33079
UAS-dilp8-RNAi	Vienna *Drosophila* Stock Center	RRID: v102604
UAS-torso-RNAi	Bloomington *Drosophila* Stock Center	RRID: BDSC_58312
UAS-phm-RNAi	Bloomington *Drosophila* Stock Center	RRID: BDSC_55392
UAS-phm-RNAi	Vienna *Drosophila* Stock Center	RRID: v104028
UAS-dib-RNAi	Vienna *Drosophila* Stock Center	RRID: v101117
UAS-shd-RNAi	Bloomington *Drosophila* Stock Center	RRID: BDSC_67356
UAS-shd-RNAi	Vienna *Drosophila* Stock Center	RRID: v108911
shd^{2}	Bloomington *Drosophila* Stock Center	RRID: BDSC_4219

UAS-cyp18a1-RNAi	Bloomington *Drosophila* Stock Center	RRID: BDSC_64923
7xEcRE-GFP	V. Henrich	N/A
7xEcRE-lacZ	Bloomington *Drosophila* Stock Center	RRID: BDSC_4517
Oligonucleotides		
Primer pair for *rp49*: GCTAAGCTGTCGCACAAATG GTTCGATCCGTAACCGATGT	Integrated DNA Technologies	N/A
Primer pair for *dilp8*: TGGTCATCGGAGTCTGTTGC TTTTGCCGGATCCAAGTCGA	Integrated DNA Technologies	N/A
Primer pair for *ets21c*: GTGCCAACAGAGGCCGATTA CTGTTGGTGGGAACTTCCGT	Integrated DNA Technologies	N/A
Primer pair for *upd3*: GCTGACCTTCCAGCAGAAAT TGCTGTGCGTTTCGTTCA	Integrated DNA Technologies	N/A
Software and algorithms		
Image J / Fiji	Schindelin et al.	https://fiji.sc/
Prism	GraphPad	https://www.graphpad.com/

Table 2.1. Key resources.

Chapter 3. Validation of an EcR probe for tissue-specific disruption of endogenous LBD-dependent interactions and support for additional EcR roles in wing disc regeneration

This chapter was partially adapted from the following paper in revision at *eLife***:

Joanna Wardwell-Ozgo, **Douglas Terry**, Colby Schweibenz, Michael Tu, Ola Solimon, David Schofeld, and Kenneth Moberg. *An EcR probe reveals mechanisms of the ecdysone-mediated swtich from repression-to-activation on target genes in the larval wing disc*. eLife. (*in revision*).

**Creation of the *UAS-EcR^{LBD}* and *UAS-EcR^{A483T}* transgenes was performed by Joanna Wardwell-Ozgo. The additional experiments and data analysis described in this chapter were designed and performed by Douglas Terry. The regeneration experiments involving *tai^{PPxA}* mutants were performed by Douglas Terry using mutants that were generated by Shilpi Verghese and are not part of the submitted papers in Chapters 2 or 3.

3.1 Introduction

The growth and patterning of developing metazoan tissues is coordinated by signals that include adhesion events between neighboring cells, secreted morphogens and ligands that act regionally within a tissue or compartment, and systemic inputs from nutrients and hormones that act at the level of the whole organism. These latter hormonal inputs synchronize growth rates and coordinate timing of developmental events across multiple tissues, and can take the form of peptides (e.g., insulin-like peptides) or cholesterol-derived steroids, which are well-known for triggering progression through major developmental transitions [52, 100]. In the fruit fly *Drosophila melanogaster*, the main steroid hormone ecdysone (Ec) is synthesized in the larval prothoracic gland (PG) and secreted into the hemolymph [52].

The active form of Ec, 20-hydroxyecdysone (20E), elicits changes in gene expression by interacting with the ligand-binding domain (LBD) of the ecdysone receptor (EcR), a type-II nuclear hormone receptor (NHR) that binds a defined palindromic DNA sequence as a heterodimer with its partner an RxR homolog Ultraspriacle (USP) [61, 101-104]. EcR/USP complexes can repress targets in the absence of 20E and activate targets as 20E titers rise [105-108]. Like other NHRs, this EcR functional plasticity is based on a model of 20E-induced allosteric changes in the LBD which evict corepressors and allow binding of coactivators [109]. Dynamic switches from repression to activation allow EcR to translate rising 20E concentrations into tissue- and stage-specific transcriptional programs that vary based on EcR isoforms present in each cell type, their patterns of genomic occupancy, and the spectrum of co-expressed EcR activators and repressors [67, 68, 72, 110, 111]. These dynamic switches in transcriptional programs allow EcR to contribute to diverse developmental processes, including apoptosis of polyploid larval cells [112, 113], proliferation of larval histoblast nests [114], collective migration of cells in the ovary [64], and transitions between developmental stages, e.g., embryo-to-larva and larva-to-pupae [52, 62, 115].

The temporal patterns of EcR transcriptional activity in developing tissues are predicted to mirror a series of developmentally programmed Ec peaks that begin in the embryo and conclude in the pupal phase [78]. These temporal gradients of Ec also have the potential to drive different expression patterns for low and high-threshold 20E-EcR targets in a manner akin to classic spatial morphogen gradients (e.g., Dpp) [116]. Consistent with this hypothesis, recent studies show that EcR dynamically redistributes across the genome of late third instar wing imaginal disc cells as 20E titers rise, implying that EcR targets shift as development proceeds, even within a single cell type [117]. One potential interpretation of this data is that enhancers

occupied by EcR only at low Ec titers are primarily regulated by EcR repression, while those only occupied at high Ec titers are primarily regulated by EcR activation. In addition, loci differentially bound by EcR across the timescale of these experiments had a lower motif density and EcR binding strength [117], suggesting that EcR recruitment to these temporally dynamic promoters might rely on cofactor recruitment or interactions with other transcription factors bound at shared enhancers. Testing these models of EcR mediated activation and repression on specific target genes is challenging given that *EcR* loss-of-function alleles or inhibition of Ec production in the PG each lead to developmental arrest [70, 118]. A more targeted approach of EcR RNAi depletion from its bound genomic sites is predicted to both relieve EcR-mediated repression and block activation, making it difficult to extrapolate roles of EcR-coregulator complexes on their targets. Similarly, overexpression of an EcR dominant negative variant (*UAS-EcR*^{F645A} dominant negative) [108] is predicted to promiscuously bind and repress EcR target sites throughout the genome, overwhelming specificity mechanisms.

To enable targeted analysis of the role of endogenous EcR and 20E-dependent co-regulators in controlling specific target genes in intact tissues, we have created a *UAS*-transgene encoding a fragment of the *EcR* coding sequence encompassing the LBD domain (EcR^{LBD}) based on a prior study suggesting that this fragment could act as a dominant negative EcR *in vivo* [119]. This EcR^{LBD} fragment lacks the DNA binding domain but is predicted to bind and sequester 20E and co-regulators that interact with the activation function-2 domain (AF2), which is embedded in the LBD, and thus will sequester factors away from endogenous EcR bound to target enhancers. The addition of Gal4/UAS provides temporal and spatial control to EcR^{LBD} mediated disruption of these interactions and visualization of downstream effects on target genes. A second EcR^{LBD} fragment was also generated that contains a mutation, Ala^{483}Thr (A483T),

which blocks interaction between the EcR^{LBD} and its corepressor Smr. This fragment will be referred to hereafter as $EcR^{LBD\text{-}A483T}$. Since $EcR^{LBD\text{-}A483T}$ is unable to bind Smr but remains capable of binding 20E, it allows us to probe which EcR regulated processes are a function of de-repression as opposed to activation of targets.

To complement the EcR^{LBD} transgenic approach, our lab used CRISPR to engineer two amino acid changes into the EcR coactivator protein Taiman (Tai). Tai is a homolog of the p160 family of Steroid Receptor Coactivators (SRC-1,2,3) in vertebrates [120, 121]. A previous study from our lab revealed direct interaction between a pair of PPxY (proline-proline-x-tyrosine) motifs in the Tai transcriptional activation domain (TAD) and two WW (tryptophan-tryptophan) domains in Yorkie (Yki), the transcriptional coactivator of the Hippo pathway [74, 122]. This study defined a role for Tai in complex with Yki in autonomous control of imaginal wing disc growth, in which Yki-driven overgrowth is dependent on interaction with Tai. In particular, the Yki-Tai interaction is required for a subset of the transcriptional targets of hyperactive Yki. These targets include *piwi* and the insulin-like peptide *Ilp8*, both of which have been shown to have roles in *Drosophila* regeneration [38, 42, 45, 46, 96, 123]. The endogenous Tai CRISPR mutant our lab generated has its PPxY motifs mutated to PPxA motifs (referred to as tai^{PPxA}), which abrogates Tai's interaction with Yki. These tai^{PPxA} mutants allow us to study the role of endogenous Yki-Tai interactions.

The data presented here validate the EcR^{LBD} and $EcR^{LBD\text{-}A483T}$ fragments as effective tools to assess the relative contribution of EcR repressors and activators to direct the control of EcR regulated processes. The well-studied EcR regulated processes of glue protein synthesis, secretion, and expectoration in larval and early pupal salivary glands (SGs) was used to assess the effects of disrupting endogenous EcR-coregulator interactions compared with RNAi

depletion of EcR or overexpression of the dominant negative EcR^{F645A}. These data reveal both key differences and similarities between these disruptions of EcR signaling. We then go on to test the effect of Tai^{PPxA} heterozygous background on imaginal wing disc regeneration following genetic *rn>rpr*^{ts} ablation and find a reduction in both imaginal wing disc regeneration and injury-induced developmental delay. Collectively, these data demonstrate the effectiveness of two new tools in investigating processes regulated by the EcR and its co-regulators.

3.2 Results

EcR^{LBD} and $EcR^{LBD\text{-}A483T}$ structure

To enable targeted disruption of interactions between EcR and co-factors in specific cells, a fragment of full-length *EcR* cDNA encoding the hinge, ligand binding domain, and C-terminal end (regions D, E, F according to nomenclature in [108] was tagged with a C-terminal red fluorescent protein tag (nls-RFP) and inserted into a *UAS* transgene (*UAS-EcRLBD*) (**Fig. 3.1**). EcR^{LBD} contains the 20E binding region and the Activation Function-2 domain (AF2), which seeds interactions with activators and repressors and contains the presumed dimerization interface with the EcR partner and RXR homolog Ultraspiracle (USP) [124]. EcR^{LBD} lacks the DNA binding domain and the isoform-specific A/B regions, which include the transactivation domain Activation Function-1 (AF1). Several mutations that affect EcR transcriptional activity lie within the EcR^{LBD} region (annotated in **Fig. 3.1**), including *Ala483Thr* (A483T), which lies within the 'Ti' domain and disrupts interaction with the fly NCoR1 repressor homolog Smr [63] and *Phe645Ala* (F645A), which is within AF2 and blocks 20E-stimulated gene expression [108, 125]. Significantly, ubiquitous expression of a similar EcR-LBD fragment using a heat shock-

inducible promoter elicits dominant-negative effects *in vivo* [119], likely by sequestering EcR regulators.

The EcR^{LBD} is predicted to bind and sequester both 20E ligand as well as co-regulators that interact via the LBD region. The EcR co-repressor SMRT-related EcR interaction protein (Smr) [63] interacts with EcR via the AF2 region. This binding has been shown to require the Ala^{483} residue and conversion of Ala^{483} to Thr ($A^{483}T$) is sufficient to disrupt Smr binding to EcR [63]. Smr is a Myb-SANT domain repressor homologous to the mammalian protein NCoR1 (nuclear receptor corepressor-1)[126] and is the most well-studied EcR repressor in *Drosophila*. Smr is known to repress EcR activity in diverse tissues. However, it has proven difficult to determine which EcR regulated processes are controlled by Smr repression and to what extent activation of EcR regulated processes is directed through de-repression of Smr repression rather than direct activation of EcR via binding to 20E ligand [63, 127]. Thus, a version of EcR^{LBD} with the $A^{483}T$ conversion was also generated, $EcR^{LBD\text{-}A483T}$, to test the effect of expressing an EcR^{LBD} fragment unable to sequester Smr on EcR regulated processes.

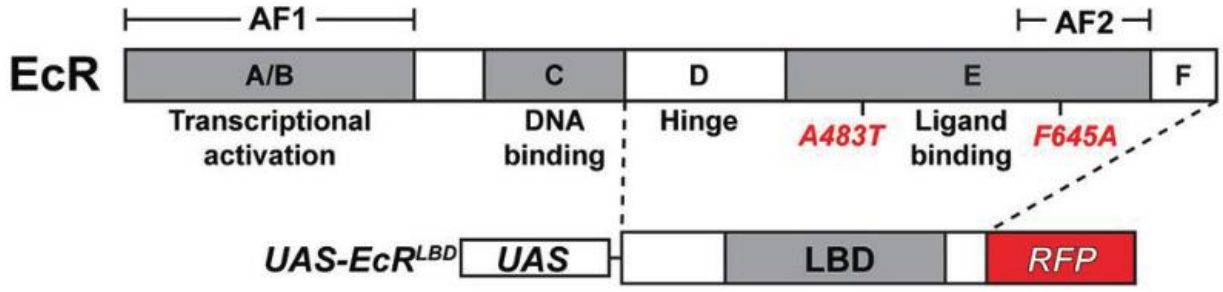

Figure 3.1 The EcR^{LBD} structure.

The EcR^{LBD} consists of the hinge, ligand binding domain (LBD) and F regions with a C-terminal RFP fusion. AF1 and AF2 domains are indicated. Mutations that disrupt EcR functions are indicated (red). The A483T mutation disrupts binding to the corepressors Smr and the F645A disrupts binding to the ligand 20E.

***EcR^{LBD}* effect on glue protein synthesis, secretion, and expectoration.**

To test the prediction that *UAS-EcR^{LBD}* sponges key EcR cofactors and perturbs 20E-regulated processes, the effect of EcR^{LBD} expression was tested on the EcR-regulated process of glue protein production, secretion, and expectoration in the larval and pupal salivary glands (SGs). GFP-tagged Sgs3 glue protein (Sgs3-GFP) synthesis is initiated by a small pulse of systemic Ec produced by the PG in mid-L3 larvae. Synthesis of Sgs3-GFP begins in the distal cells of the salivary gland and then precedes into the more proximal cells of the salivary gland (**Fig. 3.2A**) [128-130]. Secretion of Sgs3-GFP from the salivary gland cells into the lumen of the salivary gland is induced by another systemic pulse of Ec from the PG in late-L3 larvae, ~6 hours before pupariation (**Fig. 3.2A-B**). Expression of *EcR^{LBD}* in SGs with *fkh-Gal4* blocks EcR-regulated secretion of a Sgs3-GFP into the lumen of late L3 larval SGs but does not block Sgs3-GFP production (**Fig. 3.2C**). Interestingly, expression of the mutated *EcR$^{LBD\text{-}A483T}$* fragment that is no longer able to bind the co-repressor Smr does not prevent Sgs3-GFP synthesis or secretion into the SG lumen (**3.2D**). By comparison, *fkh-Gal4* driven RNAi knockdown of the *EcR* (which removes EcR from sites of genomic occupancy), RNAi knockdown of the 20E-importer *EcI* [131] (which selectively blocks 20E ligand from entering salivary gland cells), or transgenic expression of *UAS-EcR^{F645A}* (a dominant negative protein predicted to fill EcR binding sites across the genome) inhibit Sgs3-GFP glue protein synthesis as well as blocking Sgs3-GFP luminal secretion in larval SGs (**Fig. 3.2E-G**). These differences suggest that the EcR regulated processes of Sgs3-GFP synthesis and secretion into the lumen require differential regulation by EcR co-regulators.

The pulse of Ec that drives pupariation also leads to expectoration of Sgs3-GFP from the salivary glands out onto the surface of the pupa where glue proteins help the pupa stick to

surfaces [128-130]. Using the *Sgs3-Gal4* driver [108], the salivary glands can still be seen within the pupa through expression of the *UAS-RFP* transgene, but Sgs3-GFP protein has been expectorated onto the outside of the pupal case (**Fig. 3.2H)**. Expression of EcR^{LBD} in pupal SGs (0-4hr after puparium formation; APF), using the *Sgs3-Gal4* driver, inhibits Sgs3-GFP expectoration (**Fig. 3.2I**). However, expression of the mutated $EcR^{LBD\text{-}A483T}$ fragment does not affect Sgs3-GFP expectoration (**Fig. 3.2J**). The inhibition of Sgs3-GFP expectoration in the background EcR^{LBD} is consistent with inhibition of Sgs3-GFP expectoration seen with expression of EcR^{RNAi}, EcR^{F645A}, or overexpression of the P450 enzyme *Cyp18a1* that inactivates 20E [57, 132] (**Fig. 3.2K-M**). It should be noted that all of the genotypes tested eventually synthesized Sgs3-GFP, as can be seen by the Sgs3-GFP signal in the salivary glands of pupa in **Fig 3.2I,K,L**. Similarly, Sgs3-GFP is eventually expectorated in all genotypes (data not shown). This indicates that these methods of disrupt but do not completely block EcR regulated processes. Together, these data indicate that EcR^{LBD} specifically disrupts some EcR-dependent processes in larval SG cells but not others. These different phenotypic consequences of EcR^{LBD} overexpression versus EcR RNAi depletion, or EcR^{F645A} overexpression, may discriminate developmental events controlled by LBD and AF2 interactions with activators and repressors, versus those that respond to loss of EcR occupancy at genomic targets, a deficit in 20E-driven activation, or forced binding of EcR^{F645A} to sites throughout the genome.

The *A483T* mutation eliminates the ability of EcR^{LBD} to block Sgs3-GFP secretion into the larval SG lumen and WPP stage expectoration of glue proteins (**Fig. 3.2D,J,M**). These data imply either that Smr is required to coordinate 20E-induced Sgs3 production, secretion, and expectoration, or that the $A^{483}T$ mutation also disrupts binding of an unidentified co-activator that promotes these processes. A direct test of these models by RNAi knockdown of *Smr* in larval

SGs (*fkh>SmrIR*) reveals that Smr is required for Sgs3-GFP secretion (**Fig. 3.2M**), perhaps by coordinating a shift in EcR-regulated gene expression from glue protein production to secretion/expectoration. This result seems to imply that a balance of EcR repression and activation is required for proper timing of EcR-regulated developmental processes. However, we note that the salivary glands of *fkh>SmrIR* are malformed compared to other genotypes (data not shown) and it is possible Smr plays roles in additional signaling pathways that affect salivary gland development.

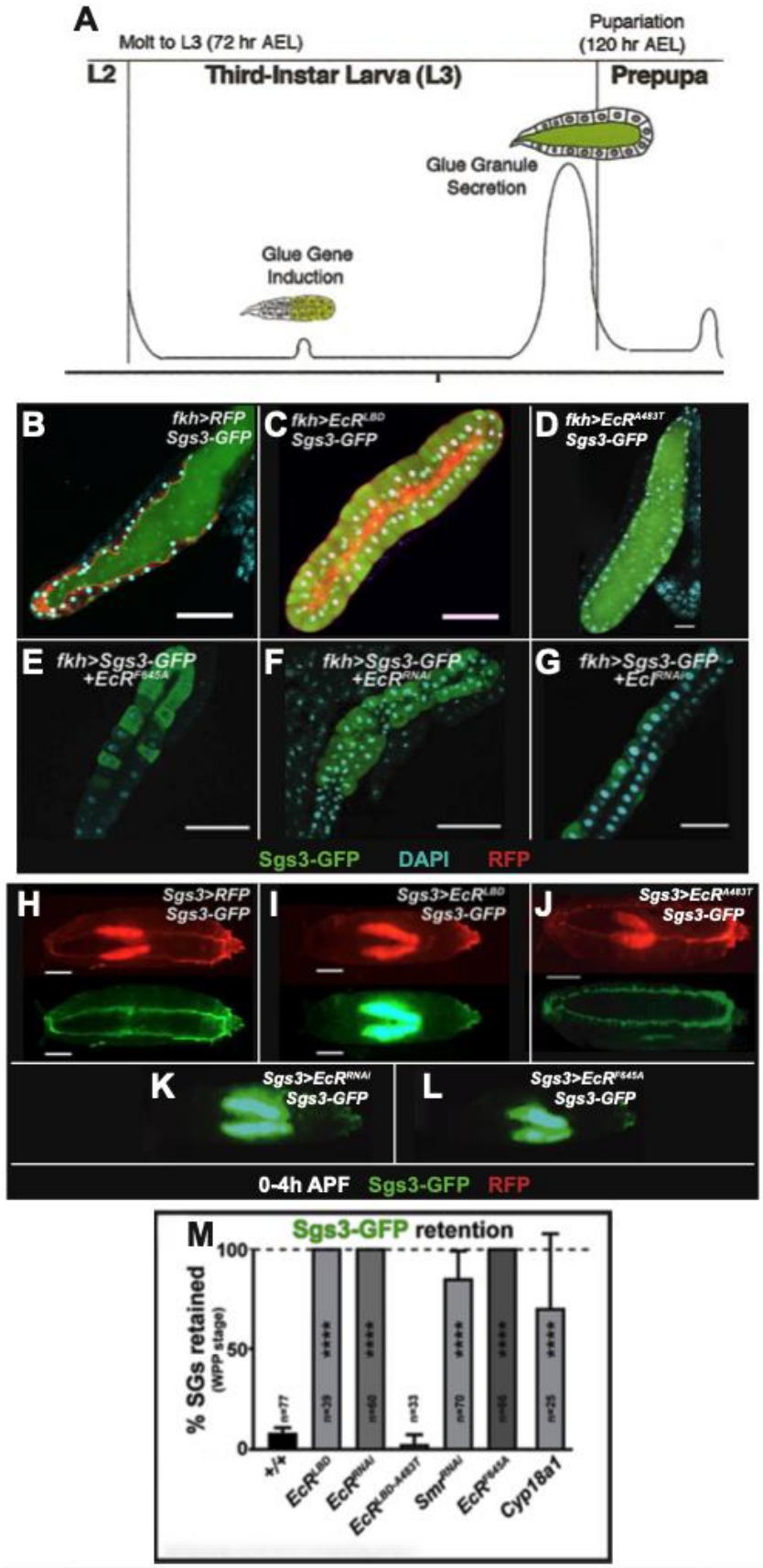
A
Molt to L3 (72 hr AEL)
Pupariation
(120 hr AEL)
L2
Third-Instar Larva (L3)
Prepupa
Glue Granule
Secretion
Glue Gene
Induction
B fkh>RFP Sgs3-GFP
C fkh>EcR^LBD Sgs3-GFP
D fkh>EcR^A483T Sgs3-GFP
E fkh>Sgs3-GFP +EcR^F645A
F fkh>Sgs3-GFP +EcR^RNAi
G fkh>Sgs3-GFP +EcR^RNAi
Sgs3-GFP DAPI RFP
H Sgs3>RFP Sgs3-GFP
I Sgs3>EcR^LBD Sgs3-GFP
J Sgs3>EcR^A483T Sgs3-GFP
K Sgs3>EcR^RNAi Sgs3-GFP
L Sgs3>EcR^F645A Sgs3-GFP
0-4h APF Sgs3-GFP RFP
M Sgs3-GFP retention
% SGs retained (WPP stage)
100
50
0
+/+
EcR^LBD
EcR^RNAi
EcR^LBD-A483T
Smr^RNAi
EcR^F645A
Cyp18a1

Figure 3.2. *EcR^{LBD}* effect on 20E-regualted glue protein synthesis, secretion, and expectoration. (A) Adapted from Biyasheva 2001. Glue protein synthesis is first induced by a small systemic pulse of ecdysone in the salivary glands of wild-type mid-L3 larvae. This glue protein synthesis begins at the distal tip of the salivary gland and spreads to more proximal salivary gland cells. Approximately 6 hours before pupariation, glue proteins are secreted into the lumen of the salivary gland. By 4 hours after puparium formation (APF), glue proteins are expectorated from the salivary glands to coat the pupae and allow the pupae to stick to vertical structures. **(B)** GFP-tagged Sgs3 glue protein (Sgs3-GFP) has been secreted into the lumen of late-L3 wild-type salivary glands. **(C)** Expression of the *EcR^{LBD}* in the salivary gland does not prevent synthesis of Sgs3-GFP, but it does inhibit Sgs3-GFP secretion into the lumen. **(D)** *EcR$^{LBD\text{-}A483T}$* expression does not block either Sgs3-GFP synthesis or luminal secretion. (**E-G)** Overexpression of the *EcR^{F645A}* or depletion of either *EcR* or the ecdysone importer *EcI* delays Sgs3-GFP synthesis and inhibits Sgs3-GFP secretion into the lumen. Scale bars for salivary glands are 100 μm (**H**) Sgs3-GFP is expectorated onto the outside of the pupae within 4 hours of puparium formation in wild-type animals. (**I**) *EcR^{LBD}* inhibits expectoration of Sgs3-GFP. (**J**) *EcR$^{LBD\text{-}A483T}$* expression does not interfere with Sgs3-GFP expectoration. (**K-L**) RNAi depletion of *EcR* or overexpression of the *EcR^{F645A}* inhibits Sgs3-GFP expectoration. Scale bars for pupae are 0.5mm. (**M**) Quantification of expectoration results. Data analysis was performed with One-way ANOVA.

Tai^{PPxA} heterozygotes display reduced regeneration and injury induced pupariation delay

We employed an established genetic ablation system [22] to assay a heterozygous tai^{PPxA} CRISPR mutation on imaginal wing disc regeneration. This genetic ablation system uses a combination of *rotund (rn)-GAL4* and *tubulin-GAL80^{ts}* to express a pro-apoptotic gene (*UAS-reaper*) in a spatially and temporally restricted manner (hereafter *rn^{ts}>rpr*) (**Fig. 2.1A**). The endogenous Tai CRISPR mutant our lab generated has its two PPxY motifs mutated to PPxA motifs (**Fig. 3.3A**). Heterozygosity for tai^{PPxA} does not lead to any growth defects during normal development (data not shown), however the tai^{PPxA} mutation has previously been shown to prevent direct Yki-Tai interaction in cell culture [74]. Given that Yki is required for imaginal wing disc regeneration [133, 134] and the Yki-Tai interaction is required during hyperactive Yki driven imaginal wing disc overgrowth [74], we used the *rn^{ts}>rpr* injury system combined with the tai^{PPxA} CRISPR mutant allele to ask if there is a physiologically relevant requirement for Yki-Tai interaction during regenerative growth. Binning adult wings into approximate "percent regenerated" groups reveals that heterozygosity for tai^{PPxA} is sufficient to impair imaginal wing disc regeneration. Previously, our lab discovered that the Yki-Tai interaction is required for hyperactive Yki-driven expression of *Ilp8* in the imaginal wing disc [74]. *Ilp8* is well known for its role as a secreted signaling peptide to delay development and allow time for regeneration to occur before developmental progression [26, 38, 44-47, 84]. Therefore, we decided to investigate if heterozygosity for tai^{PPxA} is sufficient to reduce injury-induced developmental delay following injury. We find that tai^{PPxA}/+ animals do display a reduction in injury-induced developmental delay following genetic ablation of the imaginal wing disc pouch (**Fig. 3.3C**). We also note that uninjured tai^{PPxA}/+ animals display slightly accelerated time to pupariation compared to wild-type animals (**Fig. 3.3C**). *Ilp8* has been shown to help coordinate bilateral symmetry during

normal development by transiently delaying developmental progression [47], and these data that suggest uninjured *tai*^{PPxA}/+ mutants experience accelerated development might suggest a requirement for Yki-Tai interaction in regulating *Ilp8* during normal development; however, further experiments would be needed to fully investigate this theory.

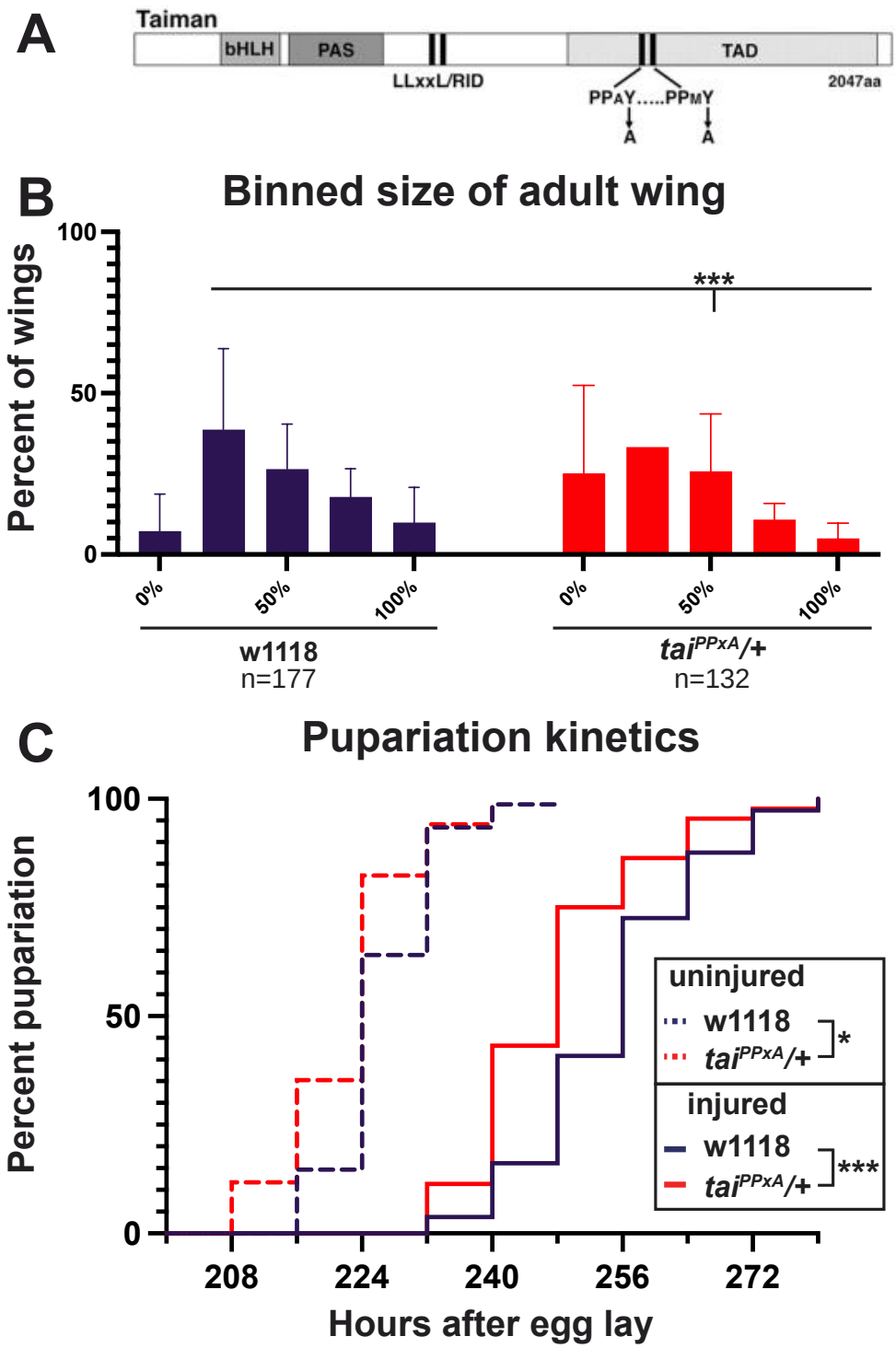

Figure 3.3. *Tai*^{PPxA} heterozygotes display inhibited wing disc regeneration and reduction in injury-induced pupariation delay. (**A**) Tai domain structure adapted from [74]. bHLH=basic helix-loop-helix, PAS=Period-Arnt-Similar, RID=receptor interaction domain,

TAD=transactivation domain. Approximate locations of the two PPxY motifs and their Y-to-A mutant forms are indicated. (**B**) Distribution of female adult wing sizes binned into five categories from 0-100% regenerated following injury and regeneration (n=number of wings and is cumulative for three experiments). Statistical significance determined by the χ^2 test. ***p<0.0001, Error bars are SD. (**C**) Kaplan-Meyer survival curve for pupariation time-points following injury with significance determined by the Log-rank (Mantel-Cox) test. n values are combined for 3 experiments for injured discs and 2 experiments for uninjured discs : *rn>rpr^{ts} w^{1118}* n=186, *rn>rpr^{ts} tai^{PPxA}*/+ n=44; *rn>+ w1118* n=41; *rn>+ tai^{PPxA}*/+ n=17 *p<0.05, ***p<0.0001.

3.3 Discussion

Steroid hormone signaling controls a diverse set of biological processes, including developmental progression, tissue growth, and fertility. The *Drosophila* Ec steroid hormone signaling pathway offers a complex steroid hormone signaling program in which to study the dynamic switches in transcriptional programs that allow for control of these disparate biological processes. New tools are needed to probe the relationships between the EcR and its endogenous co-regulators during EcR regulated processes.

Here, we employ a Gal4/UAS expressed EcR^{LBD} 'sponge' that titrates EcR co-regulators and permits assessment of expression of individual target genes *in vivo* without disrupting endogenous EcR bound at genomic sites. This tool differs from previous models of EcR disruption which employed overexpression of dominant negative *EcR* alleles (e.g., EcR^{F645A}) [125] or EcR^{RNAi} depletion that either displace or remove endogenous EcR. Instead, EcR^{LBD} will only compete away co-regulators bound to the hinge and LBD/AF2 domains of endogenous EcR. Interactions with cofactors that occur through other domains, such as the ligand independent AF1 domain [108, 135], are predicted to remain intact in cells that express EcR^{LBD}. This key difference may explain why EcR^{LBD} phenocopies some *EcR* loss-of-function phenotypes [119] but not others. For example, EcR^{F645A} and EcR^{RNAi} each disrupt production, secretion, and expectoration of glue proteins, but EcR^{LBD} only disrupts secretion and expectoration. These phenotypic differences could highlight processes that require AF1-mediated interactions or cooperative effects between AF1 and AF2, which can work together to regulate hormone receptor effects in other organisms [136-141]. Indeed, future comparisons between EcR^{LBD} and EcR^{AF1} transgenes could be an effective way to dissect roles of AF1 in 20E-EcR driven phenotypes in developing tissues. Further, as most coregulator interactions mediated

through the AF1 and AF2 domains are conserved between *Drosophila* and mammalian NHRs, these insights into EcR-cofactor interactions could also provide insight to the functions of mammalian NHRs [142, 143].

Our data using the CRISPR tai^{PPxA} allele indicate that heterozygosity for tai^{PPxA} is sufficient to impair imaginal wing disc regeneration. Previous research demonstrates that the Tai PPxY motifs are required for physical interaction between Yki and Tai as well as expression of Tai-dependent Yki targets including *Ilp8* in the context of Yki overexpression [74]. Taken together, these data imply that the Yki-Tai interaction is required for regeneration, possibly through promoting a regenerative program that includes *Ilp8*. This theory is further supported by the loss of injury-induced developmental delay we find in tai^{PPxA} injured animals. These findings will need to be followed up on to further explore the possible role for Yki-Tai interaction in driving a regenerative transcriptional program and whether this transcriptional program also requires the EcR.

3.4 Materials and methods

Drosophila husbandry

All *Drosophila* stocks were maintained at 25°C unless otherwise noted. *Sgs3-Gal4;sgs3-GFP* was a gift of A. Bashirullah. Remaining stocks were obtained from the Bloomington Drosophila Stock Center (BDSC) or the Kyoto Stock Center: *fkh-Gal4* (BL#78061), *sgs3-GFP* (BL#5884), *UAS-EcR-RNAi* (BL#9327), *UAS-Cyp18a1* (BL#19262), *UAS-RFP* (BL#30556), *UAS-Smr-RNAi* (BL#27068), *UAS-EcI-RNAi* (Kyoto#7571R-1), and *UAS-EcR*^{F645A}.

UAS-EcRLBD and *UAS-EcRA483T* transgenic lines

RedStinger (nlsRFP) coding sequence was PCR amplified from *IRER-nlsRFP* genomic DNA [144] with primers containing 5' and 3' Not1 and Xba1 restriction sites. Not1/Xba1 digested pUAST and PCR product were ligated at 16ºC. The resulting *pUAST-nlsRED* plasmid was sequence verified before being subsequently digested with EcoR1/Not1 to allow for the insertion of DNA encoding the EcR^{LBD}, hinge region and F-domain (amino acids 330-878) which were PCR amplified from *hs-EcR.LBD* genomic DNA with EcoR1/Not1 restriction sites added [101, 119]. The completed *pUAST-EcRLBD-RFP* plasmid was sequence verified. The Emory Integrated Genomics Core introduced the A^{483}T single point mutation using standard practices to generate *pUAST-EcRA483T*. Transgenic fly services were provided by BestGene, Inc (USA).

Glue protein dynamics

To measure glue protein secretion into the lumen, late (clear gut) 3rd instar *sgs3-GFP* larvae of the indicated genotypes were dissected, fixed in 4% paraformaldehyde for 30min, washed 3x

5min in 1x phosphate buffered saline (PBS), permeabilized with 1xPBS+0.3% Triton-X 100, and stained with DAPI (Sigma Aldrich #D8417) for 10min. To assess glue expectoration, *sgs3-GFP* pupae (4h APF) were imaged through their pupal case for GFP localization and intensity. Sgs3-GFP was scored as 'retained' if GFP signal could be seen within the SGs.

Regeneration experiments

We used the *w1118;; rn-GAL4, tub-GAL80ts, UAS-reaper* and *w1118;; rn-GAL4, tub-GAL80ts, UAS-eiger* genetic ablation systems to study regeneration, and *w1118;; rn-GAL4, tub-GAL80ts* as our mock ablation control [22]. These are abbreviated as rn^{ts}>*rpr*, rn^{ts}>*egr*, and rn^{ts}>+ respectively. Development was synchronized by collecting eggs on grape plates. Eggs were collected for 4 hours at 25°C then placed at 18°C. After 2 days at 18°C, 50 L1 larvae were picked and placed into churned fly food vials. For rn^{ts}>*rpr* experiments, on day 7 after egg lay (AEL) temperature shifts were performed to induce ablation. Vials were moved from 18°C to a 29°C circulating water bath for 20 hours.

Adult wing size

Only female animals were used for these experiments, as previous research has indicated that female and male flies display statistically different regenerative capacity. Populations from separate ablation experiments cannot be meaningfully compared to one another as studies from other labs have indicated seasonal variation regeneration.

Semi-quantitative: for binning experiments, adult wing size was scored following injury and regeneration into 5 categories (0%, 25%, 50%, 75%, and 100%). Results were calculated per

population, with n's representing data from at least 3 separate ablation experiments. Statistical analysis was performed in GraphPad Prism9 using the χ^2 test.

Pupariation timing experiments

Pupariation rates were quantified by counting newly formed pupae every 8 h. Timing was reported as hours after egg lay (AEL), starting at the beginning of the 4-hour egg lay period. Pupariation was determined as when animals stopped moving and darken in color. Survival curve analysis for pupariation timing experiments was performed in GraphPad Prism9 using the Log-rank (Mantel-Cox) test. Results are calculated per population, with n's representing data from at least 2 separate ablation experiments.

Chapter 4. Discussion and future directions

4.1 Summary of dissertation

Steroid hormone signaling controls a diverse set of biological processes, including developmental progression, tissue growth, and fertility in both vertebrates and *Drosophila*. Evidence has also pointed to roles for steroid hormone signaling in promoting regeneration in certain contexts. For example, mammalian steroid hormones (e.g., estrogen) promote the physiologic regeneration of deer antlers as well as mouse mammary glands [145, 146]. Further, topical estrogen application has also been shown to promote wound healing of both elderly humans and mice [147-151]. Steroid hormone signaling has also been shown to be required for limb regeneration in the fiddler crab, *Uca pugilator* [4]. In this dissertation, I demonstrate that local ecdysone steroid hormone synthesis and signaling is required for imaginal wing disc regeneration in *Drosophila melanogaster* and begin to describe the aspects of imaginal wing disc regeneration regulated by ecdysone signaling.

In Chapter 2, I investigate the role of local Ec steroid hormone synthesis in imaginal wing disc regeneration. I show that local depletion of Ec biosynthesis genes consistently impairs regrowth of injured wing discs, while KD of the gene encoding the Ec degradation enzyme Cyp18a1 enhances wing disc regeneration. Further, injury and the regenerative response in wild-type wing discs leads to a drop in EcR activity throughout the disc, followed by a rise in EcR activity specifically in the regeneration blastema; and RNAi depletion of the Ec biosynthesis gene *phm* is sufficient to prevent this rise in EcR activity in the blastema. We go on to show that blastemal Ec is required for proper injury-induced developmental delay and coordinated growth reduction. Finally, we find that expression of mRNAs encoding the key regeneration regulators Ets21C and Upd3 expression are responsive to local Ec at the site of injury.

In Chapter 3, I employ two new tools generated by postdoctoral fellows in our lab to investigate the activities of EcR and its co-regulators in development and regeneration. I used the well-studied, EcR regulated processes of salivary gland Sgs3 glue protein synthesis, secretion, and expectoration to compare the newly generated EcR^{LBD} tool to previous models of EcR disruption. I demonstrate phenotypic differences between these models that suggest the EcR^{LBD} and similar tools can be uses to gain insights into biological process specific EcR-cofactor interactions. I then make use of a CRISPR generated tai^{PPxA} allele to demonstrate a possible requirement for interaction between Yki and Tai in wing disc regeneration and injury-induced pupariation delay.

4.2 Outstanding questions and future directions

4.2.1 Ecdysteroid synthesis and signaling in the regeneration blastema

My research in Chapter 2 of this dissertation indicates that local Ec synthesis is required for imaginal wing disc regeneration. I test the requirement for Ec biosynthesis genes as far up the pathway as *phm*; however, I did not test the requirement for *neverland*, which encodes the enzyme that converts cholesterol to 7-dehydrocholesterol (7dC), or the Ec biosynthesis genes that catalyze the 'Black Box' reactions. The Black Box reactions are the steps that convert 7dC into 5β-ketodiol. They are referred to as the Black Box reactions due to the sequence and the nature of intermediaries not being fully elucidated [54, 55]. Therefore, our assessment of the local requirement for Ec biosynthesis to promote wing disc regeneration leaves a gap in our knowledge regarding which cholesterol intermediaries are required to be present in the injured wing disc. A first step in filling this knowledge gap could be screening the rest of the Ec biosynthesis gene pathway in using our regeneration paradigm. A more detailed analysis could

involve performing LC-MS/MS to determine which ecdysteroid intermediaries are present and their concentration in regenerating wing discs compared to uninjured controls. Such detailed analysis of ecdysteroid composition in a specific tissue has not been performed before, however LC-MS/MS has previously been used to screen the ecdysteroidome in whole larva [152]. Interestingly, this study indicates that, in addition to 20E, other ecdysteroid intermediaries can drive EcR regulated processes in imaginal wing discs. This opens the possibility that ecdysteroid intermediaries other than 20E are responsible for or required to promote imaginal wing disc regeneration. Resolving these questions would further our understanding of how local steroid hormone synthesis can influence local tissue growth.

4.2.2 EcR activity and targets during wing disc regeneration

We find that EcR activity, as assessed by expression of *7xEcRE-GFP* reporter, drops throughout the imaginal wing disc in the first 24hrs of regeneration. The *7xEcRE-GFP* is based off the EcREs taken from the *EcR* promoter and inserted into the *Drosophila* genome upstream of *GFP*. A limitation of this finding is that *7xEcRE-GFP* is unlikely to serve as a good readout for the activity of all EcR targets. Therefore, it is possible that the EcR activates specific targets within the blastema during the first 24hrs of wing disc regeneration, but this activity is not picked up by the *7xEcRE-GFP* reporter. *7xEcRE-GFP* expression rises by 32hrs of wing disc regeneration in scattered, individual cells located along the inner dorsal and ventral hinges and within the pouch proper and by 48hrs of regeneration becomes stronger along the ventral hinge and an area extending from the inner dorsal hinge toward the notum. This *7xEcRE-GFP* expression indicates that EcR can activate transcriptional targets in these cells during wing disc regeneration but

leaves the question of what the EcR's transcriptional targets are in the context of regeneration unanswered.

To gain an understanding of the EcR transcriptional targets during regeneration we studied the expression of candidate targets. These studies indicate that the secreted insulin-like peptide *Ilp8*, known to be involved in regulation of injury-induced pupariation delay and coordinated growth reduction [38, 45, 46, 72], is not responsive to local 20E levels in the blastema. This came as a surprise to us given our data demonstrate 20E levels in the blastema modulate both injury-induced pupariation delay and coordinated growth reduction. It remains possible that blastemal Ec signaling regulates Ilp8 signaling downstream of *Ilp8* expression via some novel Ec signaling mechanism, and this could be an interesting line of research. Alternatively, these data suggest an important role for additional signaling pathways in the regulation of injury-induced developmental delay and coordinated growth reduction. Another molecule that has recently been indicated to coordinate developmental delay through suppression of systemic Ec production in response to growth perturbation and is known to be upregulated in blastema of regenerating imaginal wing discs is the Unpaired family cytokine Upd3 [38, 48]. We find that *Cyp18a1* depletion in the blastema does upregulate *Upd3* mRNA expression in injured wing discs. This suggests that increased *upd3* expression may be, at least in part, responsible for the enhanced injury-induced developmental delay and regeneration seen in *Cyp18a1* KD discs. Expression of the key regeneration regulator gene *Ets21C* is also upregulated in *Cyp18a1* KD discs, and Ets21C has been shown to support the maintenance of the pro-regenerative transcriptional program in the blastema, including expression of *upd3* [38]. Taken together these studies indicate that an EcR transcriptional program, involving regulation of both *Ets21C* and *upd3* expression, is activated in the wing disc blastema. However, failure of *phm* KD to influence

expression of the mRNAs encoding either Ets21C or Upd3, as well as the relatively modest increase in these mRNAs seen with *Cyp18a1* KD, indicate the need for future studies to fully elucidate the pro-regenerative EcR transcriptional program.

Future studies should involve global approaches. Recently, scRNA-Seq experiments have been performed with genetically ablated discs [38, 153]. These experiments are increasing our understanding of the transcriptional programs active in distinct cellular populations during wing disc regeneration. Currently, we are analyzing data from these published experiments to determine the expression patterns of Ec biosynthesis genes during wing disc regeneration. Future scRNA-Seq experiments, could examine the effect of *phm* and *Cypa18a1* KD to elucidate the contribution of local Ec to the pro-regenerative transcriptional progam. Global ChIP-Seq experiments could also be performed to compare the genomic occupancy of the EcR between normal developmental and regenerative growth. These ChIP-Seq experiments would be able to determine if the EcR binds to specific enhancer regions during regenerative growth or if the EcR uses the same enhancer elements during regenerative growth as it does during normal developmental growth.

4.2.3 Phenotypic differences in disruption of EcR regulated processes

Expression of the EcR^{LBD} construct in the larval SG specifically disrupts secretion and expectoration of Sgs3-GFP without disrupting production of Sgs3-GFP. This differs from models of EcR disruption driven by RNAi depletion of *EcR* or expression of EcR^{F645A}, a dominant negative version of the EcR, which disrupt production of Sgs3-GFP as well as Sgs3-GFP secretion and expectoration. The specific inability of EcR^{LBD} to disrupt Sgs3-GFP production indicates that Sgs3-GFP production is involves different EcR regulation than Sgs3-GFP secretion

and expectoration. Interestingly, earlier studies of Sgs3-GFP production in the SG indicated that the EcR may not require its heterodimeric binding partner, USP, to activate Sgs3-GFP production [129]. The EcR^{LBD} fragment contains the primary binding site between EcR and USP, and it may be the case that the EcR^{LBD} can sequester USP in certain tissue contexts. If USP is specifically not required for the production of Sgs3-GFP, this would explain the ability of EcR^{LBD} to permit Sgs3-GFP production but inhibit Sgs3-GFP secretion and expectoration. Coimmunoprecipitation experiments between EcR^{LBD} could provide insights into the EcR co-regulators in tissue- and stage- specific contexts.

4.2.4 Importance of the Yki-Tai interaction during wing disc regeneration

My data indicate that heterozygosity for tai^{PPxA} is sufficient to impair wing disc regeneration and inhibit injury-induced developmental delay. The tai^{PPxA} mutation has previously been shown to block binding between Tai and Yki, the co-activator of the Hippo pathway, and the Yki-Tai interaction is required for transcriptional activation of certain Tai-dependent Yki-targets and for Yki-driven overgrowth of the imaginal wing disc [74]. Therefore, these data indicate that the Yki-Tai interaction may be required for imaginal wing disc regeneration. Given the reduction of injury-induced developmental delay observed in tai^{PPxA} heterozygotes, it is also tempting to speculate that the Yki-Tai interaction may be required for expression of *Ilp8*. However, these data cannot preclude the possibility that the effect of tai^{PPxA} heterozygosity on regeneration is mediated through disruption of Tai binding to some other co-regulator. Further studies will be needed to determine the requirement for Yki-Tai interaction in promoting the pro-regenerative transcriptional program in wing discs. These experiments will likely include global approaches

similar to the scRNA-Seq experiments proposed to resolve the transcriptional program supported by local Ec biosynthesis during regeneration.

4.3 Concluding remarks

Through the research in this dissertation, we investigated the local role of the steroid hormone Ec in regeneration of the Drosophila wing epithelium. In organisms as diverse as humans and crustaceans, steroid hormones can promote cell proliferation, wound healing, or replacement of lost appendages. However, in a widely used wounding model in Drosophila, regeneration of the larval wing is associated with a systemic loss of Ec that delays development. While investigating this apparent paradox, we discovered that although systemic activity of the EcR drops after wing injury, it locally increases within the regeneration blastema, and that local depletion of Ec biosynthesis enzymes within the blastema block the local EcR activity and impair regeneration. Significantly, reciprocal elevation of Ec levels within the blastema enhance regeneration, suggesting that transcriptional activity of the EcR protein is rate-limiting within the blastema for efficient regeneration. Probing further, we find that local manipulation of Ec biosynthesis does not alter cell division in the blastema, but rather impairs the growth coordination between injured and uninjured wing regions that is necessary to maintain developmental synchrony. At a transcriptional level, we link these local effects of Ec to altered levels of mRNAs encoding the Ets21C transcription factor, which sustains a regeneration specific transcriptional program, and the Upd3 cytokine, which is produced and secreted by wing blastema cells.

Overall, our data reveal that while systemic Ec levels drop in response to wing disc injury, a local increase in active Ec over the blastema aids in creating a unique signaling environment necessary to coordinate local and systemic aspects of the regeneration process. This

mechanism is a significant and novel addition to our understanding of how a systemic endocrine signaling pathway is locally regulated to create a privileged transcriptional environment to support tissue repair. Consequently, this work may inspire additional researchers to study the coordination of local and systemic production of endocrine signaling molecules to promote wound repair and tissue regeneration in diverse species.

REFERENCES

1. Morgan, T.H. (1901). Regeneration and Liability to Injury. Science *14*, 235-248.
2. Dinsmore, C.E. (1996). Urodele limb and tail regeneration in early biological thought: an essay on scientific controversy and social change. Int J Dev Biol *40*, 621-627.
3. Reaumur, R.A.F.d. (1712). Sur les diverses Reproduction qui se font dans les Ecrevises, les Omars, les Crabes, etc. et entr'autres sur celles de leurs Jambes and de leurs Ecailes. Historie de l'Academie Royale des Sciences, Avec les Memoires de Mathematique and de Physique pour la meme Annee, Tires des Registres de cette Academie.
4. Das, S., and Durica, D.S. (2013). Ecdysteroid receptor signaling disruption obstructs blastemal cell proliferation during limb regeneration in the fiddler crab, Uca pugilator. Mol Cell Endocrinol *365*, 249-259.
5. Tsonis, P.A., and Fox, T.P. (2009). Regeneration according to Spallanzani. Dev Dyn *238*, 2357-2363.
6. Sinigaglia, C., Alie, A., and Tiozzo, S. (2022). The Hazards of Regeneration: From Morgan's Legacy to Evo-Devo. Methods Mol Biol *2450*, 3-25.
7. Sunderland, M.E. (2010). Regeneration: Thomas Hunt Morgan's window into development. J Hist Biol *43*, 325-361.
8. Tanaka, E.M. (2003). Regeneration: if they can do it, why can't we? Cell *113*, 559-562.
9. Srivastava, M. (2021). Beyond Casual Resemblance: Rigorous Frameworks for Comparing Regeneration Across Species. Annu Rev Cell Dev Biol *37*, 415-440.
10. Chen, C.H., and Poss, K.D. (2017). Regeneration Genetics. Annu Rev Genet *51*, 63-82.
11. Goldman, J.A., and Poss, K.D. (2020). Gene regulatory programmes of tissue regeneration. Nat Rev Genet *21*, 511-525.
12. Joven, A., Elewa, A., and Simon, A. (2019). Model systems for regeneration: salamanders. Development *146*.
13. Muneoka, K., Allan, C.H., Yang, X., Lee, J., and Han, M. (2008). Mammalian regeneration and regenerative medicine. Birth Defects Res C Embryo Today *84*, 265-280.
14. Xin, M., Kim, Y., Sutherland, L.B., Murakami, M., Qi, X., McAnally, J., Porrello, E.R., Mahmoud, A.I., Tan, W., Shelton, J.M., et al. (2013). Hippo pathway effector Yap promotes cardiac regeneration. Proc Natl Acad Sci U S A *110*, 13839-13844.
15. Worley, M.I., Setiawan, L., and Hariharan, I.K. (2012). Regeneration and transdetermination in Drosophila imaginal discs. Annu Rev Genet *46*, 289-310.
16. Fox, D.T., Cohen, E., and Smith-Bolton, R. (2020). Model systems for regeneration: Drosophila. Development *147*.
17. Tanaka, E.M., and Reddien, P.W. (2011). The cellular basis for animal regeneration. Dev Cell *21*, 172-185.
18. Bilder, D. (2017). Another Nobel Prize for the Fruit Fly. In New York Times.
19. Aldaz, S., and Escudero, L.M. (2010). Imaginal discs. Curr Biol *20*, R429-431.
20. Ong, C., Yung, L.Y., Cai, Y., Bay, B.H., and Baeg, G.H. (2015). Drosophila melanogaster as a model organism to study nanotoxicity. Nanotoxicology *9*, 396-403.
21. Tripathi, B.K., and Irvine, K.D. (2022). The wing imaginal disc. Genetics *220*.

22. Smith-Bolton, R.K., Worley, M.I., Kanda, H., and Hariharan, I.K. (2009). Regenerative growth in Drosophila imaginal discs is regulated by Wingless and Myc. Dev Cell *16*, 797-809.
23. Brand, A.H., and Perrimon, N. (1993). Targeted gene expression as a means of altering cell fates and generating dominant phenotypes. Development *118*, 401-415.
24. McGuire, S.E., Mao, Z., and Davis, R.L. (2004). Spatiotemporal gene expression targeting with the TARGET and gene-switch systems in Drosophila. Sci STKE *2004*, pl6.
25. Khan, S.J., Abidi, S.N.F., Skinner, A., Tian, Y., and Smith-Bolton, R.K. (2017). The Drosophila Duox maturation factor is a key component of a positive feedback loop that sustains regeneration signaling. PLoS Genet *13*, e1006937.
26. Skinner, A., Khan, S.J., and Smith-Bolton, R.K. (2015). Trithorax regulates systemic signaling during Drosophila imaginal disc regeneration. Development *142*, 3500-3511.
27. Tian, Y., and Smith-Bolton, R.K. (2021). Regulation of growth and cell fate during tissue regeneration by the two SWI/SNF chromatin-remodeling complexes of Drosophila. Genetics *217*, 1-16.
28. Brock, A.R., Seto, M., and Smith-Bolton, R.K. (2017). Cap-n-Collar Promotes Tissue Regeneration by Regulating ROS and JNK Signaling in the Drosophila melanogaster Wing Imaginal Disc. Genetics *206*, 1505-1520.
29. Narbonne-Reveau, K., and Maurange, C. (2019). Developmental regulation of regenerative potential in Drosophila by ecdysone through a bistable loop of ZBTB transcription factors. PLoS Biol *17*, e3000149.
30. Harris, R.E., Setiawan, L., Saul, J., and Hariharan, I.K. (2016). Localized epigenetic silencing of a damage-activated WNT enhancer limits regeneration in mature Drosophila imaginal discs. Elife *5*.
31. Goyal, L., McCall, K., Agapite, J., Hartwieg, E., and Steller, H. (2000). Induction of apoptosis by Drosophila reaper, hid and grim through inhibition of IAP function. EMBO J *19*, 589-597.
32. Igaki, T., Kanda, H., Yamamoto-Goto, Y., Kanuka, H., Kuranaga, E., Aigaki, T., and Miura, M. (2002). Eiger, a TNF superfamily ligand that triggers the Drosophila JNK pathway. EMBO J *21*, 3009-3018.
33. Bosch, M., Baguna, J., and Serras, F. (2008). Origin and proliferation of blastema cells during regeneration of Drosophila wing imaginal discs. Int J Dev Biol *52*, 1043-1050.
34. Sustar, A., Bonvin, M., Schubiger, M., and Schubiger, G. (2011). Drosophila twin spot clones reveal cell division dynamics in regenerating imaginal discs. Dev Biol *356*, 576-587.
35. Herrera, S.C., Martin, R., and Morata, G. (2013). Tissue homeostasis in the wing disc of Drosophila melanogaster: immediate response to massive damage during development. PLoS Genet *9*, e1003446.
36. Worley, M.I., Setiawan, L., and Hariharan, I.K. (2013). TIE-DYE: a combinatorial marking system to visualize and genetically manipulate clones during development in Drosophila melanogaster. Development *140*, 3275-3284.
37. Worley, M.I., and Hariharan, I.K. (2022). Imaginal Disc Regeneration: Something Old, Something New. Cold Spring Harb Perspect Biol *14*.

38. Worley, M.I., Everetts, N.J., Yasutomi, R., Chang, R.J., Saretha, S., Yosef, N., and Hariharan, I.K. (2022). Ets21C sustains a pro-regenerative transcriptional program in blastema cells of Drosophila imaginal discs. Curr Biol *32*, 3350-3364 e3356.
39. Diaz-Garcia, S., and Baonza, A. (2013). Pattern reorganization occurs independently of cell division during Drosophila wing disc regeneration in situ. Proc Natl Acad Sci U S A *110*, 13032-13037.
40. Repiso, A., Bergantinos, C., and Serras, F. (2013). Cell fate respecification and cell division orientation drive intercalary regeneration in Drosophila wing discs. Development *140*, 3541-3551.
41. Verghese, S., and Su, T.T. (2016). Drosophila Wnt and STAT Define Apoptosis-Resistant Epithelial Cells for Tissue Regeneration after Irradiation. PLoS Biol *14*, e1002536.
42. Jaszczak, J.S., Wolpe, J.B., Bhandari, R., Jaszczak, R.G., and Halme, A. (2016). Growth Coordination During Drosophila melanogaster Imaginal Disc Regeneration Is Mediated by Signaling Through the Relaxin Receptor Lgr3 in the Prothoracic Gland. Genetics *204*, 703-709.
43. Halme, A., Cheng, M., and Hariharan, I.K. (2010). Retinoids regulate a developmental checkpoint for tissue regeneration in Drosophila. Curr Biol *20*, 458-463.
44. Colombani, J., Andersen, D.S., Boulan, L., Boone, E., Romero, N., Virolle, V., Texada, M., and Leopold, P. (2015). Drosophila Lgr3 Couples Organ Growth with Maturation and Ensures Developmental Stability. Curr Biol *25*, 2723-2729.
45. Colombani, J., Andersen, D.S., and Leopold, P. (2012). Secreted peptide Dilp8 coordinates Drosophila tissue growth with developmental timing. Science *336*, 582-585.
46. Garelli, A., Gontijo, A.M., Miguela, V., Caparros, E., and Dominguez, M. (2012). Imaginal discs secrete insulin-like peptide 8 to mediate plasticity of growth and maturation. Science *336*, 579-582.
47. Garelli, A., Heredia, F., Casimiro, A.P., Macedo, A., Nunes, C., Garcez, M., Dias, A.R.M., Volonte, Y.A., Uhlmann, T., Caparros, E., et al. (2015). Dilp8 requires the neuronal relaxin receptor Lgr3 to couple growth to developmental timing. Nat Commun *6*, 8732.
48. Romao, D., Muzzopappa, M., Barrio, L., and Milan, M. (2021). The Upd3 cytokine couples inflammation to maturation defects in Drosophila. Curr Biol *31*, 1780-1787 e1786.
49. Vallejo, D.M., Juarez-Carreno, S., Bolivar, J., Morante, J., and Dominguez, M. (2015). A brain circuit that synchronizes growth and maturation revealed through Dilp8 binding to Lgr3. Science *350*, aac6767.
50. Niwa, Y.S., and Niwa, R. (2016). Transcriptional regulation of insect steroid hormone biosynthesis and its role in controlling timing of molting and metamorphosis. Dev Growth Differ *58*, 94-105.
51. Niwa, Y.S., and Niwa, R. (2014). Neural control of steroid hormone biosynthesis during development in the fruit fly Drosophila melanogaster. Genes Genet Syst *89*, 27-34.
52. Yamanaka, N., Rewitz, K.F., and O'Connor, M.B. (2013). Ecdysone control of developmental transitions: lessons from Drosophila research. Annu Rev Entomol *58*, 497-516.
53. Everetts, N.J., Worley, M.I., Yasutomi, R., Yosef, N., and Hariharan, I.K. (2021). Single-cell transcriptomics of the Drosophila wing disc reveals instructive epithelium-to-myoblast interactions. Elife *10*.

54. Warren, J.T., O'Connor, M.B., and Gilbert, L.I. (2009). Studies on the Black Box: incorporation of 3-oxo-7-dehydrocholesterol into ecdysteroids by Drosophila melanogaster and Manduca sexta. Insect Biochem Mol Biol *39*, 677-687.
55. Kannangara, J.R., Mirth, C.K., and Warr, C.G. (2021). Regulation of ecdysone production in Drosophila by neuropeptides and peptide hormones. Open Biol *11*, 200373.
56. Gilbert, L.I. (2004). Halloween genes encode P450 enzymes that mediate steroid hormone biosynthesis in Drosophila melanogaster. Mol Cell Endocrinol *215*, 1-10.
57. Guittard, E., Blais, C., Maria, A., Parvy, J.P., Pasricha, S., Lumb, C., Lafont, R., Daborn, P.J., and Dauphin-Villemant, C. (2011). CYP18A1, a key enzyme of Drosophila steroid hormone inactivation, is essential for metamorphosis. Dev Biol *349*, 35-45.
58. Belles, X., and Piulachs, M.D. (2015). Ecdysone signalling and ovarian development in insects: from stem cells to ovarian follicle formation. Biochim Biophys Acta *1849*, 181-186.
59. King-Jones, K., and Thummel, C.S. (2005). Nuclear receptors--a perspective from Drosophila. Nat Rev Genet *6*, 311-323.
60. Weikum, E.R., Liu, X., and Ortlund, E.A. (2018). The nuclear receptor superfamily: A structural perspective. Protein Sci *27*, 1876-1892.
61. Yao, T.P., Forman, B.M., Jiang, Z., Cherbas, L., Chen, J.D., McKeown, M., Cherbas, P., and Evans, R.M. (1993). Functional ecdysone receptor is the product of EcR and Ultraspiracle genes. Nature *366*, 476-479.
62. Hill, R.J., Billas, I.M., Bonneton, F., Graham, L.D., and Lawrence, M.C. (2013). Ecdysone receptors: from the Ashburner model to structural biology. Annu Rev Entomol *58*, 251-271.
63. Tsai, C.C., Kao, H.Y., Yao, T.P., McKeown, M., and Evans, R.M. (1999). SMRTER, a Drosophila nuclear receptor coregulator, reveals that EcR-mediated repression is critical for development. Mol Cell *4*, 175-186.
64. Bai, J., Uehara, Y., and Montell, D.J. (2000). Regulation of invasive cell behavior by taiman, a Drosophila protein related to AIB1, a steroid receptor coactivator amplified in breast cancer. Cell *103*, 1047-1058.
65. Dasgupta, S., and O'Malley, B.W. (2014). Transcriptional coregulators: emerging roles of SRC family of coactivators in disease pathology. J Mol Endocrinol *53*, R47-59.
66. Boghog2 (2008). Type ii nuclear receptor. In Wikipedia.
67. Dye, N.A., Popovic, M., Spannl, S., Etournay, R., Kainmuller, D., Ghosh, S., Myers, E.W., Julicher, F., and Eaton, S. (2017). Cell dynamics underlying oriented growth of the Drosophila wing imaginal disc. Development *144*, 4406-4421.
68. Herboso, L., Oliveira, M.M., Talamillo, A., Perez, C., Gonzalez, M., Martin, D., Sutherland, J.D., Shingleton, A.W., Mirth, C.K., and Barrio, R. (2015). Ecdysone promotes growth of imaginal discs through the regulation of Thor in D. melanogaster. Sci Rep *5*, 12383.
69. Mirth, C.K., Truman, J.W., and Riddiford, L.M. (2009). The ecdysone receptor controls the post-critical weight switch to nutrition-independent differentiation in Drosophila wing imaginal discs. Development *136*, 2345-2353.
70. Parker, J., and Struhl, G. (2020). Control of Drosophila wing size by morphogen range and hormonal gating. Proc Natl Acad Sci U S A *117*, 31935-31944.

71. Parker, N.F., and Shingleton, A.W. (2011). The coordination of growth among Drosophila organs in response to localized growth-perturbation. Dev Biol *357*, 318-325.
72. Boulan, L., Andersen, D., Colombani, J., Boone, E., and Leopold, P. (2019). Inter-Organ Growth Coordination Is Mediated by the Xrp1-Dilp8 Axis in Drosophila. Dev Cell *49*, 811-818 e814.
73. Gokhale, R.H., Hayashi, T., Mirque, C.D., and Shingleton, A.W. (2016). Intra-organ growth coordination in Drosophila is mediated by systemic ecdysone signaling. Dev Biol *418*, 135-145.
74. Zhang, C., Robinson, B.S., Xu, W., Yang, L., Yao, B., Zhao, H., Byun, P.K., Jin, P., Veraksa, A., and Moberg, K.H. (2015). The ecdysone receptor coactivator Taiman links Yorkie to transcriptional control of germline stem cell factors in somatic tissue. Dev Cell *34*, 168-180.
75. Berreur, P., and Fraenkel, G. (1969). Puparium formation in flies: contraction to puparium induced by ecdysone. Science *164*, 1182-1183.
76. Denlinger, D.L. (1994). Metamorphosis behavior of flies. Annu Rev Entomol *39*, 243-266.
77. Lam, G., and Thummel, C.S. (2000). Inducible expression of double-stranded RNA directs specific genetic interference in Drosophila. Curr Biol *10*, 957-963.
78. Warren, J.T., Yerushalmi, Y., Shimell, M.J., O'Connor, M.B., Restifo, L.L., and Gilbert, L.I. (2006). Discrete pulses of molting hormone, 20-hydroxyecdysone, during late larval development of Drosophila melanogaster: correlations with changes in gene activity. Dev Dyn *235*, 315-326.
79. Karanja, F., Sahu, S., Weintraub, S., Bhandari, R., Jaszczak, R., Sitt, J., and Halme, A. (2022). Ecdysone exerts biphasic control of regenerative signaling, coordinating the completion of regeneration with developmental progression. Proc Natl Acad Sci U S A *119*.
80. Petryk, A., Warren, J.T., Marques, G., Jarcho, M.P., Gilbert, L.I., Kahler, J., Parvy, J.P., Li, Y., Dauphin-Villemant, C., and O'Connor, M.B. (2003). Shade is the Drosophila P450 enzyme that mediates the hydroxylation of ecdysone to the steroid insect molting hormone 20-hydroxyecdysone. Proc Natl Acad Sci U S A *100*, 13773-13778.
81. Warren, J.T., Petryk, A., Marques, G., Parvy, J.P., Shinoda, T., Itoyama, K., Kobayashi, J., Jarcho, M., Li, Y., O'Connor, M.B., et al. (2004). Phantom encodes the 25-hydroxylase of Drosophila melanogaster and Bombyx mori: a P450 enzyme critical in ecdysone biosynthesis. Insect Biochem Mol Biol *34*, 991-1010.
82. Chavez, V.M., Marques, G., Delbecque, J.P., Kobayashi, K., Hollingsworth, M., Burr, J., Natzle, J.E., and O'Connor, M.B. (2000). The Drosophila disembodied gene controls late embryonic morphogenesis and codes for a cytochrome P450 enzyme that regulates embryonic ecdysone levels. Development *127*, 4115-4126.
83. Boone, E., Colombani, J., Andersen, D.S., and Leopold, P. (2016). The Hippo signalling pathway coordinates organ growth and limits developmental variability by controlling dilp8 expression. Nat Commun *7*, 13505.
84. Gontijo, A.M., and Garelli, A. (2018). The biology and evolution of the Dilp8-Lgr3 pathway: A relaxin-like pathway coupling tissue growth and developmental timing control. Mech Dev *154*, 44-50.

85. Rewitz, K.F., Yamanaka, N., Gilbert, L.I., and O'Connor, M.B. (2009). The insect neuropeptide PTTH activates receptor tyrosine kinase torso to initiate metamorphosis. Science *326*, 1403-1405.
86. La Fortezza, M., Schenk, M., Cosolo, A., Kolybaba, A., Grass, I., and Classen, A.K. (2016). JAK/STAT signalling mediates cell survival in response to tissue stress. Development *143*, 2907-2919.
87. Cosolo, A., Jaiswal, J., Csordas, G., Grass, I., Uhlirova, M., and Classen, A.K. (2019). JNK-dependent cell cycle stalling in G2 promotes survival and senescence-like phenotypes in tissue stress. Elife *8*.
88. Hackney, J.F., Pucci, C., Naes, E., and Dobens, L. (2007). Ras signaling modulates activity of the ecdysone receptor EcR during cell migration in the Drosophila ovary. Dev Dyn *236*, 1213-1226.
89. Igaki, T., Pastor-Pareja, J.C., Aonuma, H., Miura, M., and Xu, T. (2009). Intrinsic tumor suppression and epithelial maintenance by endocytic activation of Eiger/TNF signaling in Drosophila. Dev Cell *16*, 458-465.
90. Yoo, S.J., Huh, J.R., Muro, I., Yu, H., Wang, L., Wang, S.L., Feldman, R.M., Clem, R.J., Muller, H.A., and Hay, B.A. (2002). Hid, Rpr and Grim negatively regulate DIAP1 levels through distinct mechanisms. Nat Cell Biol *4*, 416-424.
91. Hackney, J.F., Zolali-Meybodi, O., and Cherbas, P. (2012). Tissue damage disrupts developmental progression and ecdysteroid biosynthesis in Drosophila. PLoS One *7*, e49105.
92. Nogueira Alves, A., Oliveira, M.M., Koyama, T., Shingleton, A., and Mirth, C.K. (2022). Ecdysone coordinates plastic growth with robust pattern in the developing wing. Elife *11*.
93. Kiehle, C.P., and Schubiger, G. (1985). Cell proliferation changes during pattern regulation in imaginal leg discs of Drosophila melanogaster. Dev Biol *109*, 336-346.
94. DaCrema, D., Bhandari, R., Karanja, F., Yano, R., and Halme, A. (2021). Ecdysone regulates the Drosophila imaginal disc epithelial barrier, determining the length of regeneration checkpoint delay. Development *148*.
95. Santabarbara-Ruiz, P., Lopez-Santillan, M., Martinez-Rodriguez, I., Binagui-Casas, A., Perez, L., Milan, M., Corominas, M., and Serras, F. (2015). ROS-Induced JNK and p38 Signaling Is Required for Unpaired Cytokine Activation during Drosophila Regeneration. PLoS Genet *11*, e1005595.
96. Katsuyama, T., Comoglio, F., Seimiya, M., Cabuy, E., and Paro, R. (2015). During Drosophila disc regeneration, JAK/STAT coordinates cell proliferation with Dilp8-mediated developmental delay. Proc Natl Acad Sci U S A *112*, E2327-2336.
97. Pastor-Pareja, J.C., Wu, M., and Xu, T. (2008). An innate immune response of blood cells to tumors and tissue damage in Drosophila. Dis Model Mech *1*, 144-154; discussion 153.
98. Domanitskaya, E., Anllo, L., and Schupbach, T. (2014). Phantom, a cytochrome P450 enzyme essential for ecdysone biosynthesis, plays a critical role in the control of border cell migration in Drosophila. Dev Biol *386*, 408-418.
99. Wehner, D., Tsarouchas, T.M., Michael, A., Haase, C., Weidinger, G., Reimer, M.M., Becker, T., and Becker, C.G. (2017). Wnt signaling controls pro-regenerative Collagen XII in functional spinal cord regeneration in zebrafish. Nat Commun *8*, 126.

100. Danielsen, E.T., Moeller, M.E., and Rewitz, K.F. (2013). Nutrient signaling and developmental timing of maturation. Curr Top Dev Biol *105*, 37-67.
101. Koelle, M.R., Talbot, W.S., Segraves, W.A., Bender, M.T., Cherbas, P., and Hogness, D.S. (1991). The Drosophila EcR gene encodes an ecdysone receptor, a new member of the steroid receptor superfamily. Cell *67*, 59-77.
102. Yao, T.P., Segraves, W.A., Oro, A.E., McKeown, M., and Evans, R.M. (1992). Drosophila ultraspiracle modulates ecdysone receptor function via heterodimer formation. Cell *71*, 63-72.
103. Oro, A.E., McKeown, M., and Evans, R.M. (1990). Relationship between the product of the Drosophila ultraspiracle locus and the vertebrate retinoid X receptor. Nature *347*, 298-301.
104. Thomas, H.E., Stunnenberg, H.G., and Stewart, A.F. (1993). Heterodimerization of the Drosophila ecdysone receptor with retinoid X receptor and ultraspiracle. Nature *362*, 471-475.
105. Brown, H.L., Cherbas, L., Cherbas, P., and Truman, J.W. (2006). Use of time-lapse imaging and dominant negative receptors to dissect the steroid receptor control of neuronal remodeling in Drosophila. Development *133*, 275-285.
106. Schubiger, M., Carre, C., Antoniewski, C., and Truman, J.W. (2005). Ligand-dependent de-repression via EcR/USP acts as a gate to coordinate the differentiation of sensory neurons in the Drosophila wing. Development *132*, 5239-5248.
107. Schubiger, M., and Truman, J.W. (2000). The RXR ortholog USP suppresses early metamorphic processes in Drosophila in the absence of ecdysteroids. Development *127*, 1151-1159.
108. Cherbas, L., Hu, X., Zhimulev, I., Belyaeva, E., and Cherbas, P. (2003). EcR isoforms in Drosophila: testing tissue-specific requirements by targeted blockade and rescue. Development *130*, 271-284.
109. Rosenfeld, M.G., Lunyak, V.V., and Glass, C.K. (2006). Sensors and signals: a coactivator/corepressor/epigenetic code for integrating signal-dependent programs of transcriptional response. Genes Dev *20*, 1405-1428.
110. Stieper, B.C., Kupershtok, M., Driscoll, M.V., and Shingleton, A.W. (2008). Imaginal discs regulate developmental timing in Drosophila melanogaster. Dev Biol *321*, 18-26.
111. Mirth, C. (2005). Ecdysteroid control of metamorphosis in the differentiating adult leg structures of Drosophila melanogaster. Dev Biol *278*, 163-174.
112. Jiang, C., Baehrecke, E.H., and Thummel, C.S. (1997). Steroid regulated programmed cell death during Drosophila metamorphosis. Development *124*, 4673-4683.
113. Jiang, C., Lamblin, A.F., Steller, H., and Thummel, C.S. (2000). A steroid-triggered transcriptional hierarchy controls salivary gland cell death during Drosophila metamorphosis. Mol Cell *5*, 445-455.
114. Ninov, N., Chiarelli, D.A., and Martin-Blanco, E. (2007). Extrinsic and intrinsic mechanisms directing epithelial cell sheet replacement during Drosophila metamorphosis. Development *134*, 367-379.
115. Riddiford, L.M. (1993). Hormone receptors and the regulation of insect metamorphosis. Receptor *3*, 203-209.

116. Muller, B., Hartmann, B., Pyrowolakis, G., Affolter, M., and Basler, K. (2003). Conversion of an extracellular Dpp/BMP morphogen gradient into an inverse transcriptional gradient. Cell *113*, 221-233.
117. Uyehara, C.M., and McKay, D.J. (2019). Direct and widespread role for the nuclear receptor EcR in mediating the response to ecdysone in Drosophila. Proc Natl Acad Sci U S A *116*, 9893-9902.
118. Schubiger, M., Tomita, S., Sung, C., Robinow, S., and Truman, J.W. (2003). Isoform specific control of gene activity in vivo by the Drosophila ecdysone receptor. Mech Dev *120*, 909-918.
119. Kozlova, T., and Thummel, C.S. (2002). Spatial patterns of ecdysteroid receptor activation during the onset of Drosophila metamorphosis. Development *129*, 1739-1750.
120. Yan, J., Tsai, S.Y., and Tsai, M.J. (2006). SRC-3/AIB1: transcriptional coactivator in oncogenesis. Acta Pharmacol Sin *27*, 387-394.
121. Yan, J., Yu, C.T., Ozen, M., Ittmann, M., Tsai, S.Y., and Tsai, M.J. (2006). Steroid receptor coactivator-3 and activator protein-1 coordinately regulate the transcription of components of the insulin-like growth factor/AKT signaling pathway. Cancer Res *66*, 11039-11046.
122. Staley, B.K., and Irvine, K.D. (2012). Hippo signaling in Drosophila: recent advances and insights. Dev Dyn *241*, 3-15.
123. Sousa-Victor, P., Ayyaz, A., Hayashi, R., Qi, Y., Madden, D.T., Lunyak, V.V., and Jasper, H. (2017). Piwi Is Required to Limit Exhaustion of Aging Somatic Stem Cells. Cell Rep *20*, 2527-2537.
124. Laudet, V., Hanni, C., Coll, J., Catzeflis, F., and Stehelin, D. (1992). Evolution of the nuclear receptor gene superfamily. EMBO J *11*, 1003-1013.
125. Hu, X., Cherbas, L., and Cherbas, P. (2003). Transcription activation by the ecdysone receptor (EcR/USP): identification of activation functions. Mol Endocrinol *17*, 716-731.
126. Mottis, A., Mouchiroud, L., and Auwerx, J. (2013). Emerging roles of the corepressors NCoR1 and SMRT in homeostasis. Genes Dev *27*, 819-835.
127. Heck, B.W., Zhang, B., Tong, X., Pan, Z., Deng, W.M., and Tsai, C.C. (2012). The transcriptional corepressor SMRTER influences both Notch and ecdysone signaling during Drosophila development. Biol Open *1*, 182-196.
128. Andres, A.J., Fletcher, J.C., Karim, F.D., and Thummel, C.S. (1993). Molecular analysis of the initiation of insect metamorphosis: a comparative study of Drosophila ecdysteroid-regulated transcription. Dev Biol *160*, 388-404.
129. Biyasheva, A., Do, T.V., Lu, Y., Vaskova, M., and Andres, A.J. (2001). Glue secretion in the Drosophila salivary gland: a model for steroid-regulated exocytosis. Dev Biol *231*, 234-251.
130. Kaieda, Y., Masuda, R., Nishida, R., Shimell, M., O'Connor, M.B., and Ono, H. (2017). Glue protein production can be triggered by steroid hormone signaling independent of the developmental program in Drosophila melanogaster. Dev Biol *430*, 166-176.
131. Okamoto, N., Viswanatha, R., Bittar, R., Li, Z., Haga-Yamanaka, S., Perrimon, N., and Yamanaka, N. (2018). A Membrane Transporter Is Required for Steroid Hormone Uptake in Drosophila. Dev Cell *47*, 294-305 e297.

132. Rewitz, K.F., Yamanaka, N., and O'Connor, M.B. (2010). Steroid hormone inactivation is required during the juvenile-adult transition in Drosophila. Dev Cell *19*, 895-902.
133. Grusche, F.A., Degoutin, J.L., Richardson, H.E., and Harvey, K.F. (2011). The Salvador/Warts/Hippo pathway controls regenerative tissue growth in Drosophila melanogaster. Dev Biol *350*, 255-266.
134. Sun, G., and Irvine, K.D. (2011). Regulation of Hippo signaling by Jun kinase signaling during compensatory cell proliferation and regeneration, and in neoplastic tumors. Dev Biol *350*, 139-151.
135. Rosenfeld, M.G., and Glass, C.K. (2001). Coregulator codes of transcriptional regulation by nuclear receptors. J Biol Chem *276*, 36865-36868.
136. Handgraaf, S., Riant, E., Fabre, A., Waget, A., Burcelin, R., Liere, P., Krust, A., Chambon, P., Arnal, J.F., and Gourdy, P. (2013). Prevention of obesity and insulin resistance by estrogens requires ERalpha activation function-2 (ERalphaAF-2), whereas ERalphaAF-1 is dispensable. Diabetes *62*, 4098-4108.
137. Shinkaruk, S., Carreau, C., Flouriot, G., Bennetau-Pelissero, C., and Potier, M. (2010). Comparative effects of R- and S-equol and implication of transactivation functions (AF-1 and AF-2) in estrogen receptor-induced transcriptional activity. Nutrients *2*, 340-354.
138. Tolon, R.M., Castillo, A.I., Jimenez-Lara, A.M., and Aranda, A. (2000). Association with Ets-1 causes ligand- and AF2-independent activation of nuclear receptors. Mol Cell Biol *20*, 8793-8802.
139. Sheldon, L.A., Smith, C.L., Bodwell, J.E., Munck, A.U., and Hager, G.L. (1999). A ligand binding domain mutation in the mouse glucocorticoid receptor functionally links chromatin remodeling and transcription initiation. Mol Cell Biol *19*, 8146-8157.
140. Rochette-Egly, C., Plassat, J.L., Taneja, R., and Chambon, P. (2000). The AF-1 and AF-2 activating domains of retinoic acid receptor-alpha (RARalpha) and their phosphorylation are differentially involved in parietal endodermal differentiation of F9 cells and retinoid-induced expression of target genes. Mol Endocrinol *14*, 1398-1410.
141. Keeton, E.K., Fletcher, T.M., Baumann, C.T., Hager, G.L., and Smith, C.L. (2002). Glucocorticoid receptor domain requirements for chromatin remodeling and transcriptional activation of the mouse mammary tumor virus promoter in different nucleoprotein contexts. J Biol Chem *277*, 28247-28255.
142. Bastien, J., Adam-Stitah, S., Riedl, T., Egly, J.M., Chambon, P., and Rochette-Egly, C. (2000). TFIIH interacts with the retinoic acid receptor gamma and phosphorylates its AF-1-activating domain through cdk7. J Biol Chem *275*, 21896-21904.
143. Xie, X.J., Hsu, F.N., Gao, X., Xu, W., Ni, J.Q., Xing, Y., Huang, L., Hsiao, H.C., Zheng, H., Wang, C., et al. (2015). CDK8-Cyclin C Mediates Nutritional Regulation of Developmental Transitions through the Ecdysone Receptor in Drosophila. PLoS Biol *13*, e1002207.
144. Zhang, C., Casas-Tinto, S., Li, G., Lin, N., Chung, M., Moreno, E., Moberg, K.H., and Zhou, L. (2015). An intergenic regulatory region mediates Drosophila Myc-induced apoptosis and blocks tissue hyperplasia. Oncogene *34*, 2385-2397.
145. Sasidharan, V., and Sanchez Alvarado, A. (2021). The Diverse Manifestations of Regeneration and Why We Need to Study Them. Cold Spring Harb Perspect Biol *14*.
146. Easterling, M.R., Engbrecht, K.M., and Crespi, E.J. (2019). Endocrine Regulation of Epimorphic Regeneration. Endocrinology *160*, 2969-2980.

147. Ashcroft, G.S., Dodsworth, J., van Boxtel, E., Tarnuzzer, R.W., Horan, M.A., Schultz, G.S., and Ferguson, M.W. (1997). Estrogen accelerates cutaneous wound healing associated with an increase in TGF-beta1 levels. Nat Med *3*, 1209-1215.
148. Ashcroft, G.S., Mills, S.J., Lei, K., Gibbons, L., Jeong, M.J., Taniguchi, M., Burow, M., Horan, M.A., Wahl, S.M., and Nakayama, T. (2003). Estrogen modulates cutaneous wound healing by downregulating macrophage migration inhibitory factor. J Clin Invest *111*, 1309-1318.
149. Gilliver, S.C., Ashworth, J.J., and Ashcroft, G.S. (2007). The hormonal regulation of cutaneous wound healing. Clinics in Dermatology *25*, 56-62.
150. Hardman, M.J., and Ashcroft, G.S. (2008). Estrogen, not intrinsic aging, is the major regulator of delayed human wound healing in the elderly. Genome Biol *9*, R80.
151. Mukai, K., Nakajima, Y., Asano, K., and Nakatani, T. (2019). Topical estrogen application to wounds promotes delayed cutaneous wound healing in 80-week-old female mice. PLoS One *14*, e0225880.
152. Lavrynenko, O., Rodenfels, J., Carvalho, M., Dye, N.A., Lafont, R., Eaton, S., and Shevchenko, A. (2015). The ecdysteroidome of Drosophila: influence of diet and development. Development *142*, 3758-3768.
153. Floc'hlay, S., Balaji, R., Stankovic, D., Christiaens, V.M., Bravo Gonzalez-Blas, C., De Winter, S., Hulselmans, G.J., De Waegeneer, M., Quan, X., Koldere, D., et al. (2023). Shared enhancer gene regulatory networks between wound and oncogenic programs. Elife *12*.